

Investigation of a radiative cooling system with natural circulation for regulating a heat sink

Ruhan Theunissen

B. Eng.

Dissertation submitted in fulfilment of the requirements for the degree Master of Engineering at the Potchefstroom campus of the North-West University

Supervisor: Prof. C.P. Storm

November 2011

ABSTRACT

The global energy demand has seen a significant increase over the past decade. Our inseparable need for energy has created a number of serious concerns. The most important concern is the environmental impact of our energy generating methods. Another looming concern is our global fossil fuel resources that are diminishing progressively. These two major concerns have turned attention to research and development of energy efficient and alternative energy systems.

A field of alternative energy that has been untapped is nocturnal radiative cooling. The idea behind this is to utilise the cooling effect between a hot surface and the night sky. The setup is similar to that of a solar water heating system but is used for cooling instead of heating. Previous studies on radiative cooling systems have all focussed on forced circulation systems. The aim of this study is to analyse the performance of a natural circulating system.

The current knowledge on radiative cooling systems is limited and experimental research is often a costly and time consuming exercise. As a result it is difficult to get an understanding of the performance of a radiative cooling system in various operating environments. The aim of this study is to overcome this limitation by developing a theoretical model to simulate the performance of a natural circulating radiative cooling system.

A natural circulating solar water heater model was used as a basis for the natural circulating radiative cooling model. A night sky radiation model replaced the solar radiation component to give the radiative heat transfer of the panel to the night sky. Fundamental heat transfer and fluid flow theories also formed part of the model.

The theoretical model was able to give realistically accurate predictions compared to data from an experimental setup. The model made it possible to study the impact of various parameters on the system performance without the constraints of experimental setups. The performance of a natural circulating radiative cooling system was simulated over a year under different operating climates by using historical weather data.

The results obtained with the help of the model indicated that natural circulating radiative cooling is indeed able to provide a sufficient cooling effect that can be utilised in a practical manner. This study gives indication that radiative cooling systems are worthy of further development to ensure that it forms part of the current line-up of alternative energy systems.

Keywords: Radiative cooling, natural circulation, thermosyphon, night sky radiation, alternative energy.

SAMEVATTING

Die wêreld se vraag na energie het 'n drastiese toename gedurende die afgelope dekade ondervind. Die mens se onafskeidbare behoefte na energie het ongelukkig 'n aantal bekommernisse tot gevolg. Die belangrikste hiervan is die impak wat die huidige metodes van energie-opwekking op die omgewing het. 'n Ander bekommernis is dat die wêreld se reserwes van fossielbrandstof toenemend uitgeput word. Hierdie twee vernaamste bekommernisse vestig die aandag op die belangrikheid van navorsing en ontwikkeling oor effektiewe alternatiewe energiestelsels.

'n Potensiële veld van alternatiewe energie wat nog relatief onaangeraak is, is stralingsverkoeling gedurende die nag. Die beginsel daaragter is om van die verkoelingseffek tussen 'n warm voorwerp en die nag se hemelruim gebruik te maak. Die opstelling van so 'n stelsel is soortgelyk aan 'n son waterverwarmingstelsel maar dit verskaf verkoeling eerder as verhitting. Vorige navorsing op stralingsverkoeling het meestal gefokus op geforseerde sirkulasiestelsels. Die doel van hierdie studie was om die werking van 'n natuurlike sirkulasiestelsel van verkoeling te ondersoek.

Bestaande inligting oor stralingsverkoeling is beperk en eksperimentele navorsing is gewoonlik 'n tydrowende en duur proses. Gevolglik is dit moeilik om 'n goeie begrip oor die werking van stralingsverkoeling onder verskillende werkstoestande te verkry. Die doel van hierdie studie is om die genoemde beperkinge te oorkom deur 'n teoretiese model te ontwikkel wat die werking van 'n natuurlik sirkulerende stralingsverkoelingstelsel kan simuleer.

Die teoretiese model was gebaseer op 'n bestaande model wat vir natuurlike sirkulasie son waterverwarmers ontwikkel is. 'n Naghemelruim stralingsenergiemodel het die son as stralings komponent vervang om die straling hitte-oordrag tussen die paneel en die nag se hemelruim te bepaal. Fundamentele hitte-oordrag en vloeiteorie het ook deel van die simulاسie gevorm.

Die teoretiese model was in staat om realistiese en akkurate simulاسies te doen in vergelyking met die data van 'n eksperimentele opstelling. Die model het dit moontlik gemaak om die uitwerking van verskeie veranderlikes te toets sonder die genoemde beperkings van eksperimentele toetsing. Die werking van 'n stralingsverkoelingstelsel was oor 'n tydperk van 'n jaar onder verskillende klimaatstoestande gesimuleer deur van historiese weerkundige inligting gebruik te maak.

Die resultate wat met behulp van die model verkry is het aangedui dat 'n natuurlik sirkulerende stralingsverkoelingstelsel in staat is om genoegsame verkoeling te genereer. Hierdie verkoeling kan verder op 'n aanwendbare wyse opgegaar en benut word. Die bevindings van hierdie studie dui daarop dat verdere ontwikkeling van die model geregverdig is sodat dat hierdie stelsel deel van die huidige verskeidenheid alternatiewe energie stelsels kan raak.

ACKNOWLEDGEMENTS

Professor Chris Storm for giving me the opportunity to perform this study and his grateful guidance, advice and wisdom during this study.

Other staff and personnel at the North-West University school of Mechanical Engineering for their help and advice.

My Father and Mother whom I cannot thank enough for the opportunities they gave me to help me get where I am today and for their wonderful parenting.

My fellow friends who helped me focus on the lighter side of life as well and making the years of studying a memorable experience.

NOMENCLATURE

Symbol	Description	Unit	Symbol	Description	Unit
A	Panel surface area	$[m^2]$	T_1	Panel inlet temperature	$[^{\circ}C]$
A_1, A_2	Storage tank insulation surface area	$[m^2]$	T_2	Panel outlet temperature	$[^{\circ}C]$
A_{cp}	Cross section area of connecting pipes	$[m^2]$	T_{db}	Dry bulb ambient temperature	$[^{\circ}C]$
A_p	Cross section area of panel down tube	$[m^2]$	T_{dp}	Dew point temperature	$[^{\circ}C]$
B	Width of panel surface	$[m]$	T_f	Air film temperature	$[^{\circ}C]$
C_p	Constant pressure specific heat	$[J/kg \cdot K]$	T_m	Mean storage tank temperature	$[^{\circ}C]$
D_{cp}	Connecting pipes inside diameter	$[m]$	T_{sky}	Effective sky temperature	$[^{\circ}C]$
D_p	Panel down tube inside diameter	$[m]$	T_{wb}	Wet bulb temperature	$[^{\circ}C]$
f	Friction factor		V_{cp}	Fluid flow velocity in connecting pipes	$[m/s]$
g	Gravitational acceleration	$[m/s^2]$	V_p	Fluid flow velocity in panel	$[m/s]$
h	Panel convection coefficient	$[W/m^2 \cdot K]$	x_1, x_2	Insulation material thickness	$[m]$
$h_1, h_2, h_3, h_4, h_5 \& h_6$	System point height	$[m]$	x_{step}	Euler-Cauchy method step size	
h_{cp}	Connecting pipes head loss	$[m]$	α	Thermal diffusivity	$[m^2/s]$
h_f	Total system head loss	$[m]$	β	Volumetric thermal expansion coefficient	$[K^{-1}]$
h_p	Panel head loss	$[m]$	ε	Surface emissivity of panel	
h_t	Storage tank convective heat transfer coefficient	$[W/m^2 \cdot K]$	ε_{sky}	Equivalent sky emissivity	
h_t	Thermosyphon pressure head	$[m]$	θ	Time step	
k	Thermal conductivity of air	$[W/m \cdot K]$	ν	Kinematic viscosity of fluid	$[m^2/s]$
k_1, k_2	Insulation material thermal conductivity	$[W/m \cdot K]$	ρ	Density of fluid	$[kg/m^3]$
L	Length of panel surface	$[m]$	σ	Stefan-Boltzmann constant	$[W/m^2 \cdot K^4]$
L_c	Characteristic length of panel	$[m]$	φ	Panel tilt angle	$[^{\circ}]$
L_{cp}	Total length of connecting pipes	$[m]$	ϕ	Panel and connecting pipe head loss ratio	
L_p	Length of panel down tubes	$[m]$			
m	Mass of system fluid	$[kg]$			
\dot{m}	Mass flow rate	$[kg/s]$			
N	Number of down tubes in panel				
Nu	Nusselt number				
Q_{ads}	Additional heat gain	$[W]$			
Q_{conv}	Convection heat transfer	$[W]$			
Q_{load}	Heat load	$[W]$			
Q_{rad}	Thermal radiation heat transfer	$[W]$			
Q_{tank}	Total heat loss form storage tank	$[W]$			
R	Thermal resistance of insulation				
Ra	Rayleigh number				
S_1, S_2	Specific gravity				

TABLE OF CONTENTS

ABSTRACT.....	i
SAMEVATTING	ii
ACKNOWLEDGEMENTS	iii
NOMENCLATURE	iv
LIST OF FIGURES	vii
LIST OF TABLES.....	ix
1. INTRODUCTION	1
1.1. BACKGROUND	1
1.2. PROBLEM STATEMENT.....	9
1.3. STUDY OBJECTIVE.....	9
1.4. METHOD OF RESEARCH.....	10
2. LITERATURE SURVEY	11
2.1. RADIATIVE COOLING SYSTEMS.....	11
2.2. RADIATOR PANELS	12
2.3. NATURAL CIRCULATION LOOPS (THERMOSYPHON)	14
2.4. NIGHT SKY RADIATION	14
2.5. NATURAL AND FORCED CONVECTIVE HEAT TRANSFER	16
2.6. THERMAL ENERGY STORAGE	16
2.7. RADIATIVE COOLING SYSTEM CONFIGURATION	18
3. THEORETICAL MODEL ANALYSIS.....	20
3.1. INTRODUCTION	20
3.2. RADIATOR PANELS	20
3.3. PIPE NETWORK HEAD LOSSES	21
3.4. STORAGE TANK HEAT FLUX	23
3.5. EFFECTIVE SKY TEMPERATURE	24
3.6. PANEL HEAT TRANSFER	26
3.7. MEAN STORAGE TANK TEMPERATURE.....	30
3.8. NATURAL CIRCULATION FLOW (THERMOSYPHON)	33
3.9. AMBIENT TEMPERATURE AND CONDITIONS.....	36
4. EXPERIMENTAL MODEL.....	38
4.1. INTRODUCTION	38
4.2. TEST MODEL DESIGN	38
4.3. TEST MODEL SETUP	40

4.4.	EXPERIMENTAL METHOD	42
4.5.	EXPERIMENTAL RESULTS	42
5.	EXPERIMENTAL AND THEORETICAL MODEL COMPARISON	47
5.1.	INTRODUCTION	47
5.2.	OBSERVATIONS AND CORRECTIONS	47
5.3.	CORRECTED THEORETICAL MODEL RESULTS.....	55
6.	SYSTEM PERFORMANCE ANALYSIS	60
6.1.	RELATIVE HUMIDITY	60
6.2.	PANEL SURFACE EMISSIVITY	61
6.3.	CONNECTING PIPE DIAMETER	63
6.4.	PANEL AND STORAGE TANK HEIGHT DIFFERENCE	64
6.5.	PANEL TILT ANGLE.....	66
6.6.	STORAGE TANK DIMENSIONS	67
6.7.	SYSTEM PERFORMANCE CONCLUSIONS.....	70
7.	APPLIED MODEL: YEAR ROUND PERFORMANCE	71
7.1.	INTRODUCTION	71
7.2.	RADIATIVE COOLING SYSTEM DESIGN BASELINE	71
7.3.	APPLIED THEORETICAL MODEL	73
7.4.	APPLIED MODEL CONCLUSION	79
8.	CONCLUSIONS AND RECOMMENDATIONS.....	81
8.1.	CONCLUSION.....	81
8.2.	RECOMMENDATIONS AND FUTURE DEVELOPMENTS	82
8.3.	CLOSURE	83
9.	REFERENCES	84
	APPENDIX A: SAMPLE CALCULATION	86
	APPENDIX B: THEORETICAL MODEL DATA EXTRACT	93
	APPENDIX C: EXPERIMENTAL DATA EXTRACT	111

LIST OF FIGURES

Figure 1 : World primary energy demand outlook in terms of oil energy value [1].....	1
Figure 2 : Energy consumption by economic sector for South Africa in 2006 [3]	2
Figure 3 : Ammonia-water absorption refrigeration cycle [7].....	4
Figure 4 : Solar and coal energy path	6
Figure 5 : Basic flat-plate solar water heater panel.....	12
Figure 6 : Radiative cooling system.....	18
Figure 7 : Storage tank thermal resistance.....	24
Figure 8 : T_{sky} model comparison	26
Figure 9 : Kinematic viscosity of air	29
Figure 10 : Thermal conductivity of air	29
Figure 11 : Thermal diffusivity of air	29
Figure 12 : Radiator panel energy balance.....	31
Figure 13 : Storage tank energy balance.....	31
Figure 14 : Thermosyphon loop system points and heights.....	33
Figure 15 : System Temperature-Height diagram.....	34
Figure 16 : 30% Ethylene-Glycol water mixture specific gravity curve fit	35
Figure 17: Actual vs. estimated ambient temperature.....	37
Figure 18 : Test model [27]	39
Figure 19 : Actual test model.....	39
Figure 20 : Actual test model panel	39
Figure 21 : S1 Experimental data.....	43
Figure 22 : S2 Experimental data.....	44
Figure 23 : Test period temperatures	46
Figure 24 : Theoretical and test results temperature drift	48
Figure 25 : Theoretical model with additional heat gain.....	49
Figure 26 : Mass flow rate at 15 minute interval	51
Figure 27 : Mass flow rate at 1½ hour intervals	51
Figure 28 : Mass flow and energy correlation.....	52
Figure 29 : Panel temperature difference and energy correlation	53
Figure 30 : Mass flow rate at 6 hour interval.....	54
Figure 31 : Theoretical model results comparison for S1.....	56
Figure 32 : Theoretical panel heat loss for S1 simulation	57
Figure 33 : Theoretical model results comparison for S2.....	58
Figure 34 : Theoretical panel heat loss for S2 simulation	59
Figure 35 : Effect of RH on mean storage tank temperature.....	60
Figure 36 : Effect of RH on mass flow rate	61
Figure 37 : Effect of ϵ on mean storage tank temperature	62
Figure 38 : Effect of ϵ on mass flow rate.....	62
Figure 39 : Effect of pipe diameter in mean storage tank temperature	63
Figure 40 : Effect of pipe diameter on mass flow rate.....	64
Figure 41 : Effect of panel height on mean storage tank temperature	65
Figure 42 : Effect of panel height on mass flow rate.....	65
Figure 43 : Effect of tilt angle on mean storage tank temperature.....	66
Figure 44 : Effect of tilt angle on mass flow rate	67
Figure 45 : Effect of storage tank dimensions on mean storage tank temperature	68

Figure 46 : Effect of storage tank dimensions on mass flow rate	68
Figure 47 : Thermally stratified tank in- and outlet design [24].....	69
Figure 48 : Annual system performance for Johannesburg	74
Figure 49 : Annual system performance for Pretoria	76
Figure 50 : Annual system performance for Durban	77
Figure 51 : Annual system performance for Cape Town.....	78
Figure 52 : Storage tank monthly average temperature comparison	79

LIST OF TABLES

Table 1 : Coal energy conversion losses [12]	8
Table 2 : Solar energy conversion losses.....	8
Table 3 : Test model dimensions and properties	40
Table 4 : Test setup information	41
Table 5 : Design baseline summary	73
Table 6 : S1 Theoretical data extract.....	94
Table 7 : S2 Theoretical data extract.....	103
Table 8 : S1 Experimental data extract.....	111
Table 9 : S2 Experimental data extract.....	116

1. INTRODUCTION

1.1. BACKGROUND

The human race is probably one of the most energy dependant life forms ever to inhabit the earth. We have developed ways of generating and using energy in such ways that we cannot do away with it any more. Almost everything in our modern society is created with energy and is forever dependant on it. Our energy demands are expected to increase by 1.5% per year until 2030 according to the International Energy Agency [1]. Without energy at our disposal our existence is surely debatable.

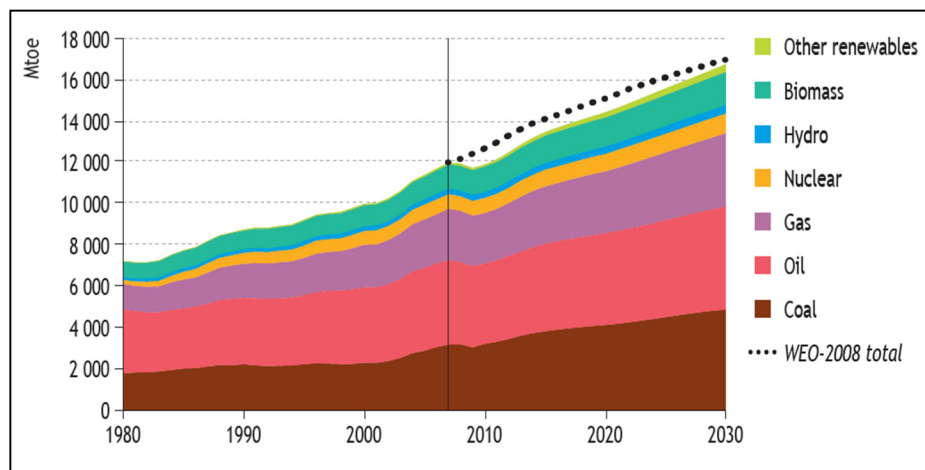


Figure 1 : World primary energy demand outlook in terms of oil energy value [1]

Our relentless energy dependence has however created a host of concerns globally in the modern day and age. An obvious and certainly most publicised concern is the impact that our current energy generating methods have on the environment. The environmental impact of fossil fuel combustion as an energy source is still a much debated topic and is yet to be quantified in full.

Apart from the environmental aspect there is another noteworthy concern looming. The price of crude oil has increased sharply during the past decade as prosperous oil fields are becoming more difficult to extract cost-effectively and rapid economic growth demands more supply [2]. The outcome of this is that energy will become a high-priced or even unaffordable commodity in the future. The price of coal has not risen as sharply as crude oil but escalating environmental policies and legislation are putting pressure on end users to find alternatives.

The underlying message in all of this is straightforward. We have to find alternative energy sources to supplement or replace fossil fuels in order to sustain our energy needs and meet stringent environmental policies. Fortunately there are a number of abundant alternative

energy sources available. Solar, wind and hydropower are popular options and vast amounts of effort and resources are currently spent on researching ways of utilising it.

Research and development of ways to tap into these alternative energy sources should continue to ensure that human society is able to move away from fossil fuels as our primary energy source.

1.1.1. Domestic Energy Use and Generation

According to statistics by the South African Department of Energy the residential sector accounted for 19.4% of the total annual energy consumption in 2006 [3], [4]. 72.8% of this energy was in the form of electricity while coal and petroleum products made up the rest. This makes up a considerable portion of the total national energy demand. Any energy saving initiatives in this sector will definitely have a noteworthy influence on the total energy consumption of the country.

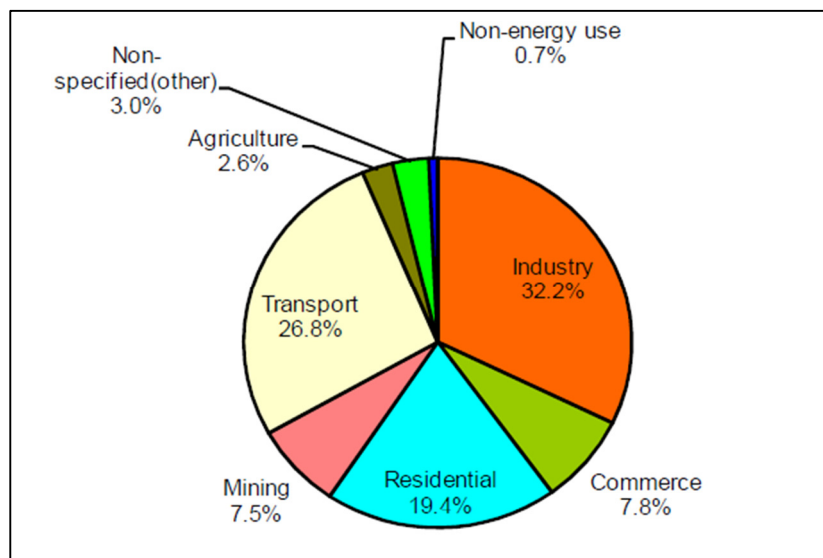


Figure 2 : Energy consumption by economic sector for South Africa in 2006 [3]

A way of reducing the energy use of a domestic house is to start using alternative energy sources on a small scale. A simple example of this is domestic solar water heating which has grown in popularity in recent years. The domestic utilisation of alternative energy sources can reach further than just solar water heating. Wind turbines and photovoltaic cells are also finding its way into domestic use. It is now possible to run a house entirely on alternative energy sources instead of an electricity supply from a municipality or national network.

The notion of using alternative energy at home is certainly gaining popularity and so called “off the grid” houses are becoming more common as technology improves and becomes more affordable. Some countries even have incentives in place for residences that are able to generate a surplus of electricity and are able to sell it back into a distribution network.

An understanding of how energy is used can help with better allocation of alternative energy sources. A typical residence has a number of main energy consumers which include water heating, refrigeration, lighting and space heating and cooling. An average of 5% of a typical South African household’s energy use goes towards refrigeration and cold storage [5].

It therefore makes good sense to explore and develop ways of applying alternative energy sources in the field of refrigeration.

1.1.2. Solar Powered Refrigeration

Refrigeration is a considerable part of our energy use. Not only is it an important part of domestic energy use but also in the commercial and industrial sector.

Modern refrigeration cycles can be divided into two main categories namely vapour compression cycles and absorption refrigeration cycles [6], [7]. The former is the most commonly used and delivers ample cooling power over a wide range of applications. The latter is not so commonly found but does still make up a noticeable sector in the market. It is not often a preferred method of cooling for various practical reasons. One reason is the generally lower efficiency or COP that absorption refrigeration has compared to vapour compression cycles.

An advantage however of absorption refrigeration is the type of energy input that is required. Absorption refrigeration cycles can be operated with only heat energy whereas vapour compression cycles require mechanical shaft power to drive a compressor [6], [7]. This means that almost any suitable source of heat can be used to power an absorption refrigeration cycle.

The capital cost of an absorption refrigeration plant is most often higher compared to vapour-compression systems but the life cycle cost can be balanced out if waste or alternative energy sources are used. This is especially true if low cost or free sources of heat are available for use. Typical sources of heat used in practice are hot exhaust gas, steam, process waste heat, fossil fuels and electricity. Another likely source of energy that has been looked into is solar thermal energy.

Previous attempts have been made to power absorption refrigeration cycles with solar thermal energy [8], [9]. These attempts proved that solar energy can indeed be used as an energy source but it has also pointed out various factors that deem these cycles unfeasible. A study done by Shiran et al [10] investigated the economic feasibility of solar powered ammonia-water absorption refrigeration cycles. This study found that high temperature, high efficiency solar collectors is the key to successful and economical operation of a solar powered cycle.

The performance and successful operation of absorption refrigeration cycles depend on a wide range of factors. One of these factors is the system pressures and temperatures at the various system points. It is important to have the correct fluid phase and temperature at each of these points for the thermodynamic cycle to work. One particularly important point in the system is the condenser outlet. Ideally this point should have the working fluid fully condensed from a gas phase to a liquid phase at a given pressure. This is however not easily achieved in practice. The reason for this is because the condenser is dependent on ambient air temperature as a heat sink.

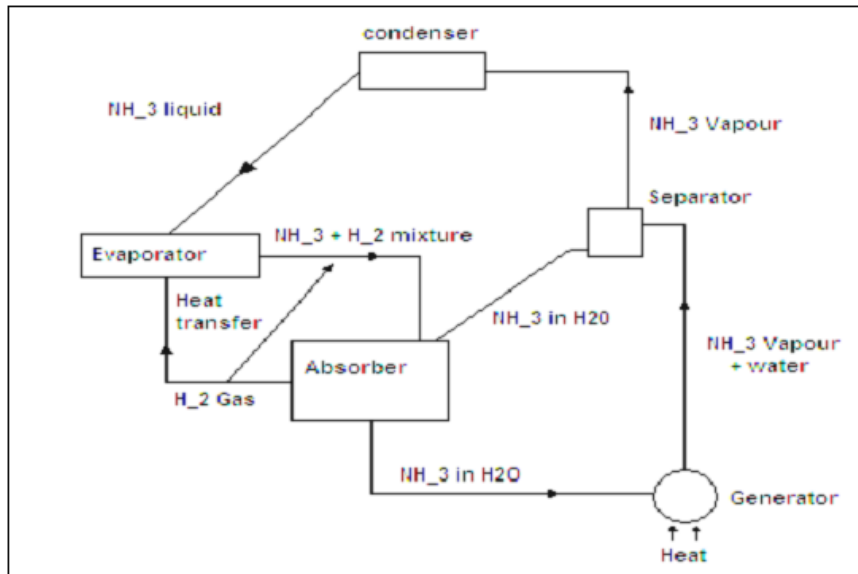


Figure 3 : Ammonia-water absorption refrigeration cycle [7]

The problem with the ambient air as a heat sink is the temperature fluctuation between day and night as well as winter and summer. A typical summer day in South Africa can reach a maximum of 30°C and cool down to around 15°C at night. This temperature difference means that a change of either the system pressure or temperature is necessary to achieve condensation of the fluid to a liquid in the condenser. Extreme condenser temperatures can result in the fluid not condensing properly if the temperature is too high or too much sub-cooling if the temperature is too low.

With conventional absorption refrigeration this is usually overcome by varying the amount of heat input to change the system pressure and this is a contributor to a lower COP. This is unfortunately not a practical solution with a solar powered cycle.

A significant problem with a solar powered system is the amount of thermal energy that is available either directly from a collector or from a thermal storage source. Solar energy systems therefore require collectors with a large surface area or thermal storage with 'n large volume and thermal capacity.

An additional supply of heat with conventional electric or fossil fuel powered cycles is easily achieved but not with solar energy. The amount of energy that is available from solar energy

either directly from a collector or stored is limited and cannot provide the necessary heat supply increase. This problem can be solved in two ways. One way is to increase the solar collector's capacity. Another way is to provide a more stable heat sink by regulating the condenser temperature.

1.1.3. Radiative Cooling Systems

An overlooked field in alternative energy is cooling by more efficient and environmentally friendly ways. One such way is heat rejection from a surface to the atmosphere in the form of thermal radiation. A simple example of this phenomenon is the cooling of the earth's surface during the night. Thermal radiation is often a forgotten form of heat transfer but it is by no means insignificant.

Thermal radiation can be utilised in many ways and various successful projects have been undertaken to take advantage of this cooling effect. One application can be to cool a fluid during the night and storing it for use during the day much like solar water heating. The storage of cold energy is now the main purpose instead of heat energy.

Radiative cooling can be achieved in the same way as the collection of solar energy. The principle of heat transfer as well as the equipment that are required is very similar. In the same way that a flat-plate solar collector is able to absorb heat it can also radiate heat from its exposed surface. This principle is backed by studies that found that flat-plate solar water heaters froze up even when the ambient temperature was still just above zero [11]. The additional cooling that caused the water inside the collector to freeze was due to the radiative cooling from the panel to the night sky. The night sky acts as a low temperature black body to which a hot surface can radiate at night.

The idea of using an energy efficient friendly cooling system can be enhanced further by abolishing a circulation pump for the fluid as well. The circulation of the fluid in the system can be achieved by a process called thermal syphoning or otherwise known as natural circulation. Thermal syphoning works on the principle of density differences between a hot and cold fluid. A hot fluid that is less dense will rise to the top in a system while a cold, denser fluid will tend to descend to the bottom of the system. This concept is used extensively in passive solar water heaters to circulate the heated water from the panel to the storage tank above the panel. This process can also be used the other way round to circulate a cooled fluid from the panel to a storage tank below the panel.

A new application of radiative cooling is a system that is able to regulate the condenser temperature of a solar powered absorption cycle as described in chapter 1.1.2. The aim of this system will be to mitigate the ambient temperature fluctuations to provide a more stable condenser operating temperature. The idea is to have radiative panels installed on the south facing side (for Southern hemisphere) of a building roof with a storage tank below in much the same arrangement as a solar water heating system.

A radiative cooling system such as this can hopefully be applied to help overcome the difficulties faced with solar powered absorption refrigeration cycles and improve its feasibility.

1.1.4. Efficient Use of Energy

The problem with alternative energy sources has always been high capital expenses that are required to utilise it. This greatly increases the life cycle cost and subsequently the cost per unit of energy. This made alternative energy economically unfeasible compared to fossil fuels in the past but recent fossil fuel price increases and environmental issues focussed attention on alternative energy sources once again.

One of the most important alternative energy sources is certainly solar energy. The utilisation of solar energy is not new and extensive research has been done in the past but its implementation in practice has been limited thus far. The high cost of efficient solar collectors makes it an expensive choice compared to fossil fuels. This notion can however be challenged if a slightly different view of energy is taken.

Another way to look at the feasibility of solar energy is to take a holistic view of how an energy source is used and the efficiency thereof. Consider the following diagram which indicates the path that two forms of energy follow from its ultimate origin, the sun, to an end use point. The two forms of energy considered in this diagram are solar thermal energy and coal energy.

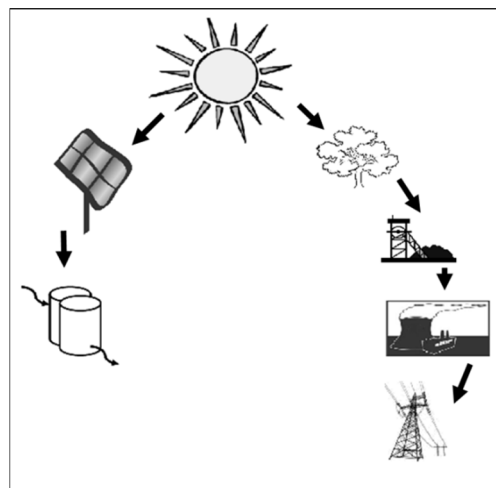


Figure 4 : Solar and coal energy path

Fossil fuels were produced from plant material that stored energy over thousands of years through photosynthesis. This is a chemical process that converts carbon dioxide and water into hydrocarbons by using energy from sunlight. The formed hydrocarbons have potential energy stored up and form the basis of all fossil fuels. The basic hydrocarbons can undergo

further chemical and physical alteration to form energy dense fossil fuels such as coal and crude oil.

The stored energy in coal is released by burning it to produce heat energy. This heat energy can be converted into other forms of energy such as kinetic energy. This is in essence the process that is followed to produce electricity from coal. The kinetic energy is used to drive an electric generator which in turn produces electricity. The conversion of energy from one form to another unfortunately undergoes losses along the way. The large number of energy conversion steps and transfers involved with electricity generation means that a significant amount of energy is lost.

Solar thermal energy on the other hand is a more direct way of tapping into the ultimate origin of energy. Solar energy is a very efficient form of energy since it undergoes fewer conversion losses along its energy path. This means that more of the original energy available remains to be used.

In order to demonstrate the efficiency of these two energy paths, consider an equal amount of energy from coal and an equal amount of energy from the sun. The end use of the energy is an absorption refrigeration cycle with a COP of 0.6 driven by solar thermal energy. It will be compared to a conventional vapour compression refrigeration cycle with a COP of 2.5 powered by electricity to drive a compressor.

The coal energy path requires that coal is burned in a power station to produce steam which is used to drive a generator which turns an electricity generator. This electricity is then distributed via a national distribution network to a point where it can power an electrical appliance. In this case it is the compressor motor of the vapour compression refrigeration cycle.

The path of solar energy is a much more direct path and has fewer losses. The thermal energy of the sun is captured with a solar collector. The captured heat is then stored in a thermal storage system to be used at times when sunshine is not present. The stored energy is used as the heat input for the absorption refrigeration cycle.

The following two tables compare the losses of these two energy paths and the amount of energy that reaches the end user.

Table 1 : Coal energy conversion losses [12]

Coal energy				
Loss	% Loss	kW Loss	kW remaining	Efficiency
Original energy in coal	0.0	0.0	100.0	100.0%
Unburnt carbon in ash after combustion	0.5	0.5	99.5	99.5%
Dry Flue gas loss	4.5	4.5	95.0	95.0%
H ₂ & fuel moisture loss	5.0	5.0	90.0	90.0%
Boiler radiation losses	0.5	0.5	89.5	89.5%
Heat sink rejection	65.0	65.0	24.5	24.5%
Turbine losses	3.4	3.4	21.1	21.1%
Generator losses	0.3	0.3	20.9	20.9%
Auxiliary power losses	1.5	1.5	19.4	19.4%
Transformer & switchgear losses	0.5	0.5	18.9	18.9%
Transmission lines losses	5.0	5.0	13.9	13.9%
Distribution system losses	2.0	2.0	11.9	11.9%
End use:				kW output
Refrigerator (COP = 2.5)				29.8
Used as heat pump (COP = 3.5)				41.7

Table 2 : Solar energy conversion losses

Solar energy				
Loss	% Loss	kW Loss	kW remaining	Efficiency
Initial solar energy	0	0.0	100.0	100.0%
Solar collector losses	30	30.0	70.0	70.0%
Thermal storage losses	15	15.0	55.0	55.0%
End use:				kW output
Refrigerator (COP = 0.6)				33.0
Used as heat pump (COP = 1.6)				88.0

It is immediately apparent that approximately 90% of the coal's initial energy is lost along the energy path. Solar power on the other hand has only lost 45% of the initial available energy. This proves the relevance of solar power in particular as a viable alternative energy source.

The better efficiency of the solar thermal energy path offsets the low COP of the absorption refrigeration cycle and makes it more favourable than a conventional vapour compression cycle when looking at the amount of cooling power output.

This whole exercise raises another question which is why fossil fuels are not used directly as an energy source since it would be much more efficient. The simple answer to this is the

convenience of electricity as a form of energy. It is relatively easy to use and distribute regardless of the substantial energy losses involved with the generation thereof. With this in mind, it can be argued whether electricity generation is a sensible use of our diminishing fossil fuel resources in applications such as this.

The importance of alternative energy sources that is directly accessible at a domestic level is once again illustrated here. A lack of research and development is a main reason of it not being a reality.

1.2. PROBLEM STATEMENT

The concept of a radiative cooling system is not new but the full potential of it has not been exploited. The feasibility of radiative cooling systems in general is still uncertain and because of this there is a reluctance to spend effort and resources on further development.

The experimental studying of system configurations and the effect of environmental conditions is a time consuming and costly exercise that could delay the development and implementation of radiative cooling systems in practice. A more theoretical research approach supported by experimental work is required in order to minimize these constraints.

The problem that is faced with such an approach is that a theoretical method is yet to be developed for a radiative cooling system. Previous studies on radiative cooling systems were only on an experimental and empirical level. The research and development of radiative cooling systems with natural circulation in particular is an untapped field with much potential.

A need therefore exists to develop a theoretical method that will assist research and development of radiative cooling systems and prove its feasibility.

1.3. STUDY OBJECTIVE

The aim of this study is to develop a theoretical model and verify it against experimental data so that it is able to simulate a radiative cooling system with natural circulation. The key attribute of this model will be to integrate the thermal syphoning concept for circulation of the fluid instead of forced circulation.

The feasibility of a radiative cooling system will be investigated with the help of this theoretical model under different meteorological climates and operating conditions expected in practice.

1.4. METHOD OF RESEARCH

This study starts off with a literature survey to look into previous attempts on radiative cooling systems and point out any shortcomings. Existing models and experimental results will be studied and possible modifications will be proposed and applied to obtain a theoretical basis for the study.

The information gathered from the literature survey will then be used for the development of the theoretical model for this study. This will involve a comprehensive analysis of a radiative cooling system in terms of pipe network, radiator panels, storage system and environmental operating conditions.

An experimental investigation of a radiative cooling system will also be conducted to verify the accuracy of the theoretical model. Any deviations between the theoretical and experimental results will be investigated and addressed by applying the necessary corrective actions to the theoretical model.

A case study will be conducted with the developed model to gauge the performance of the radiative cooling system in a practical setup. The system size and operating conditions will be examined to draw a conclusion on the feasibility of the system.

The study will end off with a conclusion about the performance and the feasibility of radiative cooling system as a heat sink regulator.

2. LITERATURE SURVEY

2.1. RADIATIVE COOLING SYSTEMS

The idea behind radiative cooling systems is to have a system that is able to dissipate heat from a thermal storage medium when conditions are favourable and then storing the chilled medium. Two key components of the system are therefore a storage medium and a surface for radiative heat dissipation. The surface is exposed to the colder night sky to radiate thermal energy from the hot surface to the night sky.

Two setups that have been proven successful for radiative cooling are roof ponds or closed systems.

Roof ponds are simple systems for storing and rejecting thermal energy. A roof pond can integrate the roof, ceiling and cooling system of a building all in one system [13]. The setup consists of a body of water that is stored on a building roof that can be exposed to the sky during the day or night to allow heating or cooling of the water. An insulating system above the roof pond is needed for control when the roof pond is exposed to the sky. For heating purposes the roof pond is exposed during the day for heating. It is closed or insulated during the night to prevent heat loss. The opposite is done during the night for cooling. It is exposed at night to reject heat from the water and is closed and insulated during the day to prevent heat gains. The heated or cooled water that is stored can then be used for whatever purpose at any time.

A disadvantage of roof pond systems is the complication of installing such a system in a building. The roof structure has to be able to support the substantial weight of the storage pond. Another aspect that adds to the complexity is the covering over the body of water. A shutter or louver system is required that can open and close as needed to insulate the body of water from the outside conditions.

A more practical and less complicated system is the closed system. This type of system configuration consists of a flat panel that is exposed to the night sky which is connected to a well-insulated storage tank. A heat transfer fluid is circulated through the panel at night to dissipate heat. These systems are based on solar water heating systems and have a similar setup with regards to equipment albeit with some minor modifications.

Radiative cooling systems with flat-plate radiator panels were investigated by Al-Nimr et al. [14], Dobson [15] and Ito & Muira [16]. These studies analysed the performance of radiative cooling systems on an experimental basis. The studies done by Dobson and Ito & Muira achieved cooling rates of between 40 and 80 W/m² depending on the environmental conditions.

The study conducted by Ito & Muira analysed the influence of the flow rate on the temperature of the storage tank. The results indicated that low flow rates bring about the same reduction of temperature in the storage tank as high flow rates. This effect was also

observed in the study done by Al-Nimr et al. These two cases suggest that a natural circulation system should achieve sufficient cooling rates in spite of the very low flow rates.

A drawback with all types of radiative cooling systems is the influence of weather conditions on the performance. The study done by Ito & Muira found that radiative cooling systems are best suited for climates where cold clear, dark (moonless) nights with a low humidity are predominant. This limits the application of radiative cooling systems to some extent.

It was apparent from the previous studies on radiative cooling systems that it can indeed be applied as a successful method of cooling.

2.2. RADIATOR PANELS

A radiative cooling system consists of a radiative panel and a storage tank as described in the previous chapter. The panel is a very important part of the system and its design can have a significant effect on the system performance.

The design of a radiative cooling system panel is very similar to that of a flat-plate solar water heating system. The flat-plate solar collector is in essence a very simple and robust piece of equipment. A lot of research and development has also been carried out over many years to analyse and improve the performance of these collectors. This vast source of information fits this study very well due to the similarities between solar collectors and radiative panels.

The characteristics of flat-plate solar water heaters are described by Duffie & Beckman [8] and Jansen [9]. The basic design consists of an upper and lower manifold tube connected by a number of smaller vertical tubes. A metal sheet is usually attached to the vertical tubes to act as a fin for increasing the heat transfer area. Flat-plate solar water heaters are boxed and insulated with a transparent glass cover over the exposed surface. This is to minimise any convective heat transfer losses to the air in contact with the collector. The exposed surface is coated with high emissivity black paint to minimise the reflectance of the surface and ensure maximum absorption of solar energy.

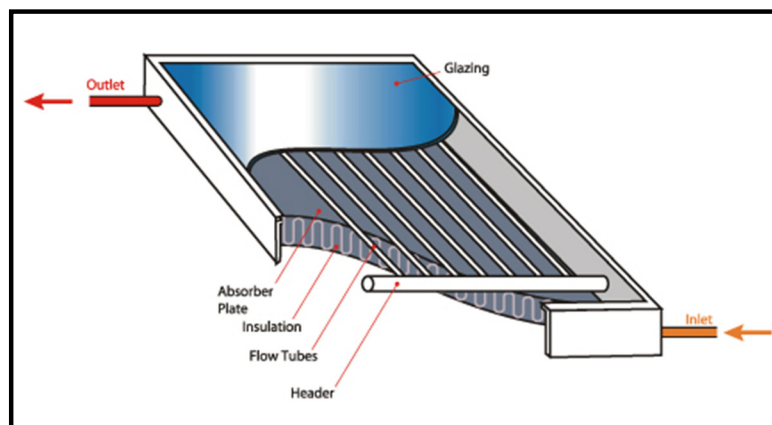


Figure 5 : Basic flat-plate solar water heater panel

The basic flat plate solar collector as described is also able to radiate heat from its surface rather than absorbing it. One element of the design that is not necessary for the radiation of heat is the glazing. The glass cover can be removed altogether to utilise the convection heat transfer component as well.

The performance of flat-plate solar collectors used for radiation cooling has been investigated by Erell & Etzion [17]. This study analysed the parameters that affects the performance of a radiative cooling panel. Erell & Etzion also found that there are a number of small but significant differences between a panel used for radiative cooling and flat-plate solar heating. Important parameters of a radiative cooling panel are the following

- Spacing between pipes. This should be kept to a minimum or eliminated altogether according to Erell & Etzion.
- Turbulent flow. This improves heat transfer but will add to pipe network losses.
- Length of the radiator panel. This parameter determines the amount of time that the fluid spends inside the panel.
- Mass flow rate. A high flow rate will reduce the temperature difference between the panel in- and outlet. This will give a higher mean surface temperature which will increase the heat transfer rate. A practical limit is one that takes into consideration the heat transfer conditions of the panel as well as power required for pumping.

Erell & Etzion concluded that if the radiator panel mean temperature is higher than the ambient air temperature, the fin efficiency increases and consequently the panel efficiency. This is due to an increase in convective heat transfer and a larger exposed surface for thermal radiation. On the other hand, the fin efficiency decreases if the ambient temperature is higher than the mean plate temperature. This causes a heat transfer from the ambient air to the panel, reducing the net heat transfer. Radiative heat transfer is still favoured by the increased surface but the convective heat transfer counteracts this. The design of a radiative cooling panel thus depends on the environmental conditions in which it will operate.

Another study conducted by Meir et al [18] investigated the performance of polymer-based radiator panels as a low cost alternative to metal panels. This study concluded that a polymer-based radiative cooling system can also achieve sufficient cooling under moderate climate conditions. An advantage of the polymer-based radiative cooling system over other conventional panels is the lower investment costs. A disadvantage is less efficient performance if compared to panels constructed from metals.

Harrison & Walton [19] investigated the effect of white painted surfaces on radiation cooling. The study focused on commercially available white paints containing titanium oxides (TiO_2). A white painted surface should in theory have the same radiative cooling performance as a black painted surface. This is because the white surfaces have the same spectral emissivity as a black surface. A white painted surface has an advantage during the day over a black painted surface. It is less susceptible to direct sunlight that can cause unwanted heat gains in the panel.

In practice the radiator panel can be integrated as part of a building roof structure. A study by Dimoudi & Androutsopoulos [20] investigated a prototype panel that consisted of a pipe network laid out on a flat concrete roof building. A steel plate was then fixed to the pipe network. The study also made use of a white painted panel surface as suggested by

Harrison & Walton [19]. Dimoudi & Androutsopoulos found that their system is able to contribute positively to the cooling requirements of a building. The study also found that the water flow rate can significantly influence the performance of a radiative cooling system. Good cooling power can be achieved by maintaining the panel temperature above the ambient dry bulb temperature by altering the flow rate of the water. This temperature difference creates an energy transfer between the ambient air and the panel as well.

2.3. NATURAL CIRCULATION LOOPS (THERMOSYPHON)

The radiative cooling systems in the referred studies have all been operated by a forced convection method. Circulation of the fluid through the panels has been achieved by a small pump. The aim of this study is to abolish the pump and use natural circulation.

Natural circulation or a thermosyphon as it is otherwise known works on the principle of density differences of a fluid inside a closed system or loop. A hot fluid is less dense than a cold fluid. A hot fluid will therefore tend to accumulate at the top of a system and more dense cold fluid will accumulate at the bottom. The concept of natural circulation has been applied successfully in solar water heaters for many years. As the fluid is heated in the panel it rises to the top towards the storage tank. The colder water in the bottom of the storage tank descends to the bottom of the system towards the inlet of the panel.

A comprehensive method for estimating the performance of natural circulation solar water heater systems was done by Close [21]. Close developed a mathematical model to predict the flow rate of a natural circulation loop for given input parameters. The accuracy of the model was verified by Close with experimental setups. The theoretical model provided a close enough estimation of the storage tank temperatures and system performance according to Close. The model proposed by Close is a very simple method and has been used in several solar water heater studies since.

This model provides a base upon which further natural circulating system studies can be done. Natural circulation is an integral part of the radiative cooling system for this study. The model by Close was initially developed for solar water heating systems but it can be altered for radiative cooling systems.

2.4. NIGHT SKY RADIATION

Thermal radiation can be described as the energy that is emitted from a surface with a nonzero temperature to a surface with a lower temperature [22]. The energy is transferred by electromagnetic waves and does not require a medium through which the energy is transferred. Thermal radiation will therefore be most effective in a vacuum.

The rate at which thermal radiation takes place per unit area is termed the emissive power (E) of the surface and is measured in W/m^2 . The emissive power of a surface is described by the Stefan-Boltzmann law:

$$E_b = \sigma T_s^4 \quad (1)$$

T_s is the absolute temperature of the surface in Kelvin and σ is the Stefan-Boltzmann constant equal to $5.67 \times 10^{-8} \text{ W/m}^2\text{-K}^4$. This equation describes an ideal emitter, in other words no loss of energy occurs during the heat transfer process. This ideal emitter is also called a blackbody.

It is however not possible to achieve ideal radiation from a real surface. The efficiency of a real surface's radiation heat transfer is termed the emissivity (ϵ). This property depends on the material and its surface finish and colour. The emissive power of a real surface is given by the following equation:

$$E_b = \epsilon \sigma T_s^4 \quad (2)$$

The net radiation heat transfer between two ideal surfaces can be calculated with the following equation [8], [22]:

$$q = \sigma A(T_1^4 - T_2^4) \quad (3)$$

with σ the Stefan-Boltzmann constant, A the area of the surface in m^2 and T the temperatures in Kelvin. This formula also describes the radiation between two ideal surfaces. The radiation between two real surfaces is again influenced by the emissivity of the surfaces and also their orientation towards each other.

The radiation heat transfer of a radiative cooling system will be between the panel surface and the night sky. The panel is considered to be the hotter surface and the night sky the colder surface.

Night sky radiation or nocturnal radiation is the transfer of heat from a hot surface to the cooler night sky. In this case the panel and the night sky. The problem faced with night sky radiation is how to determine the temperature of the night sky, also called the effective sky temperature. Extensive studies have been done to provide a method for determining this effective sky temperature.

One method of determining this night sky temperature is proposed by Duffie & Beckman [8] and another method is described by Pérez-García [23]. The models are both mathematical methods to estimate the effective night sky temperature. The models by Duffie & Beckman and Pérez-García both provide a night sky temperature value that can be substituted in equation (3).

2.5. NATURAL AND FORCED CONVECTIVE HEAT TRANSFER

The heat transfer from an unglazed radiator panel also has a convective heat transfer component. The convective heat transfer takes place between the panel surface and the air in contact with the panel. Two types of convective heat transfer are considered namely natural and forced convective heat transfer.

Forced convection heat transfer is the heat transfer between a surface and a moving fluid [22], [7]. The motion of the fluid is brought on by external forces acting on it. Wind blowing over the radiator surface is a form of forced convection in the case of a radiative cooling panel. The heat transfer depends on the boundary layer caused by the flow of the air over a surface.

With natural or free convection the fluid motion is caused by buoyancy forces present in the fluid that is in contact with a hot or a cold surface. This buoyancy forces are the effect of a density difference and a body force that is proportional to the density present in the fluid [22]. The effect of natural convection heat transfer is usually neglected but since the overall heat transfer of a radiative cooling system is small it could have a noticeable effect.

Natural convection heat transfer from the radiative panel will occur during windless conditions while forced convection will occur during windy conditions. Since the natural convection heat transfer is significantly smaller than forced convection heat transfer it provides a worst case scenario if it is assumed that windless conditions are prevalent.

2.6. THERMAL ENERGY STORAGE

The idea of radiative cooling systems is to dissipate heat energy during the night and use the cooled fluid during the day. This implies that the cold energy has to be stored in some way.

According to Dincer & Rosen [24] there are two ways of storing thermal energy. The thermal energy can be stored by increasing or decreasing the temperature of a substance in the form of sensible heat, or by changing the phase of a substance in the form of latent heat. The two ways can also be used in combination. Thermal energy storage (TES) is therefore used to temporarily store high or low temperature energy for later use.

The problem with energy sources such a solar energy, or radiative cooling in this case is that the supply and demand of energy usually does not coincide. Radiative cooling is available only at night but demand for cold water may be during the day time when cooling is not possible. Thermal energy storage makes it possible to store the energy during the time of supply when no demand is present.

Commonly used substances used for thermal energy storage include oil, water and rock. These energy storage mediums are inexpensive and readily available. As mentioned before the energy is stored in the form of sensible heat. A drawback of this type of energy storage

is the large volume required for a certain amount of energy storage due to the low specific heat capacity of these storage mediums.

Another less common but very promising thermal energy storage method is phase change materials (PCM). These materials are able to store energy in the form of latent heat when a substance undergoes a phase change. The thermal energy is stored or released when the substance changes from one phase to another. A practical form of latent heat storage is ice. An advantage of phase change materials is that it requires considerably less volume compared to sensible heat storage.

Phase change materials still require research and development in material and system design in order for it to be used effectively. Water as a storage medium on the other hand has been used for ages and its behaviour and properties are well understood.

Dinçer & Rosen provides a comprehensive guide to thermal energy storage materials and system design. A few basic principles according to them for an effective water thermal storage system are the following:

1. The tank should be stratified and the mixing of stratification layers should be minimised during charging and discharging.
2. Dead zones in the storage volume should be minimised.
3. The heat losses and gains from the tank should be minimised.

A study done by Hasnain [25] describes three possible thermal storage systems for cool storage in particular. The three most important and effective mediums are chilled water, ice and eutectic salts. Each of these systems has its advantages and disadvantages in terms of temperature range, storage capacity per volume and system cost.

Chilled water storage is by far the most used due to its simplicity and low cost. Water has a very good thermal storage capacity compared to any other commonly used fluids. A disadvantage of chilled water storage is the required system volume. The required size can become unfeasibly large depending on the demand that is designed for. Water storage systems are therefore limited to certain applications.

Ice storage is the other possibility but it is more complex and high system costs rules it out in most cases. Ice is used as a phase change storage medium and has a much higher heat storage capacity per volume compared to water which makes it more practical in large storage capacity systems.

Another drawback of ice storage that has to be considered is the operating temperature. The operating temperature is limited to be in the range of freezing temperature of water which is around zero degrees Celsius. Ice storage also has the tendency to accumulate on the cooling surface and have to be removed continuously to maintain proper performance. The layer of ice acts as a heat transfer barrier and reduces the cooling coil performance considerably.

The third and most recent advance in thermal storage is eutectic salts. Like ice storage the storage capacity of these salts depends on the latent heat required during phase changes. Eutectic salts also do not expand and contract significantly during freezing and melting which makes it useful in larger storage capacity systems. Unlike ice it is possible to create eutectic

salts for a wide range of temperatures. Eutectic salts certainly have a number of advantages over other storage mediums but more research and development is still required to provide a practical solution.

Thermal storage is a key part of any radiative cooling system. The literature pointed out the importance of storage mediums for different applications and also the related system design for optimal performance.

2.7. RADIATIVE COOLING SYSTEM CONFIGURATION

An important characteristic of a radiative cooling system with natural circulation is the position of the storage tank and panel relative to each other. For natural circulation to take place with radiative cooling the storage tank should be positioned below the panel.

This is the exact opposite of what is required for solar water heaters with natural circulation where the storage tank has to be positioned above the panel [26].

The purpose of this is to allow the cooled, denser fluid from the panel to accumulate at the bottom of the system. At the same time the warmer, less dense fluid inside the storage tank will accumulate at the top of the system. In order for radiative cooling with natural circulation to take place the outlet of the storage tank should therefore be positioned at the top of the tank and the inlet at the bottom and otherwise for the panel.

A previous study by Theunissen & Brink [27] tested such a system configuration. It was concluded from the study that radiative cooling with natural circulation is indeed possible by using the abovementioned system configuration.

The relative position of inlets and outlets, flow direction and accumulation of hot and cold fluid for a radiative cooling system is illustrated in Figure 6.

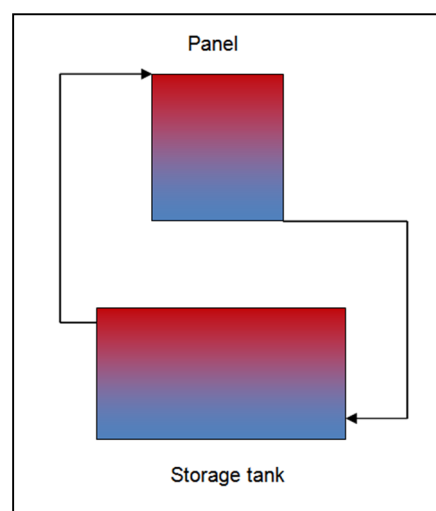


Figure 6 : Radiative cooling system

The panels should preferably be left unglazed to make use of the convective heat transfer component as well. A louver system can also be used to shade the panel from unwanted solar or other thermal radiation.

The storage tank and connecting pipes should be well insulated to minimise unwanted heat gains. The very low flow rate and temperature differences of a natural circulating loop can be influenced easily by unwanted heat gains thus reducing the performance significantly.

The previous study by Theunissen & Brink pointed out the importance of a good system configuration and will certainly be taken into consideration with this study.

3. THEORETICAL MODEL ANALYSIS

3.1. INTRODUCTION

The main purpose of the theoretical model is to predict and analyse the performance of a radiative cooling system. A complete understanding of the theories governing radiative cooling systems are needed in order to develop the model.

The main aspects that will be analysed and modelled are the following:

- Thermosyphon flow rate
- System heat loss/ gain
- Operating conditions.

The various system parameters required to model the system are described in the following paragraphs.

3.2. RADIATOR PANELS

The radiator panels used in this study consisted of vertically inclined parallel tubes in a top-down arrangement, connected to horizontal inlet and outlet manifolds at the top and bottom.

The design and analysis of radiator panels can be an elaborate study on its own in terms of tube spacing, tube diameter, fluid flow dynamics and so forth. For this reason the radiative panel in this study was considered as a control volume with inputs and outputs for flow, temperature and energy transfer. It was therefore not necessary to study the panel design in detail.

Many studies have been done in the past on the detail design and analysis of flat-plate solar water heater collectors [8], [9], [28]. The findings of these studies were applied to this study because of the many design similarities between flat-plate solar collectors and radiative cooling panels.

One aspect of the panels that had to be considered in more detail was the fluid flow head losses. The panel has a pressure drop in the manifolds and down tubes. This pressure drop had to be considered in the theoretical model because of its influence on the flow rate.

The panel head loss was included in the pipe network head losses and is explained in the next paragraph.

3.3. PIPE NETWORK HEAD LOSSES

The pipe network of the system consists of the connecting pipes between the radiator panel and storage tank and the panel manifolds and downpipes.

The head losses of the pipe network are required to determine the mass flow rate of the system. The method for calculating the mass flow rate is explained in chapter 3.7. In short the thermosyphon head is set equal to the friction loss head of the pipe network.

To calculate the head losses due to friction caused by surface roughness and pipe network components the Darcy-Weisbach [29] equation was used as a base. A shortcoming of this method is that it is not ideally suited for flow with very low Reynolds numbers. The Darcy-Weisbach equation is suited for steady state developed flow conditions. With the low flow rates of thermosyphon flow it is uncertain whether the flow is laminar or turbulent and fully developed or not.

A method used by Zerrouki et al. [30] for calculating the flow of a natural circulating solar water heater was based on the Darcy-Weisbach equation and provided reasonable accuracy for predicting the system head losses. This method was applied to the theoretical model to calculate the system head losses.

The method as by Zerrouki is as follows:

The total head losses of the system are split up into the head loss of the connecting pipes between the panel and storage tank and the head loss of the panel itself.

$$h_f = h_{cp} + h_p \quad (4)$$

According to Zerrouki the head losses of the panel are proportional to the head losses of the connecting pipes. This ratio of the head losses is given by:

$$\Phi = \frac{h_{cp}}{h_p} \quad (5)$$

Substituting this into equation (4) gives:

$$h_f = h_p(1 + \Phi) \quad (6)$$

This equation now represents the total head loss of the connecting pipes and panel. The head loss of the panel can now be substituted by the appropriate head loss equation.

The head loss for the collector pipes from the Darcy-Weisbach equation is given as:

$$h_p = \frac{\rho f V_p^2 L_p}{2 D_p} \quad (7)$$

with the friction factor, f , calculated by:

$$f = \frac{64\nu}{D_p V_p} \quad (8)$$

Substituting equation (8) into equation (7) gives:

$$h_p = \frac{32\rho V_p L_p \nu}{D_p^2} \quad (9)$$

The same theory used to obtain the head loss of the panel can be applied to obtain the head loss equation for the connecting pipes. This gives:

$$h_{cp} = \frac{32\rho V_{cp} L_{cp} \nu}{D_{cp}^2} \quad (10)$$

For N number of tubes in the panel, the continuity of flow for the fluid applies:

$$\rho V_p N A_p = \rho V_{cp} A_{cp} \quad (11)$$

The area was replaced by the circular area formula:

$$A = \frac{\pi}{4} D^2 \quad (12)$$

Equation (11) together with the head losses of the panel and connecting pipes of equation (9) and (10) was substituted into the ratio ϕ in equation (5) giving:

$$\phi = N \left(\frac{L_{cp}}{L_p} \right) \left(\frac{D_p}{D_{cp}} \right)^4 \quad (13)$$

Substituting equation (13) and (9) into equation (6) now gives:

$$h_f = \left(\frac{32\rho V_p L_p v}{D_p^2} \right) \left(1 + N \left(\frac{L_{cp}}{L_p} \right) \left(\frac{D_p}{D_{cp}} \right)^4 \right) \quad (14)$$

The velocity of the fluid can be substituted by:

$$V_p = \frac{\dot{m}}{\rho N A_p} \quad (15)$$

Equation (14) now becomes:

$$h_f = \left(\frac{128\dot{m} L_p v}{\pi N D_p^4} \right) \left(1 + N \left(\frac{L_{cp}}{L_p} \right) \left(\frac{D_p}{D_{cp}} \right)^4 \right) \quad (16)$$

With this equation it is possible to determine the mass flow rate of the thermosyphon by equating the thermosyphon head to the head loss of the pipe network from equation (16).

3.4. STORAGE TANK HEAT FLUX

The storage tank is examined as an individual control volume to determine the factors that have an influence on its performance.

Factors that certainly have an influence on the performance of the storage tank are unwanted heat gains or losses.

The storage tank heat gain or loss is due to the transfer of heat from the hotter surroundings to the much colder stored fluid. The heat transfer energy is accounted for in the theoretical model since it will influence the temperature of the stored fluid and subsequently the radiative cooling system's performance.

The heat is mainly transferred by conductive and convective heat transfer [22]. The thermal resistance of the storage tank is made up out of the conductive resistance of the insulating material and the convective resistance of the air surrounding the tank.

The storage tank had two layers of insulation material and the convective boundary layer of the air. The storage tank is a thin wall steel vessel and its resistance was considered negligible in this case. The surface temperature of the steel wall is considered equal to the mean storage tank temperature. The equivalent thermal resistance circuit of the heat transfer from the storage tank to the surroundings is shown in Figure 7.

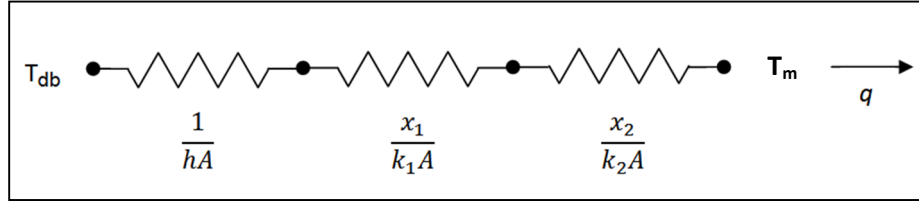


Figure 7 : Storage tank thermal resistance

The total thermal resistance of the storage tank is given as:

$$R = \sum R_t = \frac{1}{h_t A_1} + \frac{x_1}{k_1 A_1} + \frac{x_2}{k_2 A_2} \quad (17)$$

The values of k_1 , k_2 , x_1 , x_2 are constants and depends on the thermal properties of the insulation material. The value of h_2 was assumed constant and can be obtained from predetermined values of boundary layer convection coefficients for tanks.

The overall heat loss from the fluid inside the storage tank to the surrounding air is now calculated as follows:

$$Q_{tank} = \frac{(T_{db} - T_m)}{R} \quad (18)$$

This heat transfer energy was used later on in paragraph 3.7 to determine the mean storage tank temperature.

3.5. EFFECTIVE SKY TEMPERATURE

The radiation heat transfer from the panel to the colder night sky requires a temperature difference between the panel and the night sky. The problem is that the night sky temperature, to which the panel radiates, is difficult to measure directly. This problem was overcome by using a method described by Pérez-García [23] to relate the effective sky temperature to the ambient dry bulb temperature.

The method used by Pérez-García is as follows:

The effective sky temperature T_{sky} is given by the following equation:

$$T_{sky} = (\epsilon_{sky})^{0.25} T_{db} \quad (19)$$

It is important to note that T_{db} must be in Kelvin. The variable ϵ_{sky} is the equivalent sky emissivity. The equivalent sky emissivity is determined by two equations for day and night conditions respectively. Both of these equations are a function of the dew point temperature

T_{dp} . The two equations are used separately to determine the equivalent sky emissivity for clear day or night conditions.

The equation for day time is:

$$\varepsilon_{sky} = 0.727 + 0.60 \left(\frac{T_{dp}}{100} \right) \quad (20)$$

and the night time equation is:

$$\varepsilon_{sky} = 0.741 + 0.62 \left(\frac{T_{dp}}{100} \right) \quad (21)$$

It is important that T_{dp} is in degrees Celsius [$^{\circ}\text{C}$] for equation (20) and (21). Only equation (21) was in this study used since the radiative cooling system will normally operate during the night.

The equivalent sky emissivity can be substituted into equation (19) to calculate the effective sky temperature for the radiative heat transfer.

The model described by Pérez-García was also compared for consistency with two other models suggested by Duffie and Beckman [8], [26]. For reference, model 1 was the method described above by Pérez-García. Model 2 and 3 were the two methods described by Duffie & Beckman. Model 3 is a method described in the first edition of Duffie & Beckman [8] while the other method was found in the second edition of Duffie & Beckman [26].

Model 2 calculates the effective sky temperature as follows:

$$T_{sky} = T_{db} \left[0.711 + 0.0056T_{dp} + 0.000073T_{dp}^2 + 0.013 \cos(15t) \right]^{0.25} \quad (22)$$

with T_{sky} and T_{db} in Kelvin and the dew point temperature T_{dp} in degrees Celsius and t the number of hours after midnight.

Model 3 is the other method described by Duffie & Beckman [8] and calculates the effective sky temperature as follows:

$$T_{sky} = 0.0552 \cdot T_{db}^{1.5} \quad (23)$$

with T_{sky} and T_{db} again in Kelvin.

All three of the models were calculated at a relative humidity of 50% at different dry bulb temperatures at midnight. The results of the three different models are shown in Figure 8. From the results it was apparent that there is not much difference between the three models. It was concluded that any one of the three methods can be used with reasonable accuracy.

For the case of this study the method of Pérez-García is used since the dry bulb temperatures are known and it is not dependant on time as the case is with model 2.

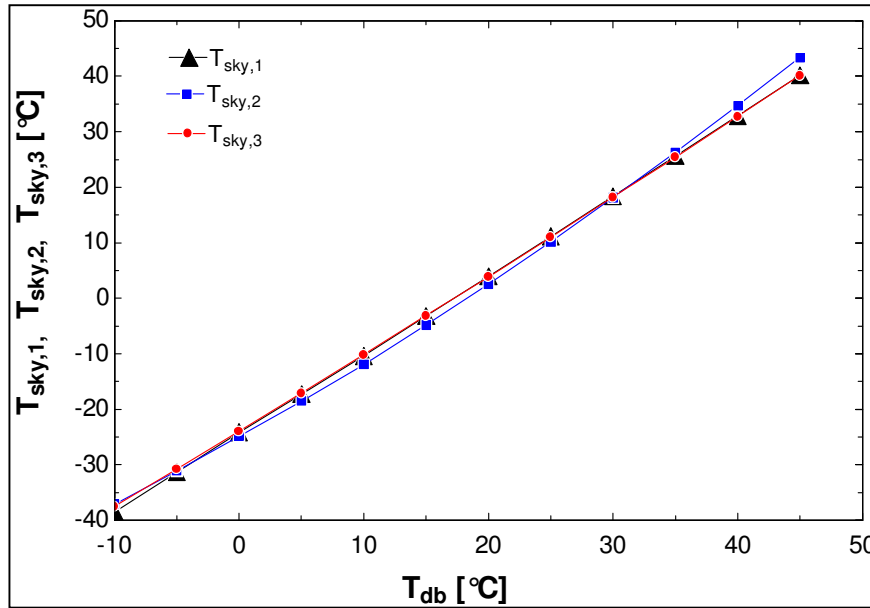


Figure 8 : T_{sky} model comparison

The effective sky temperature was used in the next chapter to calculate the thermal radiative heat transfer from the panel surface to the night sky.

3.6. PANEL HEAT TRANSFER

The heat transfer from the radiator panel consists of two parts namely the thermal radiation and convective heat transfer. Heat transfer only takes place from the upper surface of the panel exposed to the night sky. The underside of the panel is considered to be well insulated.

These two means of heat transfer from the panel surface are discussed in the following paragraphs.

3.6.1. Radiation Heat Transfer

The most important means of heat transfer of the systems is the thermal radiation from the panel to the colder night sky. The study by Close [21] suggests that the mean temperature of the panel is assumed equal to the mean storage tank temperature T_m . This assumption

was verified with experimental data by Close. The experimental data from a previous study by Theunissen et al [27], on a radiative cooling system also confirmed this assumption.

The thermal radiation heat transfer [22] between the panel surface, with temperature T_m and the effective night sky with temperature T_{sky} is:

$$Q_{rad} = \varepsilon \sigma A (T_{sky}^4 - T_m^4) \quad (24)$$

with T_{sky} and T_m in Kelvin.

The emissivity ε depends on the radiative properties of the panel's surface. For the case of the radiative system examined in this study the emissivity was based on a matt black painted metal surface.

Dust and contamination on the panel surface can have an effect on the emissive properties of the surface and will affect the efficiency of the panel. For this study it was assumed that the panel is free of dust or other contamination.

The term σ is the Stefan-Boltzmann constant for radiation.

$$\sigma = 5.67051 * 10^{-8} [W/m^2 K^4]$$

The area, A , of the exposed surface has a considerable effect on the performance of a radiative panel. The radiative heat loss is directly proportional to the exposed area. There are however practical considerations that limits the size of the panels.

The equation for thermal radiation was used to incorporate the surface emissivity and panel size on the performance of a radiative cooling system.

3.6.2. Convective Heat Transfer

Heat transfer from the panel surface also occurs in the form of convective heat transfer, especially with an unglazed radiative panel. Convective heat transfer consists of two types namely free and forced convection. Free convection is due to buoyancy forces of air in contact with a hot or cold surface thus creating flow currents. Forced convection heat transfer is caused by forced flow conditions, in this case wind conditions over the panel.

For this study it was assumed that only free convective heat transfer is present. Free convection normally results in lower heat transfer rates opposed to forced convection. The assumption made will therefore give results for a worst-case scenario during a windless night.

The panel surface temperature was again assumed equal to the mean storage tank temperature as mentioned in the previous section. The convective heat transfer from the panel surface to the surrounding air is calculated by:

$$Q_{conv} = hA(T_{db} - T_m) \quad (25)$$

The variable h is the convection heat transfer coefficient. The value of h depends on the boundary layer conditions caused by the flow of a gas or fluid over a surface. For free convection the flow is caused by buoyancy forces as the air is heated or cooled and a density difference develop.

The calculation of the free convection heat transfer coefficient is a complex procedure and different cases exist for various geometric shapes, tilted surfaces etc. The procedure used in this study for calculating the free convection heat transfer coefficient is described in detail in Incropera et al. [22].

The first step of the procedure to calculate h is to determine the Rayleigh number. The equation for calculating the Rayleigh number is:

$$Ra = \frac{g\beta(T_m - T_{ab})(L_c)^3}{\nu\alpha} \quad (26)$$

with

$$\beta = \frac{1}{T_f} \quad (27)$$

For an inclined surface the gravitation acceleration constant g is replaced by $g \cdot \cos\phi$ with ϕ the angle of the inclined surface to the horizontal.

The variable T_f is the film temperature of the air in contact with the panel surface and is calculated as follows:

$$T_f = \frac{T_m + T_{ab}}{2} \quad (28)$$

The surface temperature of the panel was again assumed equal to the mean storage tank temperature according to Close [21].

The next step was to obtain the properties of the particular fluid, in this case air, for use in equation (26).

The properties of air (ν , α and k) was found in tables [22] at certain temperatures. A problem with the data from the tables was the very large temperature intervals. This would have led to imprecise calculations in the theoretical model.

To overcome this problem the values found in the tables were used to do a curve fit to be able to determine the properties at any given temperature.

Figure 9 to Figure 11 indicates the plots obtained from the data tables and their respective linear equations. All of the properties follow a near linear relation and a straight line equation was assumed for all of the curve fits.

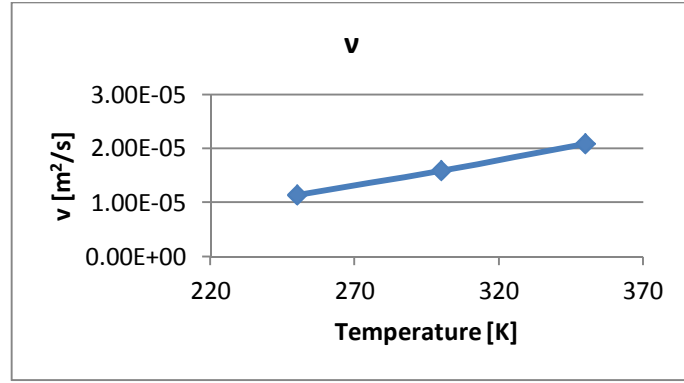


Figure 9 : Kinematic viscosity of air

$$\nu = 1.35159 * 10^{-5} + 9.5 * 10^{-8} \left(\frac{T_{db} + T_m}{2} \right) \quad (29)$$

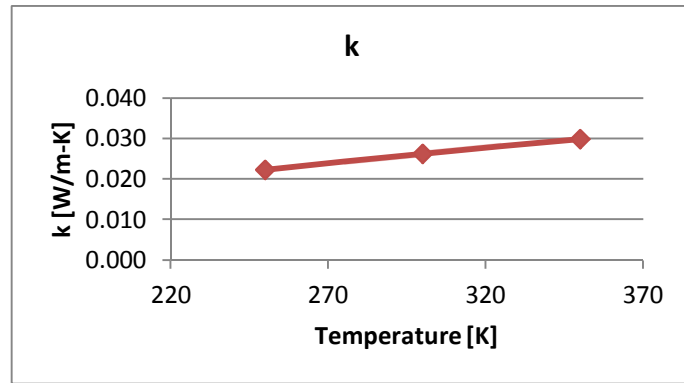


Figure 10 : Thermal conductivity of air

$$k = 0.0241 + 7.7 * 10^{-5} \left(\frac{T_{db} + T_m}{2} \right) \quad (30)$$

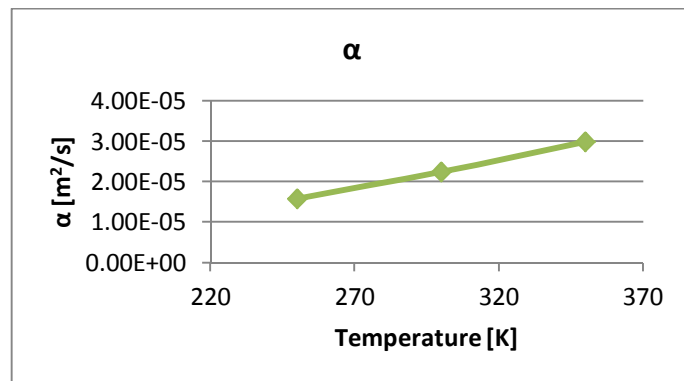


Figure 11 : Thermal diffusivity of air

$$\alpha = 1.90077 * 10^{-5} + 1.4 * 10^{-7} \left(\frac{T_{db} + T_m}{2} \right) \quad (31)$$

The next step of the convective heat transfer calculations required calculating the Nusselt number. The Rayleigh number and properties of air that was obtained in the previous steps were used to determine the Nusselt number.

The recommended method by Incropera et al. [22] for calculating the Nusselt number for the upper surface of a hot surface is as follows:

$$Nu = 0.54 \cdot Ra^{\frac{1}{4}} \text{ for } (10^4 \leq Ra \leq 10^7) \quad (32)$$

$$Nu = 0.15 \cdot Ra^{\frac{1}{3}} \text{ for } (10^7 \leq Ra \leq 10^{11}) \quad (33)$$

With the Nusselt number now known it is possible to calculate the free convection coefficient with the following equation.

$$h = Nu \cdot \frac{k}{L_c} \quad (34)$$

With L_c the characteristic length of the panel defined as:

$$L_c \equiv \frac{A}{2(L + B)} \quad (35)$$

The free convection coefficient h was now used to calculate the convective heat transfer from the panel surface in equation (25).

The convective heat transfer from the panel can cause a heat gain or loss from the panel if the dry bulb temperature is higher or lower than the panel surface temperature. This heat gain or loss was added to the radiative heat loss to give a net heat transfer from the panel.

3.7. MEAN STORAGE TANK TEMPERATURE

A method was developed by Close [21] to estimate the performance of natural circulating solar water heaters. This method has been used since in many other studies for simulating natural circulating solar water heaters. The model by Close has been altered to use radiative cooling from the panel instead of solar heat gain for this study.

The model as developed by Close and with the alterations is as follows:

The starting point of the method is the energy balances over the panel and radiative panel. By examining the storage tank and radiator panel separately the instantaneous energy balances of both the storage tank and panel were obtained.

Energy balance over the radiator panel:

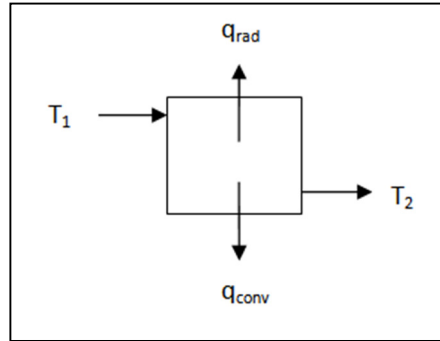


Figure 12 : Radiator panel energy balance

$$Q_{rad} + Q_{conv} + \dot{m} \cdot Cp \cdot T_2 = \dot{m} \cdot Cp \cdot T_1 \quad (36)$$

Energy balance over storage tank:

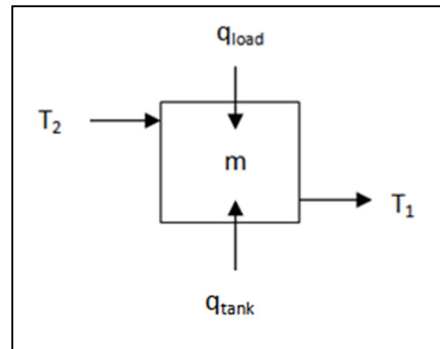


Figure 13 : Storage tank energy balance

$$Q_{tank} + Q_{load} + \dot{m} \cdot Cp \cdot T_2 = \dot{m} \cdot Cp \cdot T_1 + c \cdot \frac{dT_m}{d\theta} \quad (37)$$

By combining equation (36) and (37) the following equation was obtained:

$$c \cdot \frac{dT_m}{d\theta} = -Q_{rad} - Q_{conv} + Q_{load} + Q_{tank} \quad (38)$$

The radiation and convection heat transfer were substituted by the radiative and convective heat transfer equations described in paragraph 3.6 and given as:

$$Q_{rad} = \varepsilon \sigma A (T_{sky}^4 - T_m^4) \quad (39)$$

and

$$Q_{conv} = hA(T_{db} - T_m) \quad (40)$$

Equation (38) now becomes:

$$c \cdot \frac{dT_m}{d\theta} = \varepsilon \sigma A (T_{sky}^4 - T_m^4) + hA(T_{db} - T_m) + Q_{load} + Q_{tank} \quad (41)$$

This differential equation can now be solved for T_m at a time step θ . The differential equation was solved with the Euler-Cauchy numerical method [31]. Although this is a crude method for solving differential equations, it did provide sufficient accuracy for the model. Equation (41) solved for T_m with the Euler-Cauchy method now becomes:

$$T_{m(n+1)} = T_{m(n)} + x_{step} \cdot \left[\frac{(\varepsilon \sigma A (T_{sky}^4 - T_m^4) + hA(T_{db} - T_m) + Q_{load} + Q_{tank}) \cdot Timestep}{c} \right] \quad (42)$$

with the Euler-Cauchy step size $x_{step} = 1$.

The time step variable in equation (44) is to convert the Watts to the amount of energy in Joule transferred in the given time step. The time step was chosen according to the interval of the experimental measured temperature readings. A 15 minute interval used in this case.

The variable c is the total thermal capacity of the fluid and the storage tank material of the system and is calculated by:

$$c = m * Cp + c_{tank} \quad (43)$$

The thermal capacity of the tank material was considered negligible in this case given its small thermal capacity and mass relative to the fluid.

With equation (42) it is possible to determine the mean storage tank temperature change over a period of time at a given dry bulb and effective sky temperature.

3.8. NATURAL CIRCULATION FLOW (THERMOSYPHON)

After solving the differential equation for T_m , the thermosyphon flow rate of the system needed to be determined. The thermosyphon head had to be determined as well in order to calculate the flow rate. In the study by Close [21] the thermosyphon head is set equal to the friction head of the system in order to calculate the thermosyphon flow rate.

$$h_t = h_f \quad (44)$$

The thermosyphon head is generated by the density differences of the fluid as it is cooled or heated throughout the system.

Figure 14 indicates the system points and their respective heights that were used to determine the fluid's temperature distribution throughout the system. Figure 15 shows the theoretical temperature distribution of the fluid as it moves through the system.

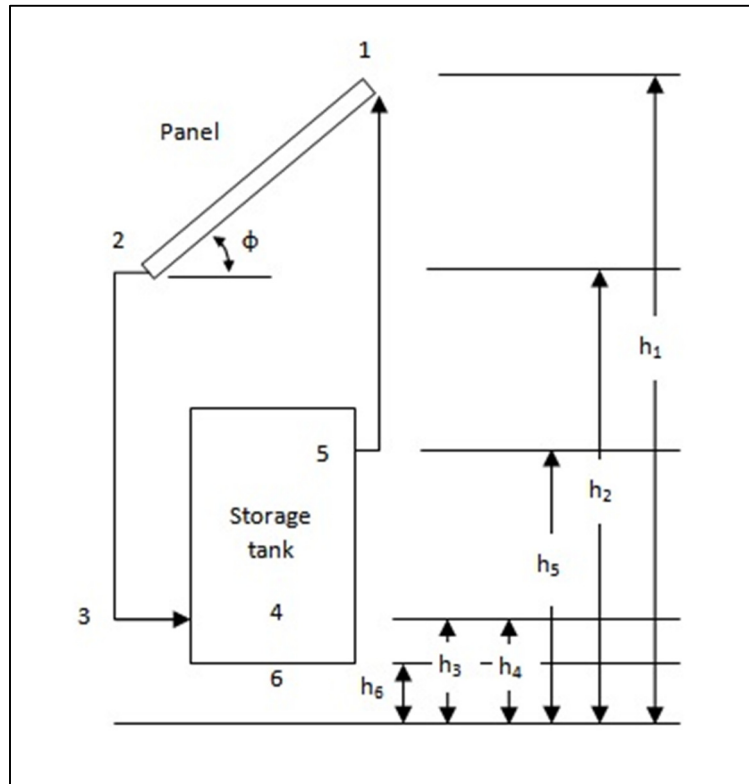


Figure 14 : Thermosyphon loop system points and heights

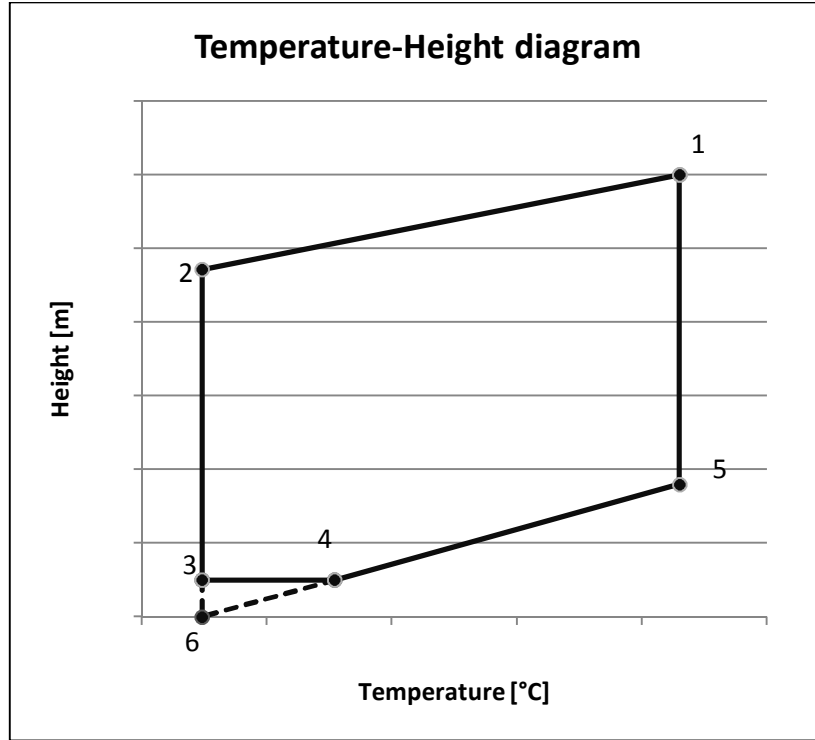


Figure 15 : System Temperature-Height diagram

The thermosyphon head h_t is represented by the enclosed area of the graph between points 1,2,3,4 and 5. Point 6 is the small volume of fluid between the storage tank inlet and the bottom of the storage tank. Due to thermal stratification the coldest fluid will accumulate beneath the inlet. This reduces the thermosyphon head to some extent and consequently the thermosyphon flow rate.

According to Close the relation between the temperature and specific gravity can be assumed linear. This implies that Figure 15 also indicates the specific gravity distribution in the system. The temperature differences $(T_1 - T_2)$ can now be substituted by the specific gravity $(S_1 - S_2)$.

The area inside the graph indicated in Figure 15 is obtained with standard area and geometry formulas and theorems. The final derived equation for the area inside the temperature-height diagram is:

$$h_t = (S_1 - S_2) \left((h_1 - h_3) - 0.5(h_1 - h_2) - 0.5 \left(\frac{(h_5 - h_3)^2}{(h_5 - h_6)} \right) \right) \quad (45)$$

A parabolic curve fit was done with the existing data to be able to find the specific gravity of the fluid for any given temperature. In the case of this study the specific gravity data for a 30% Ethylene-Glycol in water mixture was used to do the curve fit. Figure 16 shows the given specific gravity data points and the resulting curve fit.

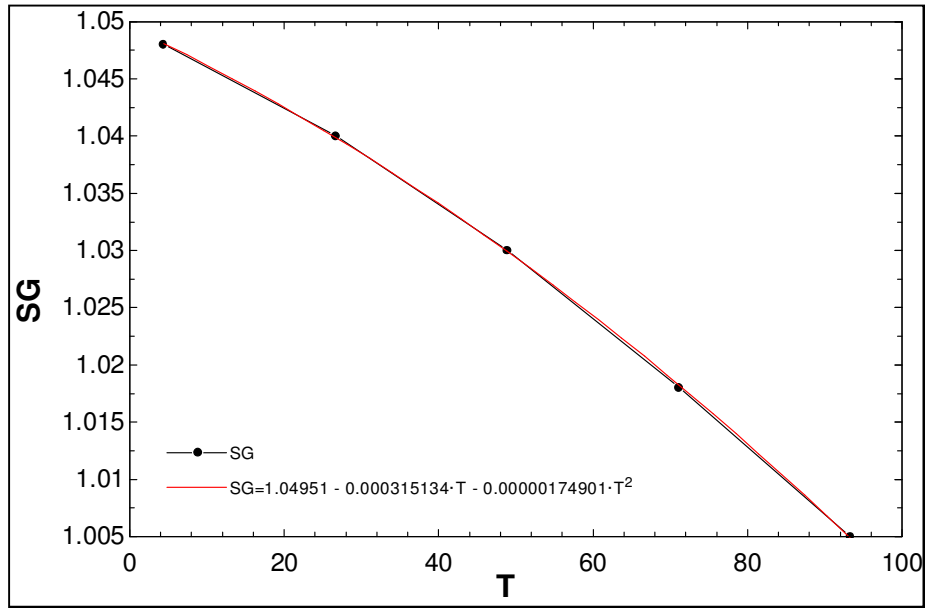


Figure 16 : 30% Ethylene-Glycol water mixture specific gravity curve fit

The curve fit equation used for calculating the specific gravity at a given temperature is:

$$S = 1.049 - 3.151 \cdot 10^{-4} \cdot T - 1.749 \cdot 10^{-6} \cdot T^2 \quad (46)$$

By substituting equation (46) into the specific gravity difference ($S_1 - S_2$) the following equation was obtained:

$$S_1 - S_2 = -1.749 \cdot 10^{-6}(T_1^2 - T_2^2) - 3.151 \cdot 10^{-4}(T_1 - T_2) \quad (47)$$

The term $(T_1^2 - T_2^2)$ can be split up into:

$$T_1^2 - T_2^2 = (T_1 + T_2)(T_1 - T_2) \quad (48)$$

with

$$T_m = \frac{T_1 + T_2}{2} \quad (49)$$

Substituting this into equation (47) gives:

$$S_1 - S_2 = -2 \cdot (1.749 \cdot 10^{-6})(T_1 - T_2) \cdot T_m - 3.151 \cdot 10^{-4}(T_1 - T_2) \quad (50)$$

The minor and major friction head losses in the system were calculated with the method described in paragraph 3.3. The thermosyphon head h_t and the friction head h_f from equation (16) and (45) was substituted into equation (44) to give:

$$(S_1 - S_2) \left((h_1 - h_3) - 0.5(h_1 - h_2) - 0.5 \left(\frac{(h_5 - h_3)^2}{(h_5 - h_6)} \right) \right) = \left(\frac{128 \dot{m} L_p \nu}{\pi N D_p^4} \right) \left(1 + N \left(\frac{L_{cp}}{L_p} \right) \left(\frac{D_p}{D_{cp}} \right)^4 \right) \quad (51)$$

The specific gravity difference $(S_1 - S_2)$ was substituted by equation (50) and $(T_1 - T_2)$ by equation (37) to give the final equation for calculating the thermosyphon mass flow rate:

$$\begin{aligned} & \left(\frac{Q_{tank} + Q_{load} - c \cdot \frac{dT_m}{d\theta}}{\dot{m} C_p} \right) (-2 \cdot 1.749 \cdot 10^{-6} \cdot T_m - 3.151 \cdot 10^{-4}) \\ & \cdot \left((h_1 - h_3) - 0.5(h_1 - h_2) - 0.5 \left(\frac{(h_5 - h_3)^2}{(h_5 - h_6)} \right) \right) \\ & = \left(\frac{128 \dot{m} L_p \nu}{\pi N D_p^4} \right) \left(1 + N \left(\frac{L_{cp}}{L_p} \right) \left(\frac{D_p}{D_{cp}} \right)^4 \right) \end{aligned} \quad (52)$$

Equation (52) was solved with T_m known to determine the mass flow rate \dot{m} of the thermosyphon loop. With the obtained mass flow rate and T_m it was also possible to calculate the panel inlet and outlet temperatures with equations (36) and (49).

3.9. AMBIENT TEMPERATURE AND CONDITIONS

The ambient temperature for use in the calculations can be approximated by a sine function. This will give a crude ambient temperature profile between day and night. A problem that was observed in experimental data was that only day time temperature follows a sine curve while the night time temperature follows a more linear function.

A curve fit was done with average ambient temperatures recorded during the test period and the actual and estimated temperatures are shown in Figure 17. The sine function overestimates the temperature at night which would give results that are not realistic and accurate when used in the theoretical model. This limits a continuous sine function to predict the ambient temperature over a 24 hour period.

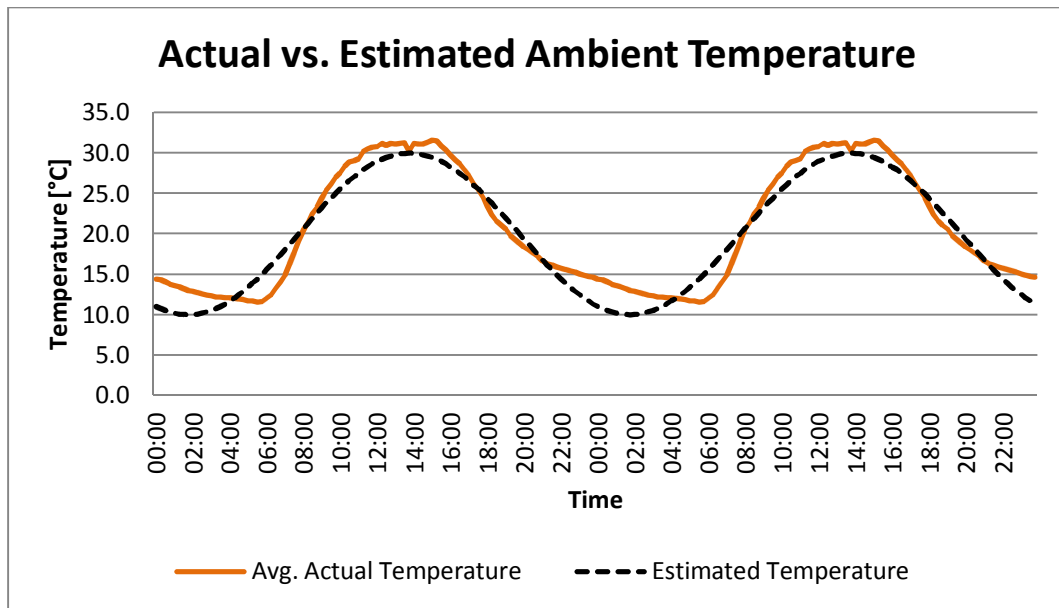


Figure 17: Actual vs. estimated ambient temperature

An estimated ambient temperature is also not able to take into account changes in weather patterns or other abnormal weather conditions. The wet bulb temperature required to determine the relative humidity is even more difficult to predict because of the various factors it is influenced by.

The difficulty to predict the ambient temperature and relative humidity accurately meant that an alternative had to be used.

Previously recorded data from the experimental setup was used instead as the ambient dry bulb and wet bulb input temperatures for the theoretical model. This also meant that the theoretical model could be compared with the experimental setup under the same environmental conditions.

4. EXPERIMENTAL MODEL

4.1. INTRODUCTION

An experimental setup was used to evaluate the results of the theoretical model. The purpose of this was to point out any differences or shortcomings between the model and an actual setup.

The design and evaluation of the test model was based on a previous study undertaken [27] to study the concept and possibilities of radiative cooling with natural circulation.

4.2. TEST MODEL DESIGN

The test model consisted of a radiative cooling system mounted on a frame that replicated a common pitched roof of a residential house onto which it is likely to be installed. The height and pitch angle of the frame was chosen to replicate this. Details and specifications of the setup are given in Table 3 and Table 4 in the next paragraph.

Two similar radiative cooling systems were used for testing side by side. Each system was made up out of a radiative panel connected to a storage tank with connecting pipes.

Both of the systems were identical except that one system was equipped with an adjustable electric heating element to simulate a heat load on the system.

The other system did not have a simulated heat load. The purpose of this system was to serve as a reference to the other system to gauge the mean storage tank and panel inlet and outlet temperatures.

For reference purposes the system equipped with the heat load was labelled System 1 (S1) and the other system labelled System 2 (S2). A layout of the system is given in Figure 18 below.

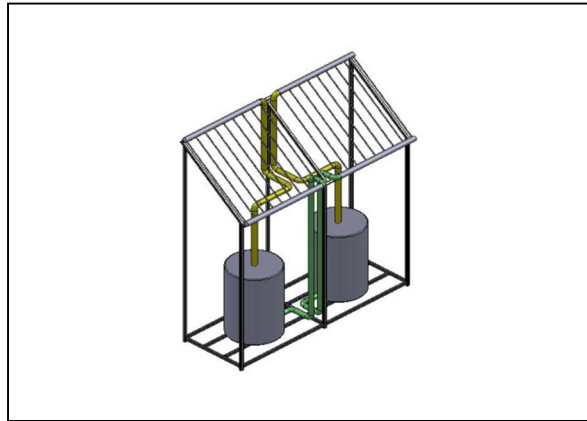


Figure 18 : Test model [27]



Figure 19 : Actual test model



Figure 20 : Actual test model panel

4.3. TEST MODEL SETUP

4.3.1. Test model dimensions and properties

The dimensions, properties and physical characteristics of the experimental setup played an important role in the performance of the system. It was also important to have these specifications as input parameters for the theoretical model when the comparison was done.

The specifications of the test model setup are as follows:

Table 3 : Test model dimensions and properties

Property	Unit	Value
Panel		
Length	[m]	1
Width	[m]	1
Number of down tubes		9
Tube spacing	[mm]	100
Tube diameter	[mm]	15
Inlet and Outlet manifold diameter	[mm]	45
Tilt angle	[°]	40
Surface emissivity, ϵ		0.7
Storage tank		
Capacity	[ℓ]	233
Height	[m]	0.88
Diameter	[m]	0.58
Connecting pipes		
Diameter	[mm]	50
Total length (Measured between inlets and outlets)	[m]	3.85
Storage tank insulation		
Layer 1		Glass fibre
Layer 2		Polyester fibre
Total thickness	[mm]	60
Overall k-value	[W/m ² K]	0.045
Fluid		
Type		Water-Ethylene glycol mixture
Percentage solution (Ethylene-Glycol in water)	[%]	30%
Total capacity (Includes storage tank, panel and connecting pipes)	[ℓ]	247
Test model dimensions (Refer to Figure 14)		
Panel inlet, h_1	[m]	2.7
Panel outlet, h_2	[m]	2.06
Storage tank inlet, h_3	[m]	0.03
Storage tank outlet, h_5	[m]	0.88
Storage tank base, h_6	[m]	0

The table below gives other relevant information of the test setup:

Table 4 : Test setup information

Property	Unit	Value
S1 Mean storage tank temperature	[°C]	15
S2 Mean storage tank temperature	[°C]	14
Average air pressure at location	[kPa]	85
Test start date		21 st September 2010
Test end date		31 st October 2010

4.3.2. Location and positioning

The test model was set up at Potchefstroom, in the North-West province of South Africa (S26 41.088 E27 05.818). The meteorological information and psychometric data used in the calculations were all based on this location.

A south facing orientation of the panels was chosen to minimise the effect of solar radiance on the panel surface during the day.

The test setup had a clear line of sight from the panel's surface to the night sky. No trees or nearby buildings obscured the line of sight to maximise the performance of the system.

The test location represented an average condition that the system will be exposed to in practice. The result therefore gave a good understanding of the performance of the system under typical circumstances.

4.3.3. Measuring instrumentation

The test model was evaluated by recording temperatures at various points in the system. The panel inlet, outlet, storage tank, ambient dry bulb and wet bulb temperatures were recorded on both systems.

The temperatures were measured by using K-type thermocouples connected to a computer equipped with a data logger. The temperatures were recorded in 15 minute intervals by the data logger and were appended in a computer file.

The panel in- and outlet temperatures were measured by installing a thermocouple directly in the flow path of the panel inlet and outlet manifolds. The storage tank temperature was measured at the centre point of the tanks to give an average tank temperature.

Another thermocouple recorded the dry bulb ambient temperature at the test location. The wet bulb temperature was also measured at the same location and was used to determine the real time relative humidity.

The heating element that was used to simulate the heat load on the system was a normal electric resistance water heating element and had a maximum rating of 2 kW. The heating element input was controlled with a variable alternating current transformer to be able to set it at a specific heat load input. A kilowatt-hour meter was also connected to the heating element to measure the heat load input over a time period.

The mass flow rate of the thermosyphon effect was not measured directly. The main reason for this is the very small magnitude of the mass flow rate. It was not possible to install a flow measuring device directly in the flow path because of the significant head loss it would have created. A flow measuring device that do not obstruct the flow path and is able to measure such low flow rates would have been unfeasibly expensive for this study. Instead the flow rate was determined indirectly from the panel inlet and outlet temperatures and an energy balance of the storage tank.

4.4. EXPERIMENTAL METHOD

The test period was from the 21st of September 2010 to the 31th of October 2010. During this time the temperatures were continuously recorded with the equipment described above.

The heating element on System 1 was altered during the testing period. The testing started off with the element at zero Watt input. The test setup operated at this setting for a period of one week to establish the baseline temperatures of both systems. After this the heating element was adjusted to 30 Watt input. The heating element input remained at this for a period of two weeks. The heating element input was then increased to 40 Watts. This setting was kept so for a period of two and a half weeks until the end of the test period. The gradual increase of the heating element input was to examine its effect on the mean storage tank temperature and panel heat dissipation.

No significant alterations were made to the test model during this time apart from the heat load.

4.5. EXPERIMENTAL RESULTS

The results obtained from the test model were processed and compiled to analyse the performance of the system over the test period. The test model's results are discussed briefly in this section.

The first evaluation of the system performance was done on the data of a typical night of operation. The recorded data of a typical 48 hour period is given in Figure 21 and Figure 22 for System 1 and System 2 respectively. These specific sets of data were the night of the 5th of October 2010.

The graphs indicate the measured dry bulb, panel inlet, panel outlet and average storage tank temperatures of the two systems over 48 hours. The relative humidity is determined from the wet bulb temperature and also indicated.

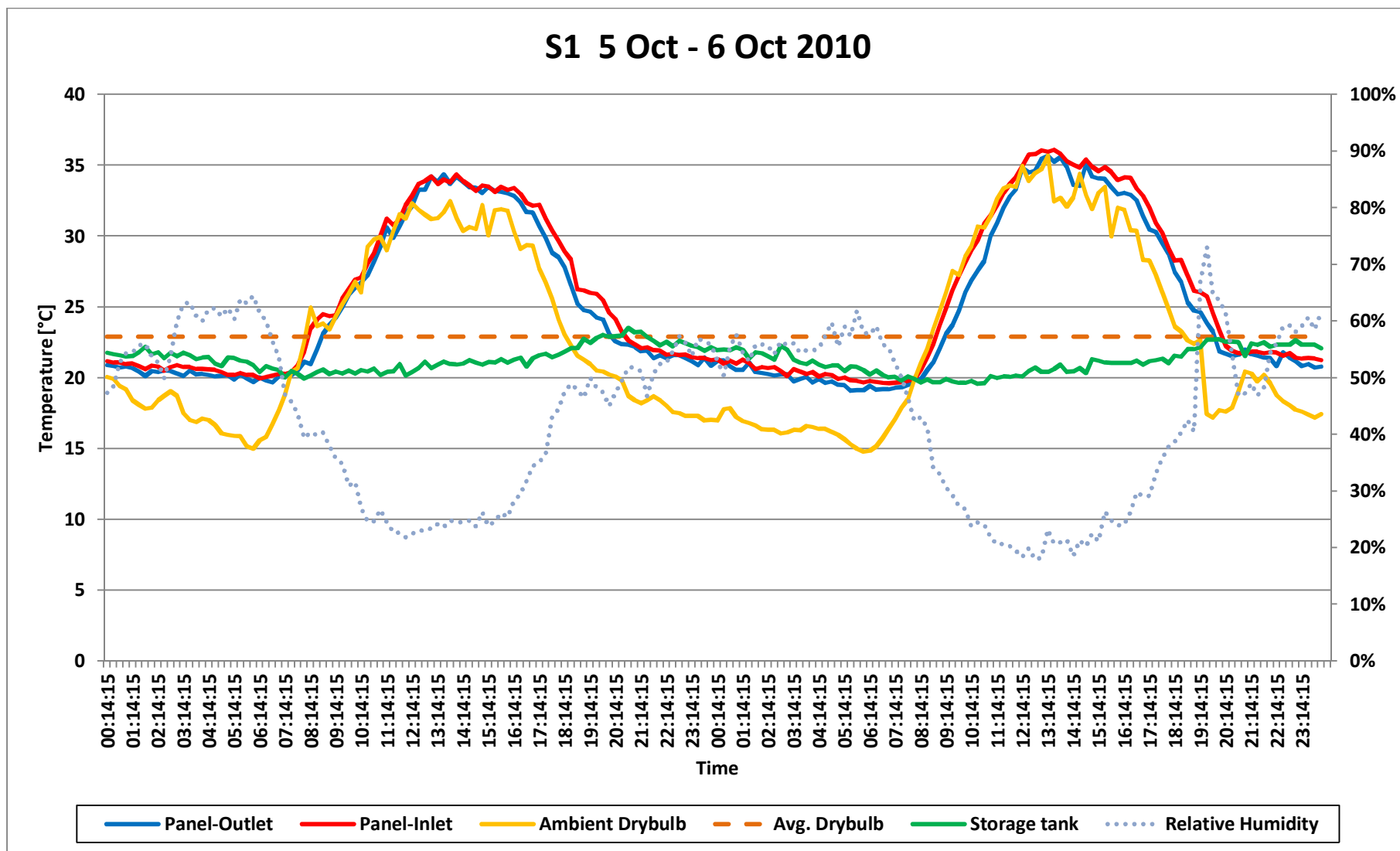


Figure 21 : S1 Experimental data

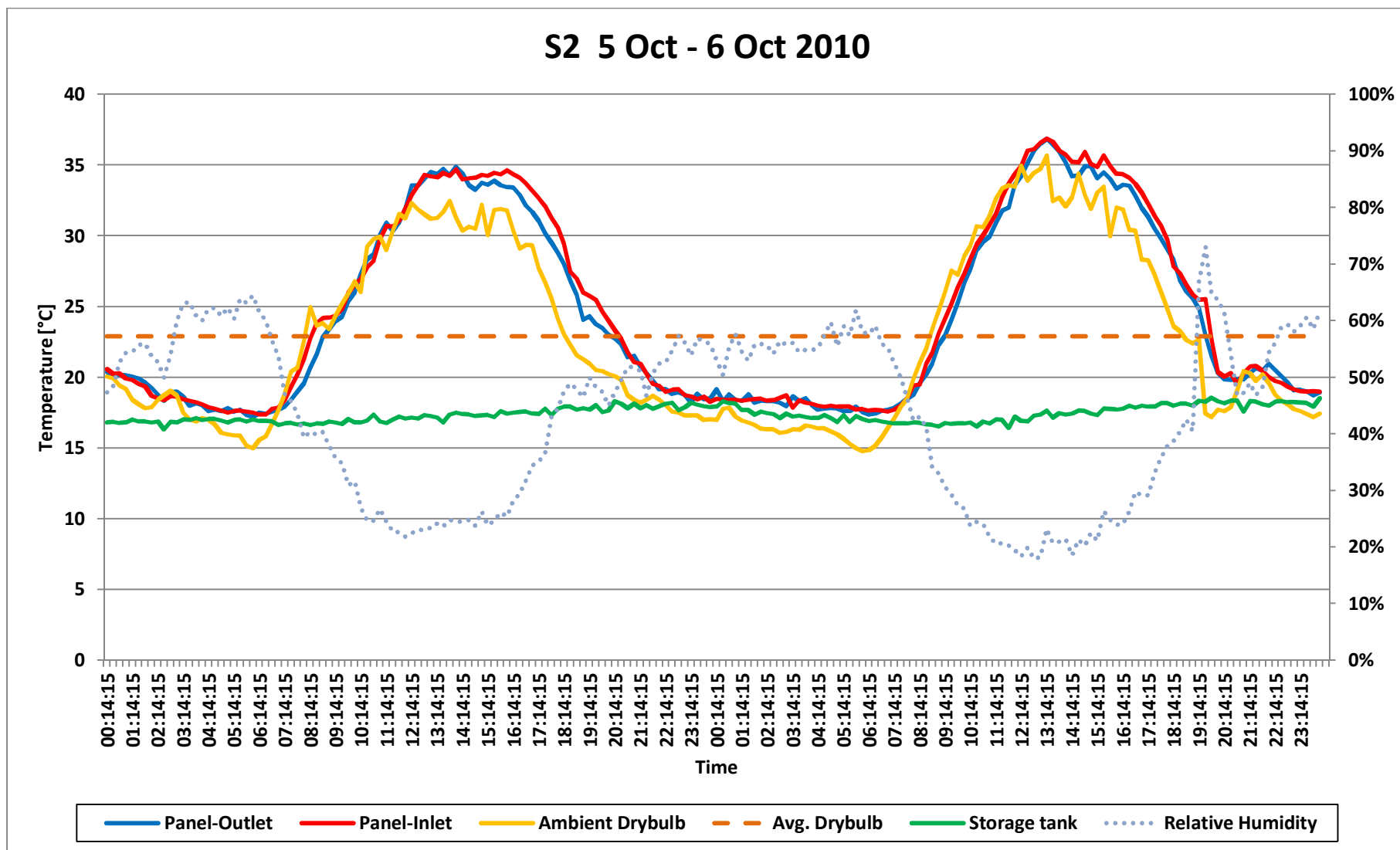


Figure 22 : S2 Experimental data

From the recorded data in the graphs it was observed that the systems generally started to show a change in storage tank temperature from about 22:00 PM. By this time the ambient temperature usually dropped sufficiently for the system to start functioning. The residual heat retained during the day in the panels and the fluid inside it was also dissipated by this time.

The effect of the heat load was noticeable when the storage tank temperatures of System 1 and System 2 were compared. System 2 had a much lower average storage tank temperature than System 1. The effects of a higher storage tank temperature are also observed with this in mind. System 1 showed a greater temperature change during the night than System 2. This is due to the panel surface being warmer causing an increase in the radiative heat transfer from the panel.

The desired damping effect of the system is clearly observed if the ambient temperature is compared to the storage tank temperature of System 1. The ambient temperature fluctuated in the order of 20 to 25°C between minimum and maximum, whereas the storage tank temperature fluctuation was less than 5°C. From this small extract of data it was already apparent that this damping effect can be used to the advantage to provide a more stable heat sink for a refrigeration cycle.

The recorded data of the test model setup for the entire period of testing are shown in Figure 23. The graph indicates the storage tank temperatures of System 1 and System 2 and also the ambient dry bulb temperature. The average dry bulb temperature of each day is also indicated.

The difference between the storage tank temperatures of System 1 and System 2 was clearly seen in the graph. The effect of the heat load was noticed again in the storage tank temperature deviation on the 30th of September when it was switched on.

The temperatures over the long term also indicated that a significant damping effect is achievable. The data over this period of time indicated that it is possible to keep the storage tank temperature at or below the average ambient temperature. The average dry bulb temperature therefore served as a baseline temperature for the system's performance. An average storage tank temperature below the average dry bulb temperature is advantageous, since it signifies an improved lower heat sink temperature that is created for the refrigeration cycle.

The data obtained in the experimental phase of the study are to be used to verify the results of the theoretical model against. The verification and validation of the theoretical model is discussed in the next chapter.

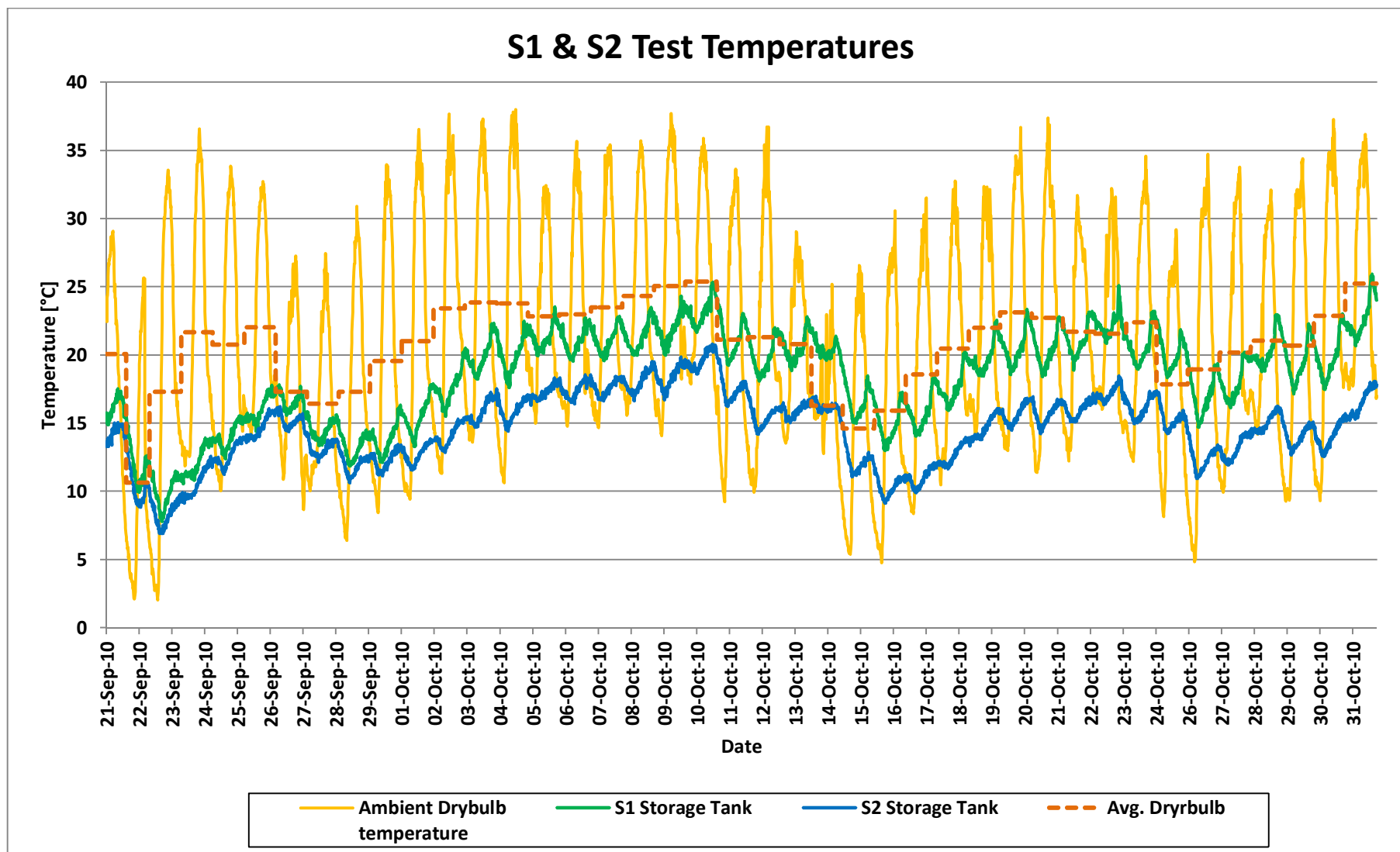


Figure 23 : Test period temperatures

5. EXPERIMENTAL AND THEORETICAL MODEL COMPARISON

5.1. INTRODUCTION

The accuracy of the theoretical model to predict the system performance was compared against the results obtained from the experimental model.

The theoretical model was configured to replicate the experimental setup. The dimensions and properties given in Table 3 and Table 4 were used as system parameters. The recorded ambient dry and wet bulb temperatures were also used as input for the theoretical model in order to gauge its results under the same environmental conditions as the experimental setup.

The results of the theoretical model and test setup were compared against each other and the observations are discussed in this chapter.

5.2. OBSERVATIONS AND CORRECTIONS

Careful analysis of the results initially indicated a fairly good correlation between the results of the theoretical model and the experimental setup. A number of inconsistencies did however occur and was investigated further in order to improve the theoretical model's accuracy.

The observations and the subsequent corrections made in the comparison are described in detail in the next sections.

5.2.1. Temperature Deviation

The first noticeable difference that was observed in the comparison was a steady rise in temperature over time in the test model data which the theoretical model did not indicate. Figure 24 illustrates this observed temperature drift.

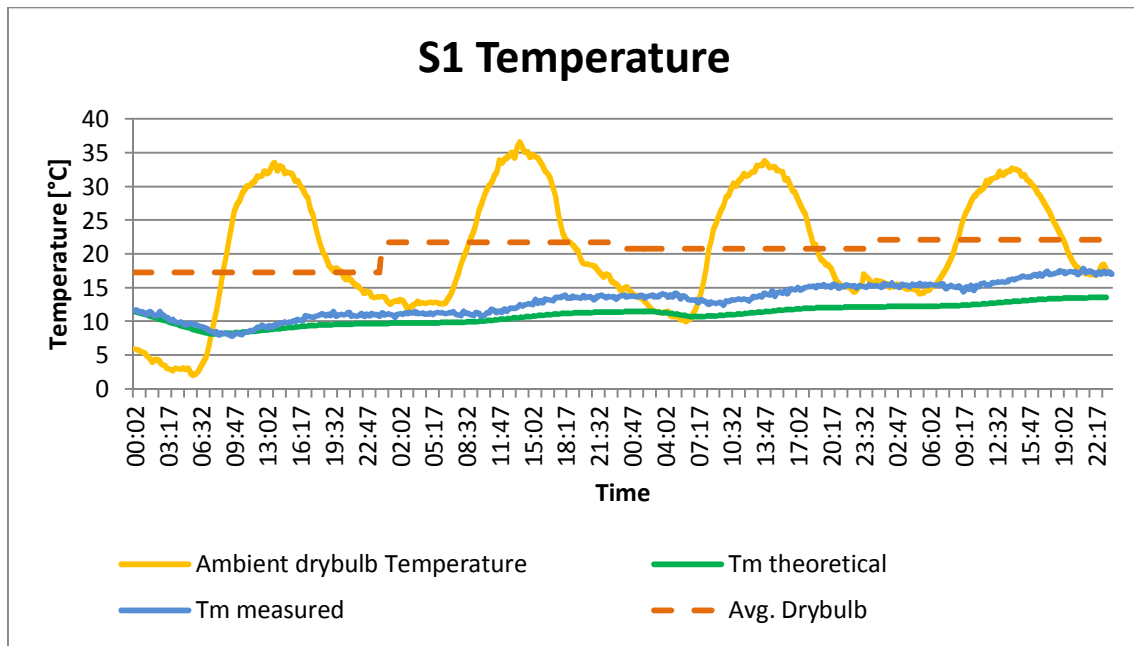


Figure 24 : Theoretical and test results temperature drift

Further investigation suggested that the temperature increase can be caused by solar irradiance on the storage tanks and also a small amount of conductive heat transfer at the tank in- and outlet points. This creates a small heat flux into the storage tank causing the gradual storage tank temperature increase. This observation pointed out a deficiency in the theoretical model since it did not take into account heat transfers of this type and scale.

With a trial and error method it was concluded that the unexplained heat gains were in the order of 10 to 20 Watts during the daytime hours. As a result a constant 15 Watts was added as a heat load input to the storage tank's energy balance.

With the addition of this additional heat gain the theoretical model now demonstrated a very good correlation with the test model data. The effect of the additional heat gain in the theoretical model is illustrated in Figure 25.

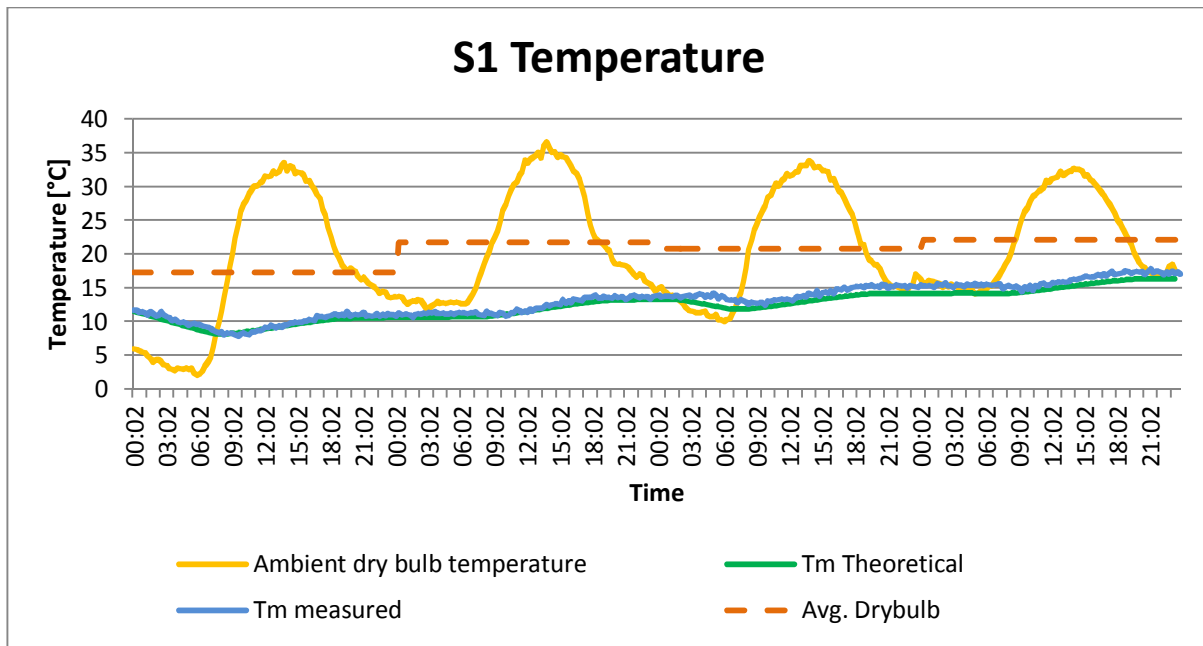


Figure 25 : Theoretical model with additional heat gain

A limitation of the model is to predict system performance during nights with cloud cover. Cloud cover significantly reduces the effective sky emissivity explained in chapter 3.5. As a result the theoretical model overestimates the amount of heat loss from the radiative panel's surface during overcast nights.

The effect of cloud cover was observed in the data of 12 to 13 October 2010 when another temperature difference was noticed between the theoretical and experimental data. The night of the mentioned date was known to be overcast.

It was noticed in the test model data that the storage tank temperature did not decrease during this time even though the dry bulb temperature was favourable for radiative cooling (lower than the average storage tank temperature). The theoretical model on the other hand indicated normal radiative heat transfer from the panel at this temperature thus incorrectly reducing the storage tank temperature.

The deviation during this one night slightly distorted the theoretical results thereafter resulting in a lower predicted storage tank temperature than the measured temperature.

Since it is difficult to directly measure or predict cloud cover it was not factored into the theoretical model. Fortunately the number of overcast days was small in proportion to the number of days with clear sky conditions. The overestimation of the storage tank temperature decrease during overcast nights is therefore considered negligible.

5.2.2. Flow Rate Correlation

The mass flow rate was calculated with the theoretical model and was compared to the mass flow rate obtained from the experimental measured results.

As mentioned previously in paragraph 4.3.3 the test model's flow rate was obtained by an indirect method. The method that was used is as follows:

The first step was to determine the amount of energy transferred from the storage tank over a given time. This was done by using the following equation:

$$Q = mCp(\Delta T) \quad (53)$$

The change in temperature (ΔT) was for the given time interval. A time interval of 15 minutes was used to match to the time interval of the measured results.

The instantaneous energy transfer of the storage tank is then:

$$W = \frac{Q}{Time} \quad (54)$$

Since the storage tank's energy transfer is done by the panel, equation (54) is therefore also the instantaneous energy transfer of the panel.

With the Watts from the panel known as well as the panel inlet (T_{in}) and outlet (T_{out}) temperatures it was possible to calculate the mass flow (\dot{m}) rate of the system. This was done by considering the energy balance of the panel:

$$W = \dot{m}Cp(T_{in} - T_{out}) \quad (55)$$

The method described above was used to calculate the thermosyphon mass flow rate for the test model data. The theoretical model's mass flow rate was then compared against this data.

Figure 26 illustrates the results obtained by the theoretical model and the indirect method used for the measured data for the 15 minute intervals.

It was immediately apparent that the theoretical model and the test model data did not correlate well. The data were scrutinised to determine the cause of this significant inconsistency. This process revealed a number of responsible factors.

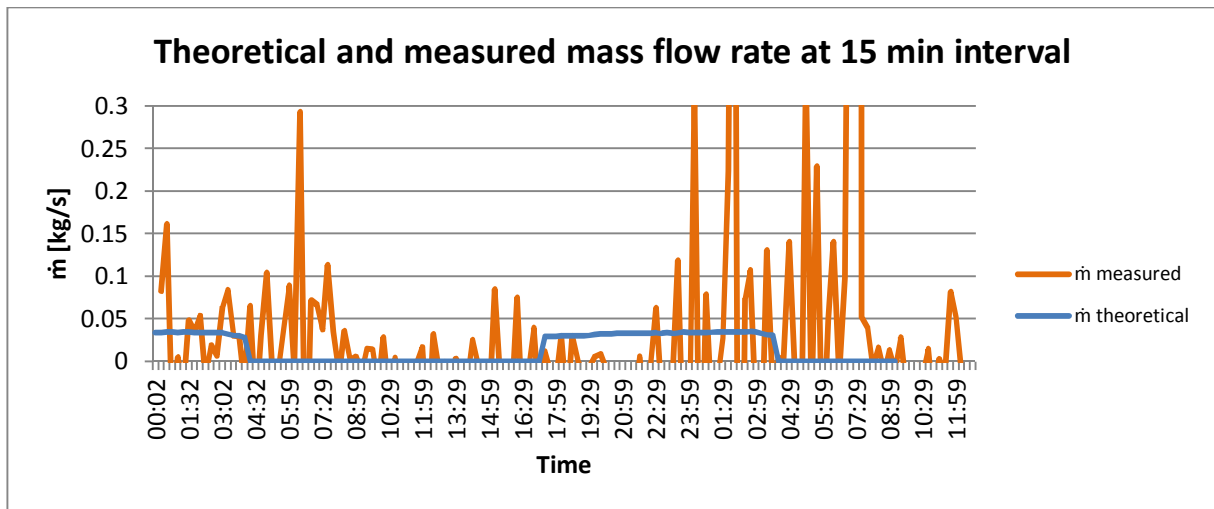


Figure 26 : Mass flow rate at 15 minute interval

It was concluded that the most influential factor was the accuracy and response of the measuring equipment used. After studying the measured data it was noted that the values of the temperatures can fluctuate significantly within $\pm 1^\circ\text{C}$ in a matter of seconds due to the measuring equipment's sensitivity. A corrective action for this is to use a larger time interval to give an average temperature reading.

An interval of 15 minutes was considered to be inaccurate. An even larger time interval was tried and a time interval of 1 ½ hours proved to give better results. The larger time interval indeed evened out the temperature fluctuations of the 15 minute intervals to some extent. The results of this attempt is indicated in Figure 27

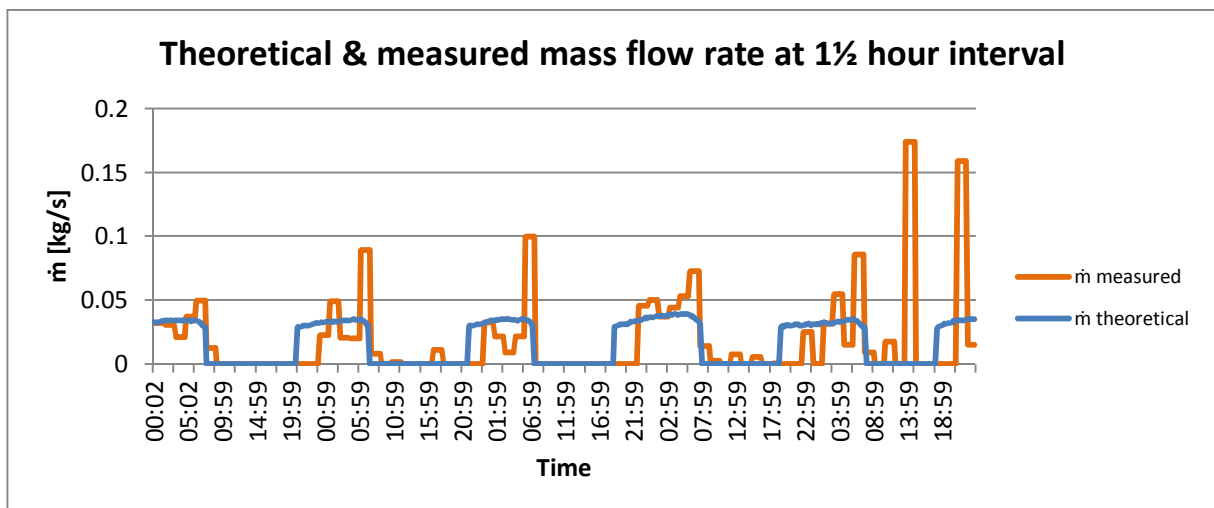


Figure 27 : Mass flow rate at 1½ hour intervals

The measured and theoretical flow rates compared better at the larger interval of 1½ hours although some inconsistencies can still be observed. The cause of these inconsistencies that are still present was investigated further to find out if it was caused by temperature fluctuation of the measuring instruments. The K-type thermocouples that were used have a tolerance of $\pm 1.5^{\circ}\text{C}$.

The investigation began by taking into consideration the mass flow rate and energy balance of the storage tank. Mathematically this has to be a fixed relation and it should provide a linear relationship between the mass flow rate and energy transferred if heat gains/losses are neglected.

The mass flow rate and energy transferred from the storage tank was evaluated with measured data of 10 days and using the method described in the beginning of the paragraph. The results were plotted in a scatter plot diagram and are shown in Figure 28 below.

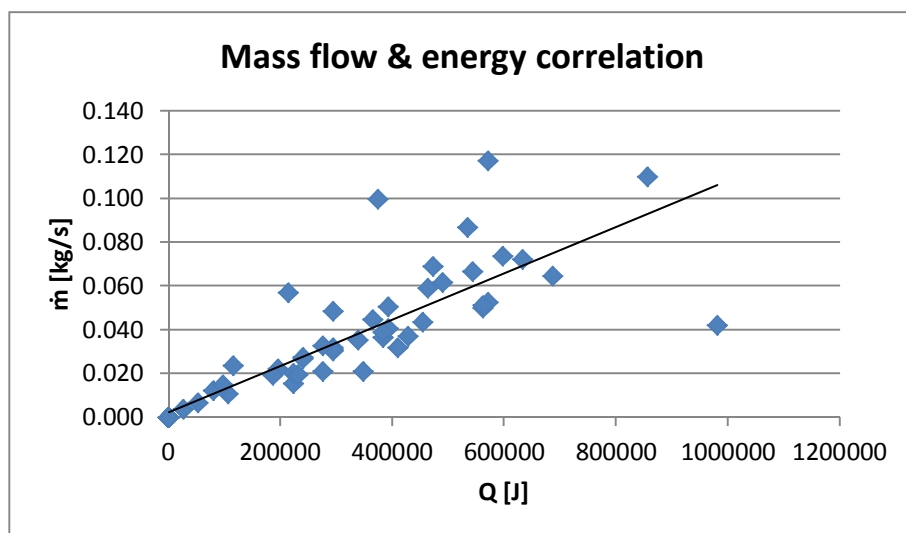


Figure 28 : Mass flow and energy correlation

The data shown in Figure 28 indicated that the mass flow rate differ significantly in some cases for a given energy loss from the storage tank. This should not be the case since it has to be a good linear correlation theoretically. All of the variables used in the calculations were examined to determine which had the largest impact on the inconsistent mass flow rates.

One set of variables used in the mass flow rate calculations are the inlet and outlet temperatures of the panel. This appeared to be the only variable that could have an effect on the mass flow rate since all the other values used in the calculations are constant values.

The panel temperature difference was plotted against the energy transfer of the storage tank in a scatter plot diagram. This should again give a linear correlation theoretically. The results are shown in Figure 29.

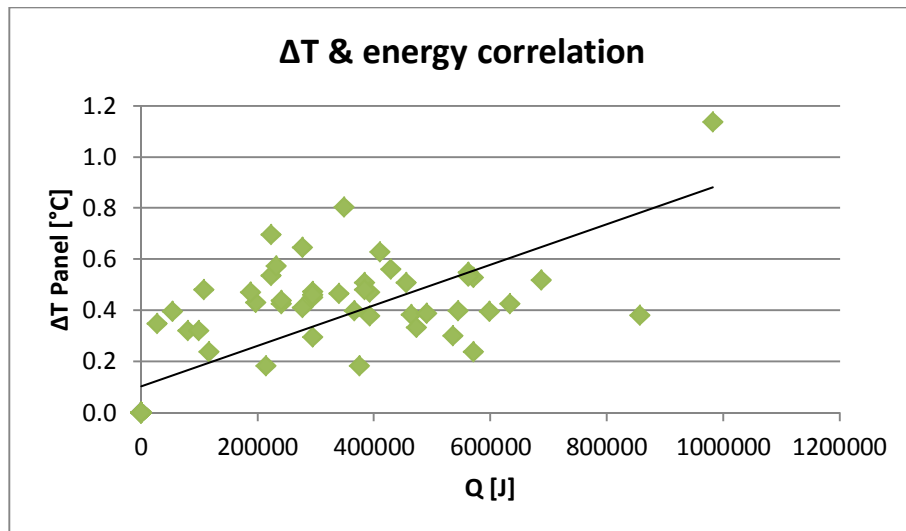


Figure 29 : Panel temperature difference and energy correlation

From Figure 29 it was immediately apparent that the panel temperature difference does not correlate well to the energy transfer from the storage tank. This suggests that the irregular panel inlet and outlet temperatures are the main contributing factor of the inconsistent mass flow rates.

The temperature difference between the panel inlet and outlet is very small and a fluctuation of even 0.1 of a degree can influence the temperature difference considerably. This results in the mass flow rate being incorrectly calculated.

An even larger time interval was chosen to try and even out the temperature fluctuation. For this run a time interval of 6 hours was chosen. This larger time interval provided an average mass flow rate for the two halves of a typical night of operation from 18:00 to 24:00 and 24:00 to 6:00. The results from the mass flow rate calculations for the 6 hour time interval is given in Figure 30.

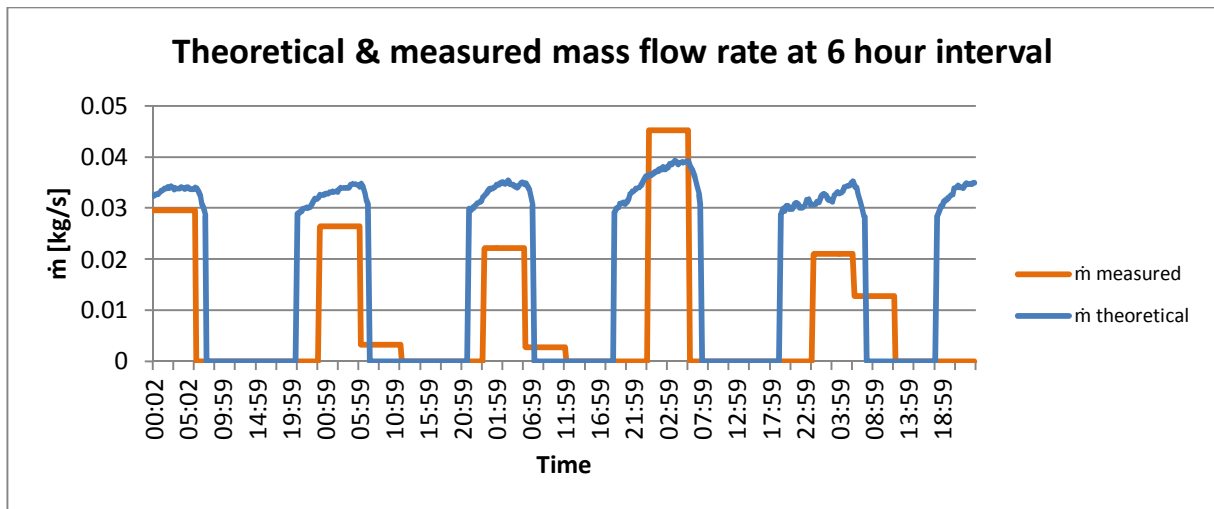


Figure 30 : Mass flow rate at 6 hour interval

The experimental mass flow rate is now more in accordance with the theoretical mass flow rate although some small differences can still be observed. The spikes observed with the 15 minute and 1½ hour time intervals are now averaged out.

Another possible influence on the theoretical mass flow rate is the fluid head losses of the system's pipe network.

The equation used for calculating the pipe network head losses in the theoretical model only provides a rough estimation. Fluid flow head losses at very low flow, low Reynolds numbers are very difficult to measure and calculate accurately. The outcome of this is that the current theoretical methods are only able to provide approximations of the head losses.

It is therefore a possibility that the pipe network head losses is over or underestimated in the theoretical model. This subsequently causes the calculated mass flow rate to be lower or higher than the actual mass flow rate. This is a likely cause of the small difference that is still observed between the theoretical and experimental mass flow rates in Figure 30.

All the influencing factors described in this section made the verification of the theoretical model difficult in terms of the mass flow rate. In spite of this the theoretical model still gave realistic mass flow rates and was not considerably different from the test model's data.

It was concluded that the theoretical model is able to predict the system mass flow rate with good enough precision for the purpose of this study considering the small magnitude of the flow.

5.3. CORRECTED THEORETICAL MODEL RESULTS

The corrections proposed in the previous sections were applied to the theoretical model in order to improve its accuracy. Results were generated again with the corrected theoretical model and compared to the test model results.

The results of the final model and the test model over the test period are given in the figures found in the following pages. The data is only represented graphically in this chapter. A detailed extract of the data is given in Appendix B and C.

The theoretical model was compared to the storage tank temperatures of System 1 in Figure 31 and System 2 in Figure 33. The theoretical energy transfer from the panel as experienced with the simulations of System1 and System 2 are also respectively given in Figure 32 and Figure 34.

It was observed that the corrected theoretical model closely followed the storage tank temperature trends of the test model data for both systems.

The panel heat loss in Figure 32 indicated that the heat loss is on average between 80 to 100 W/m² of panel during the night at a constant heat load input of 30 Watts. It was also noted that a higher mean storage tank temperature results in an increase of panel heat loss when compared with Figure 34. The heat loss for System 2 without a heat load and a resulting lower storage tank temperature was around 60 Watts per square meter of panel.

These satisfactory results led to the conclusion that the theoretical model is able to accurately enough predict the performance of a radiative cooling system. The model can be used to predict and analyse the performance of a scaled up radiative cooling system.

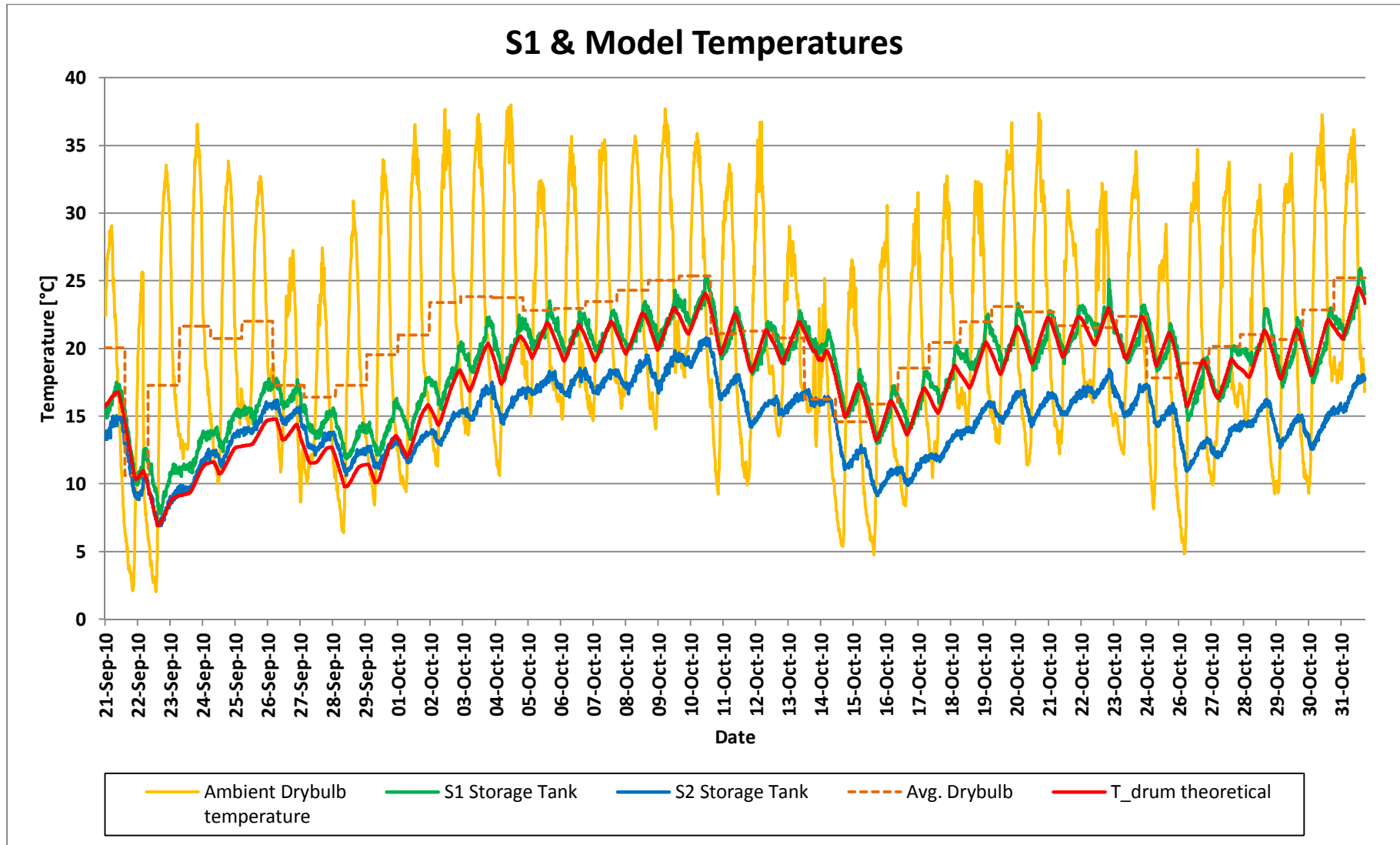


Figure 31 : Theoretical model results comparison for S1

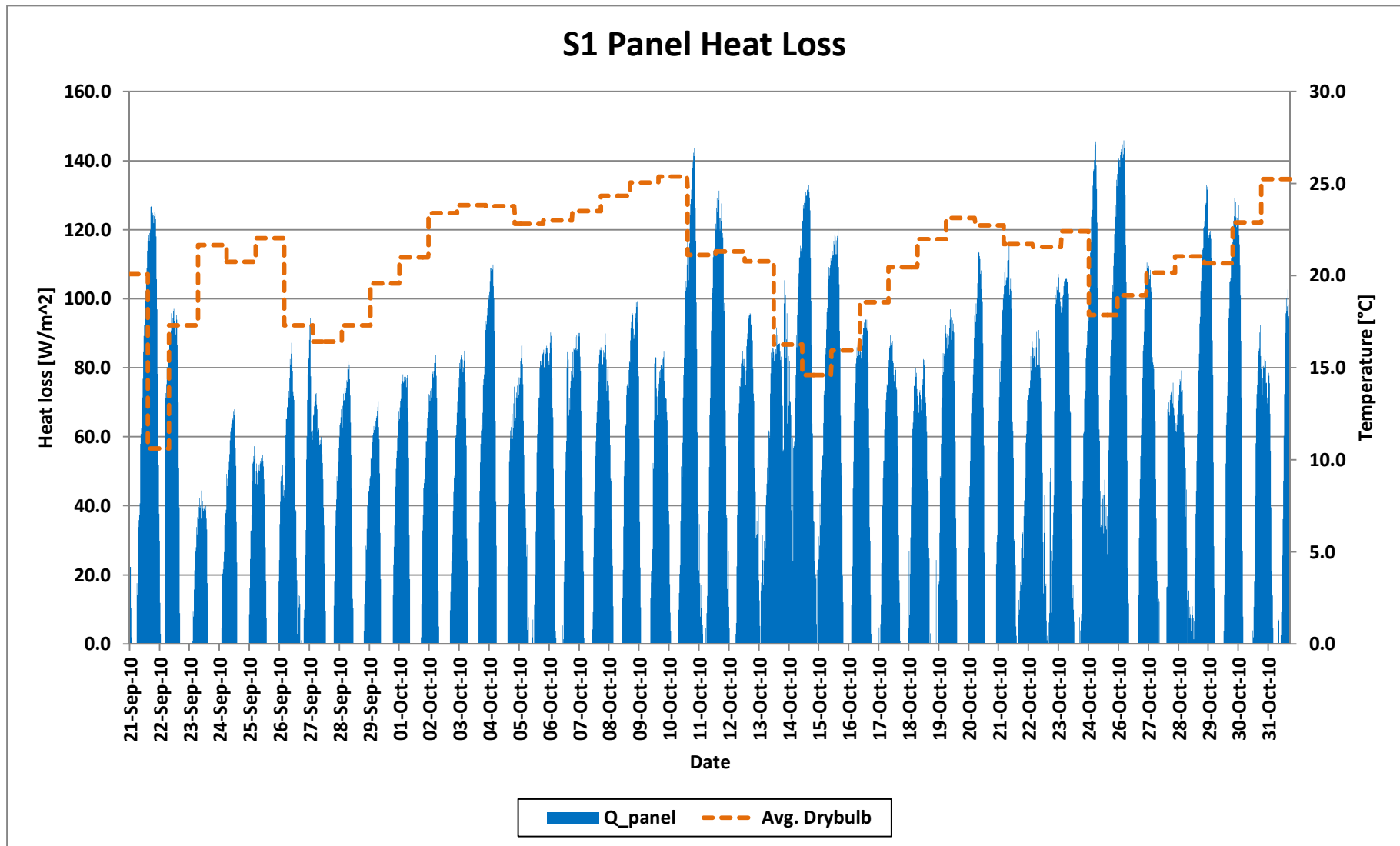


Figure 32 : Theoretical panel heat loss for S1 simulation

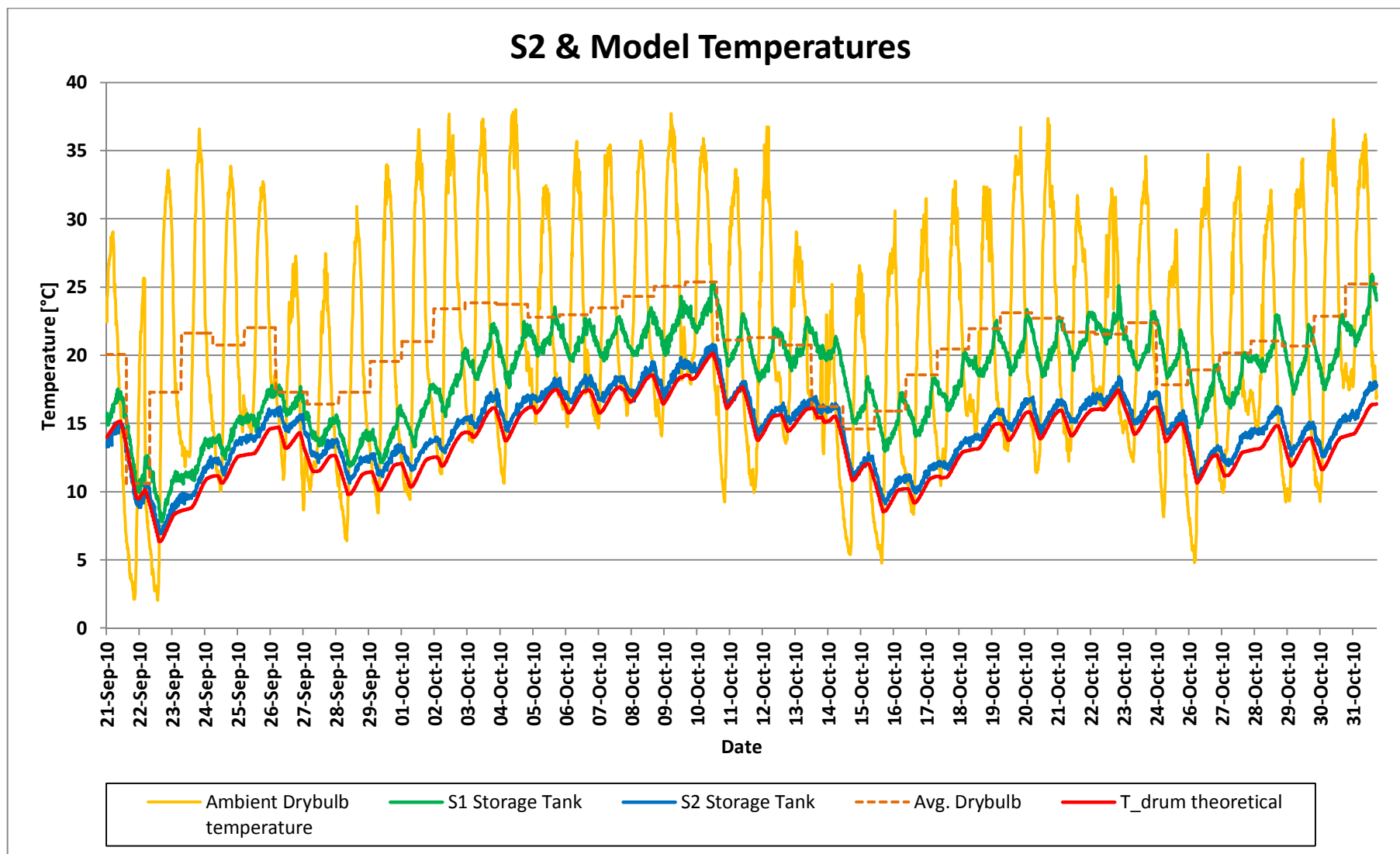


Figure 33 : Theoretical model results comparison for S2

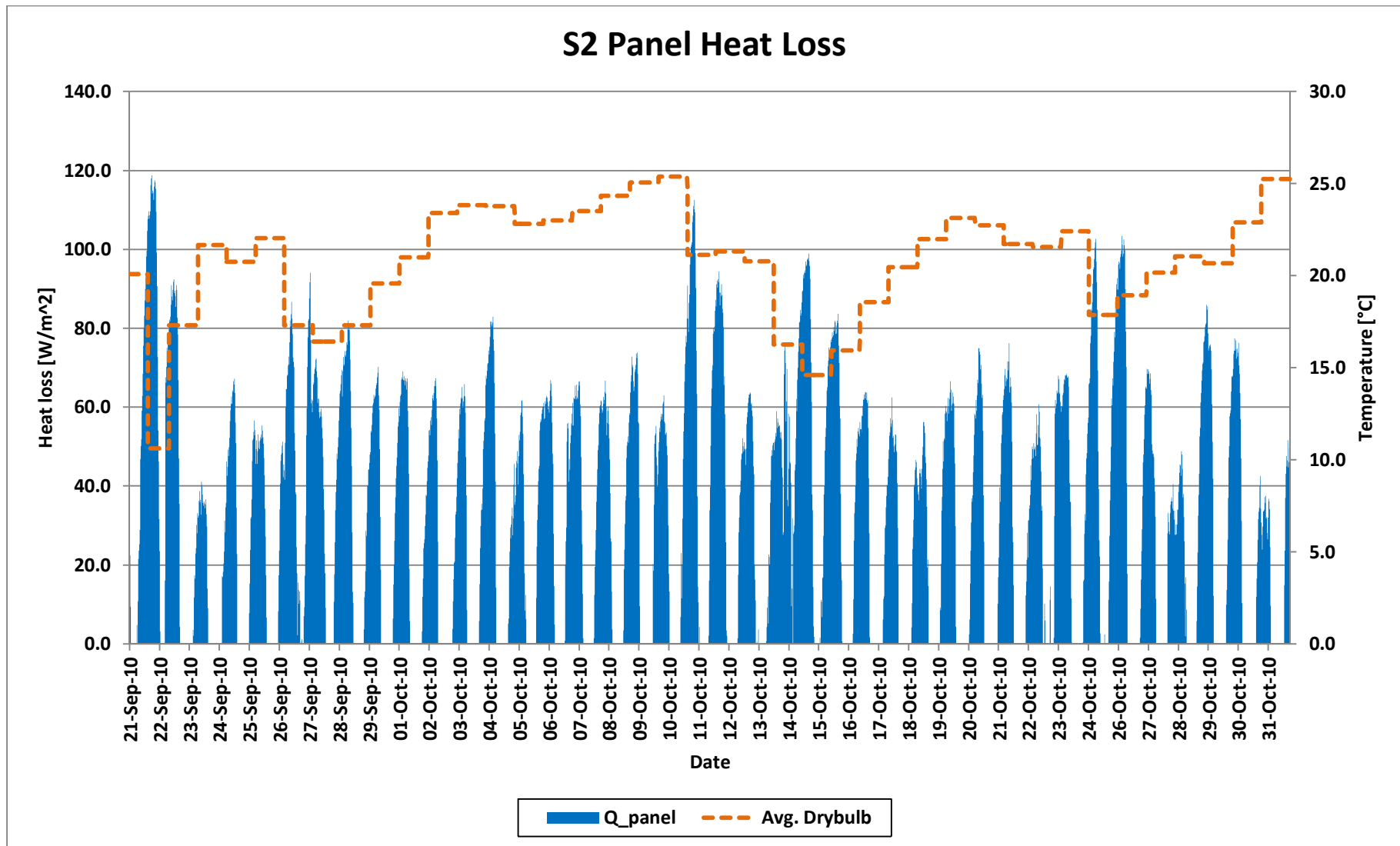


Figure 34 : Theoretical panel heat loss for S2 simulation

6. SYSTEM PERFORMANCE ANALYSIS

The theoretical model was applied to study the effects of various system parameters on the performance. This was done in order to get a better understanding of the performance of a radiative cooling system in general before moving on to a scaled up system.

The evaluation was done by changing one system parameter at a time and studying its effect on the mass flow rate, storage tank temperature and panel heat loss.

The various parameters that were altered and the resulting effect on the system performance are described in the following paragraphs.

6.1. RELATIVE HUMIDITY

From previous studies [27] and the literature study it was known that the relative humidity of the air can affect the radiative heat transfer to the night sky.

The relative humidity was varied from 10% to 100% in the theoretical model to determine its effect on the system performance. The relative humidity was kept constant over the time in this case opposed to the actual relative humidity which fluctuates with time.

The effect of relative humidity on mass flow rate and mean storage tank temperature is given in Figure 35 and Figure 36.

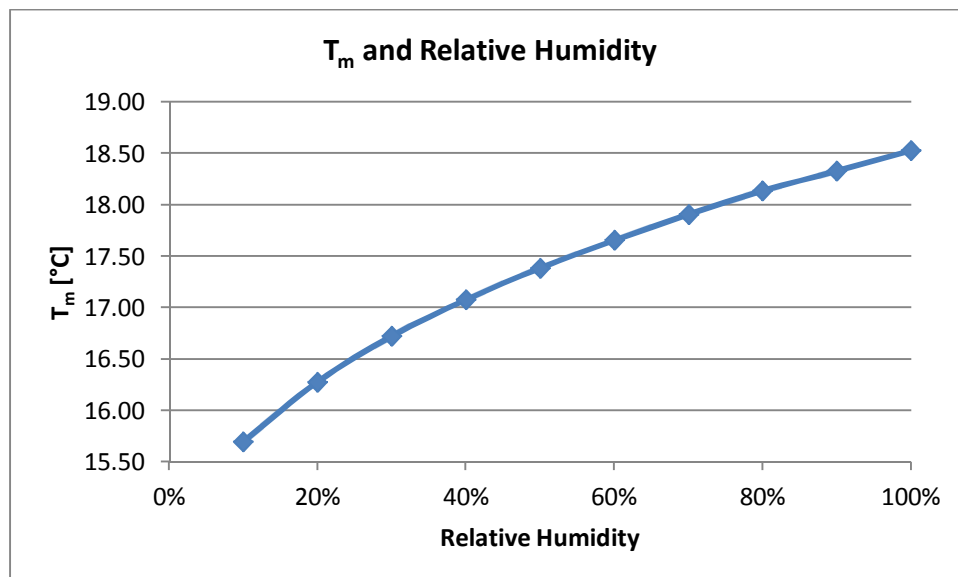


Figure 35 : Effect of RH on mean storage tank temperature

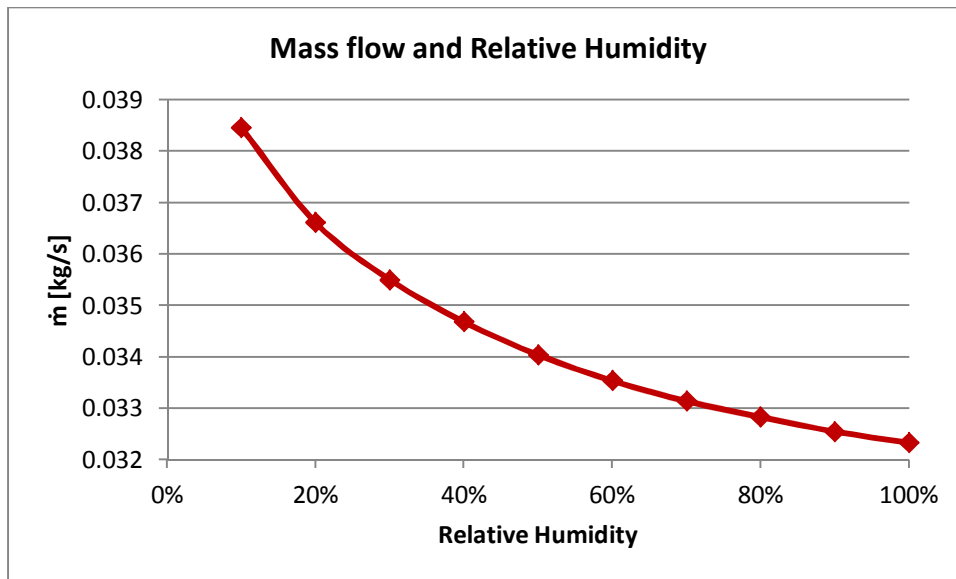


Figure 36 : Effect of RH on mass flow rate

In both the preceding figures it was observed that the relative humidity had a considerable effect on the performance as expected. The mass flow rate decreased and the mean storage tank temperature increased with an increase in relative humidity. This implies that less heat loss occurs from the panel at a high relative humidity.

The effect of the relative humidity is as such, because of the effective sky temperature that is influenced by the relative humidity. A high amount of moisture in the air is in effect an obstruction in the path of the thermal radiation path between the panel and the night sky.

From these results it was concluded that the relative humidity is an important factor that has to be considered in the design and implementation of a radiative cooling system. A radiative cooling system therefore performs best if used in dry climates with low humidity.

6.2. PANEL SURFACE EMISSIVITY

The panel surface emissivity is a property that is dependent on the material properties of the panel and its surface coating. The surface emissivity should remain constant but a number of factors can influence this property in practice.

A significant problem with a radiative cooling system is contamination on the panel surface thus lowering its surface emissivity. This can include dust, water residue or even a change in the surface coating due to discolouration. A lower panel surface emissivity reduces the thermal radiation from the surface thus reducing the system performance.

The effect of the panel surface emissivity on the performance is given in Figure 37 and Figure 38.

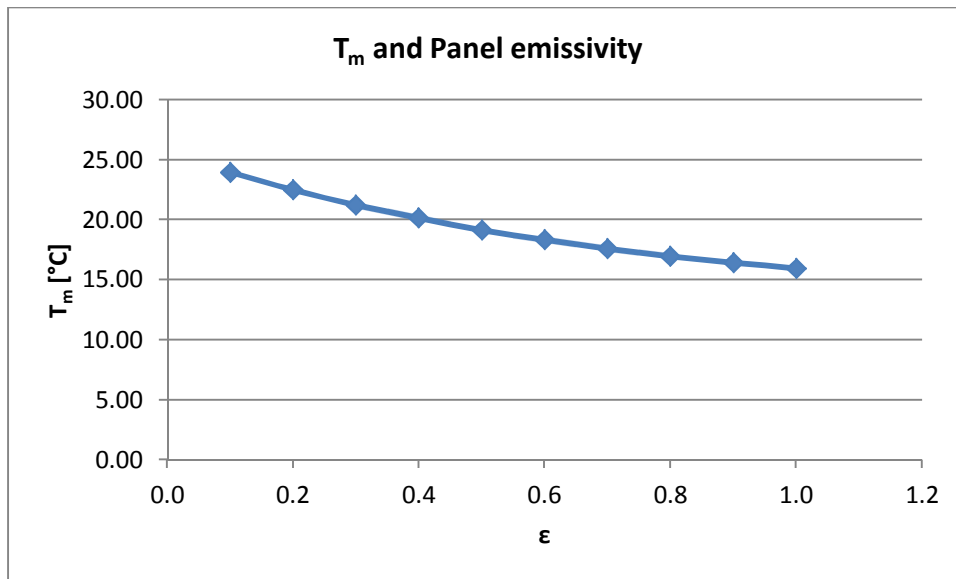


Figure 37 : Effect of ϵ on mean storage tank temperature

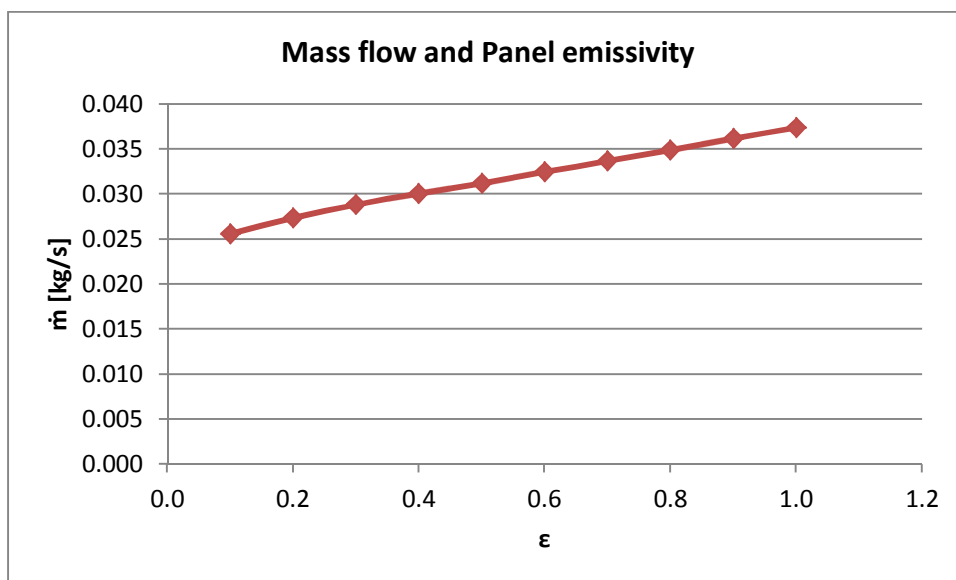


Figure 38 : Effect of ϵ on mass flow rate

It is evident from the graphs that a higher emissivity leads to lower average storage tank temperatures and increased mass flow rates.

In practice a surface emissivity as low as 0.1 is rarely encountered but the rest of the values in the range of 0.6 to 0.9 are very likely in practice. In this range it is still noticeable that a decrease in emissivity is able to reduce the system performance.

It is therefore advisable that a surface coating with a high emissivity is used to provide the best performance. In practice the panel surface should be kept clean to fully utilise the emissive properties of the surface coating.

6.3. CONNECTING PIPE DIAMETER

The connecting pipes between the panel and the storage tank in- and outlets are an important component that has to be analysed. The aim of this investigation was to determine if small diameter pipes will reduce the performance compared to large diameter pipes.

The diameter of the pipes connecting the storage tank and panel was varied from 15 mm to 60 mm inside diameter. These are practical pipe sizes likely to be used in a radiative cooling system. The results are given in Figure 39 and Figure 40.

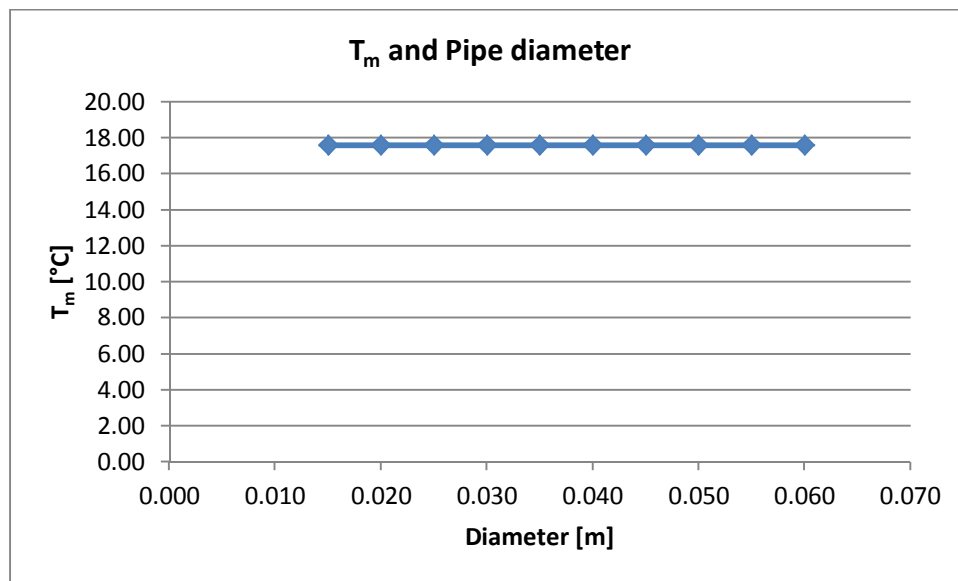


Figure 39 : Effect of pipe diameter in mean storage tank temperature

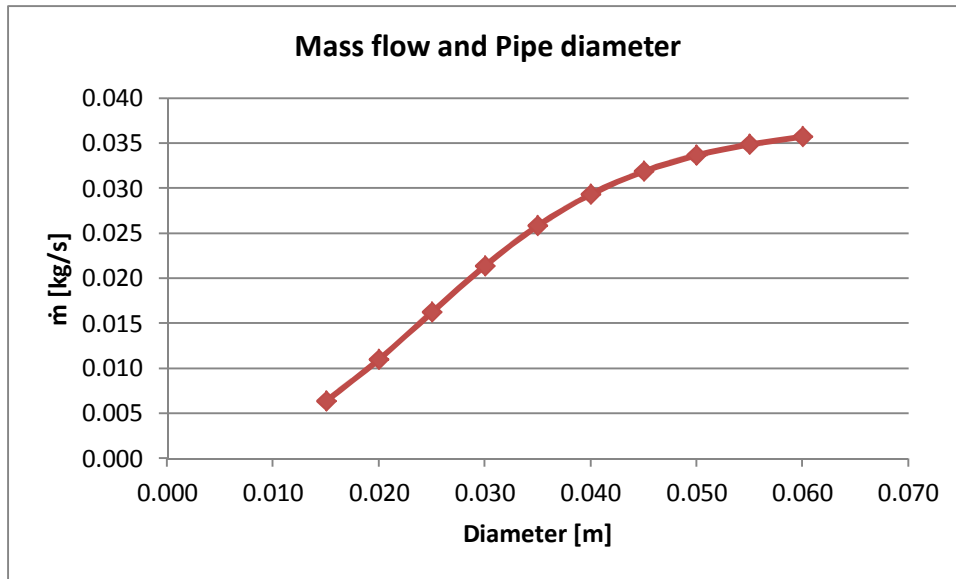


Figure 40 : Effect of pipe diameter on mass flow rate

It was clearly evident from the results that the connecting pipe diameter had no effect on the mean storage tank temperature. The mass flow rate did however show a change with different pipe diameters. The constant storage tank temperature means that the energy transfer remained constant regardless of the pipe diameter.

A small diameter pipe reduces the mass flow rate resulting in a larger temperature difference over the panel and otherwise for larger pipe diameters.

It is evident from the results that the connecting pipe diameter had no significant effect on the system performance. Financial implications and practicality are most likely to be governing factors for a radiative cooling system's connecting pipe design.

6.4. PANEL AND STORAGE TANK HEIGHT DIFFERENCE

The height difference between the panel and the storage tank is a factor that is likely to be influenced by the geometry of the building onto which such a system will be installed in practice. It is therefore important to investigate the effect of this system parameter on the performance.

The distance between the storage tank bottom and panel inlet was varied between 1 metre and 5 metres to study its effect and the results are plotted in Figure 41 and Figure 42.

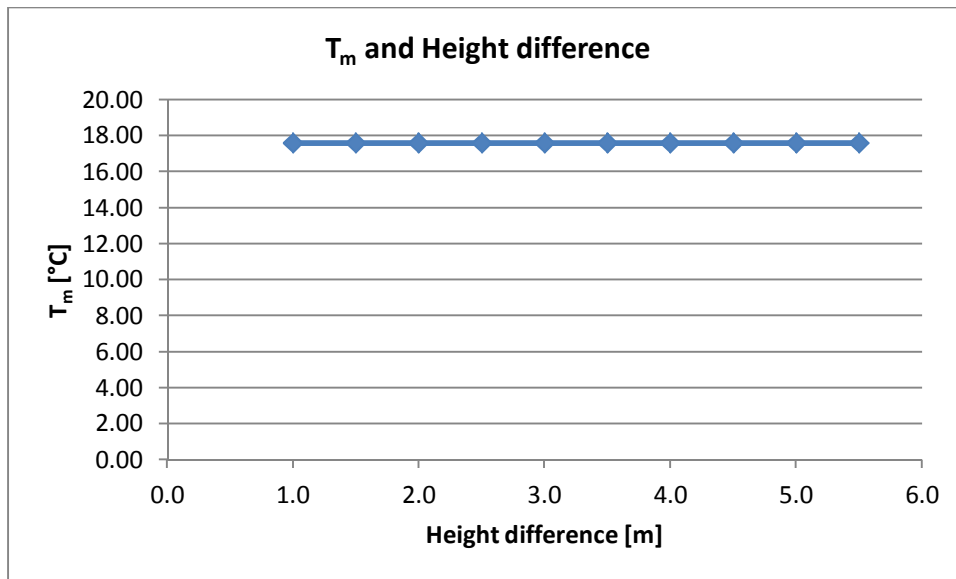


Figure 41 : Effect of panel height on mean storage tank temperature

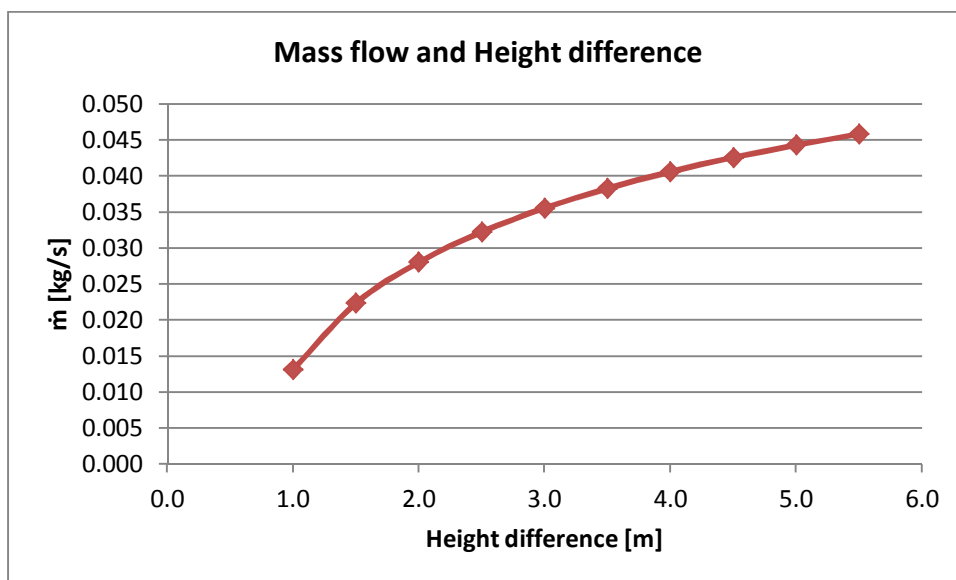


Figure 42 : Effect of panel height on mass flow rate

It was noted in Figure 42 that the panel height had a significant effect on the mass flow rate. The mass flow rate increased as the panel height increased.

Figure 41 on the other hand showed no change in the mean storage tank temperature with a change in height. It was concluded that the panel height had the same effect as the connecting pipe diameter that was investigated in paragraph 6.3. The amount of heat energy transferred remains constant regardless of mass flow rate. The only effect is a change in the panel outlet temperature.

From this investigation it was concluded that the system performance is not influenced by the height difference between the panel and storage tank. Any building constraints will

therefore have no effect in a practical system. It should however be kept in mind that the panel outlet should not be lower than the storage tank outlet, to enable thermosyphon flow.

6.5. PANEL TILT ANGLE

The tilt angle of the panel is also likely to be influenced by the building geometry along with the height difference described in the previous paragraph.

The tilt angle of the panel was varied between 10° and 60° relative to the horizontal to study the effect on the mass flow rate and the mean storage tank temperature. The results for different tilt angles are plotted in Figure 43 and Figure 44.

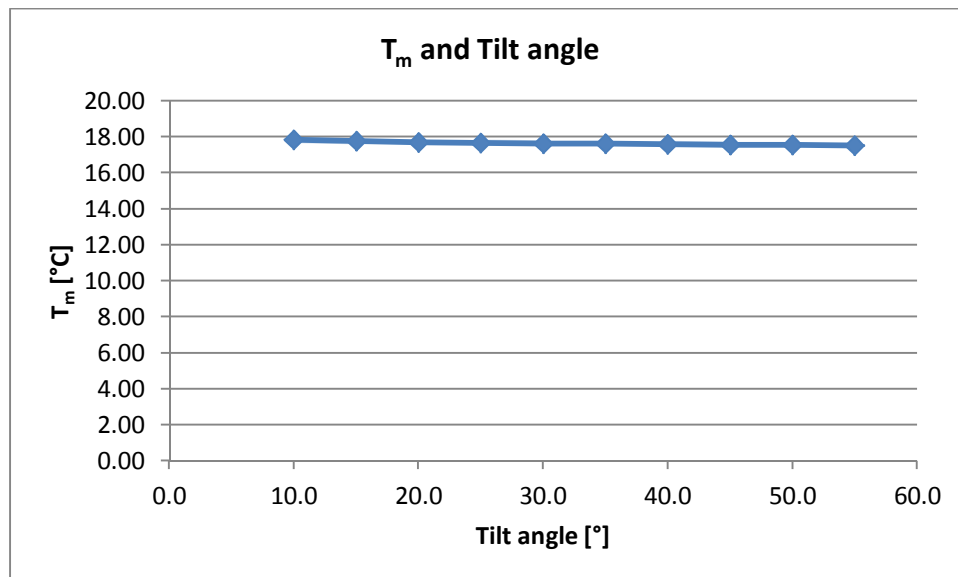


Figure 43 : Effect of tilt angle on mean storage tank temperature

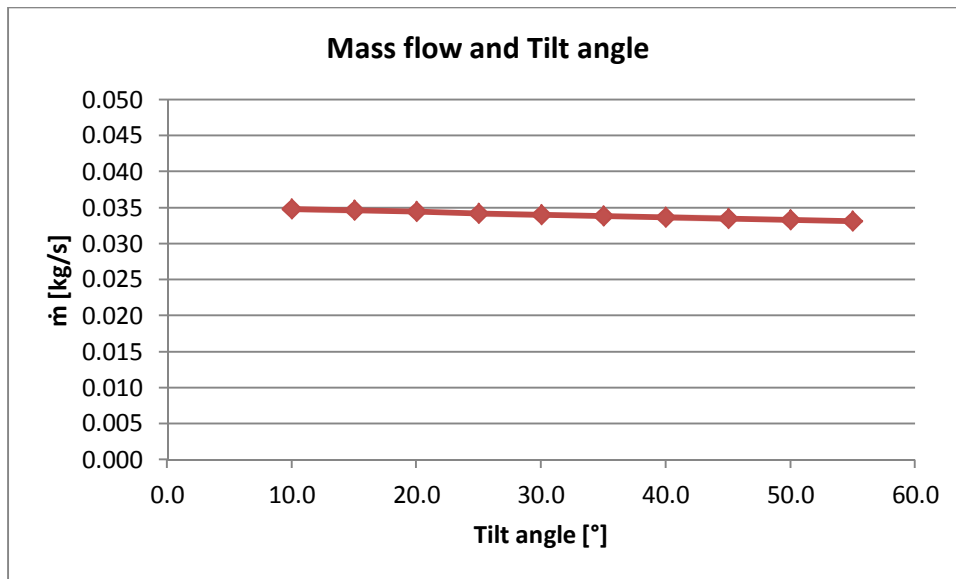


Figure 44 : Effect of tilt angle on mass flow rate

Both graphs indicate that different tilt angles had a very small effect on the mass flow rate and mean storage tank temperature.

For flow stability and to help initiate the thermosyphon flow the panel should be inclined by more than zero degrees. For this reason a minimum tilt angle of 10° was chosen for this analysis. The panel tilt angle should also be such that the panel has a clear line of sight to the night sky. Any nearby building or vegetation obscuring this path would significantly reduce the performance of the system.

It is advised to have the panel at an incline. This is to allow the denser cold water in the panel to flow downwards more easily.

From the results it was therefore concluded that the system performance is not significantly affected by the panel tilt angle if constrained by building geometries.

6.6.STORAGE TANK DIMENSIONS

The storage tank is an important part of the radiative cooling system. One particularly important aspect of the storage tank is its height and diameter relation. Standard “Off the Shelf” storage tanks are likely to be used in practice to keep system costs down. It is therefore important to determine if the storage tank dimensions have any significant effect on the system performance.

The effect of the storage tank dimensions was analysed by varying the storage tank height and diameter for a fixed volume. This gave two extreme scenarios for the storage tank

design. The one extreme is a shallow large diameter tank and the other is a high, small diameter tank. The results of this analysis are given in Figure 45 and Figure 46.

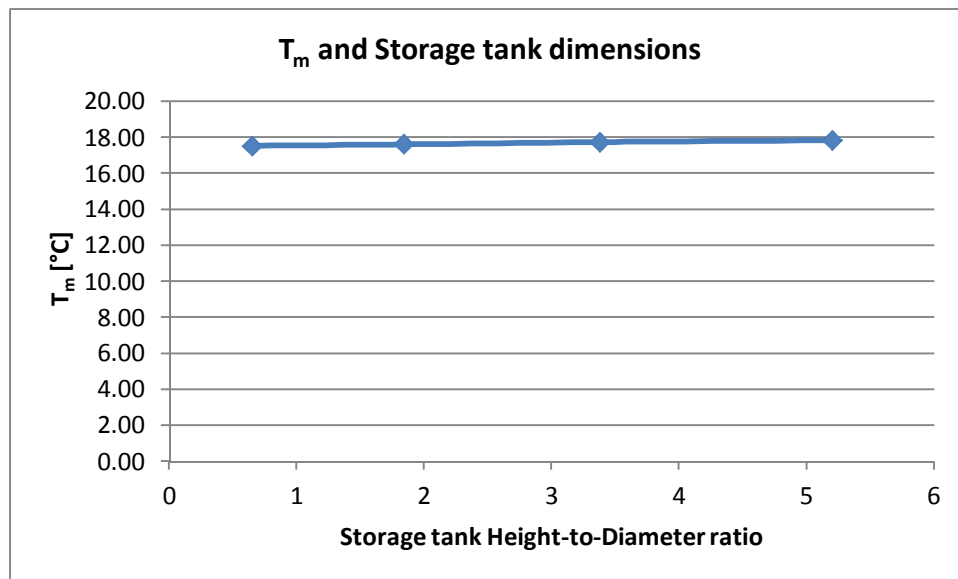


Figure 45 : Effect of storage tank dimensions on mean storage tank temperature

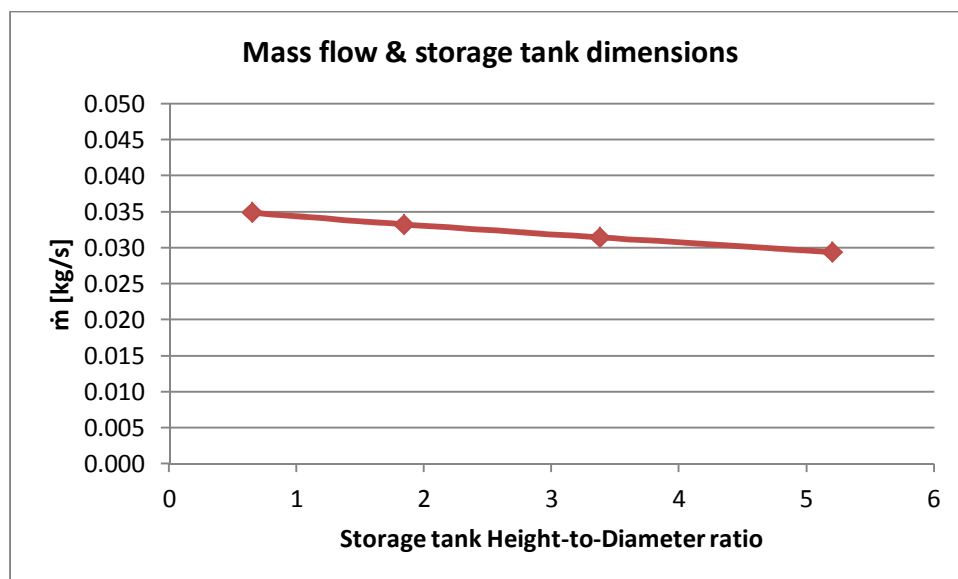


Figure 46 : Effect of storage tank dimensions on mass flow rate

The analysis on the storage tank dimensions indicated that the mean storage tank temperature and mass flow rate was not significantly influenced. This analysis however did not include the effect of stratification inside the storage tank on the performance. In practice it is better to have a high, small diameter tank. Thermal stratification layers are more easily formed in this setup and are not disturbed as easily.

The main consideration for the storage tank design is the amount of energy that needs to be stored. The storage tank must be able to provide enough stored energy to keep the temperature fluctuation within a specified range for a given time period. This consideration also has financial implications in practice.

The position of the inlet and outlet is also of high importance for the storage tank design. According to Dincer & Rosen [24] it is possible to get so called dead zones in the tank with poorly positioned in- and outlets. This effectively reduces the amount of useable storage capacity. The effect of the storage tank in- and outlets are shown in Figure 47 below. The inlet and outlet should be positioned as far apart as possible to maximise the storage capacity.

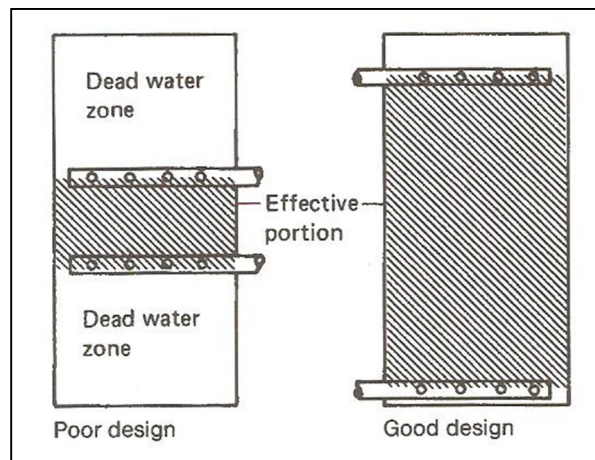


Figure 47 : Thermally stratified tank in- and outlet design [24]

Another aspect mentioned by Dincer & Rosen is the temperature difference between the in- and outlet. The optimal temperature difference according to them is at least 5-10 °C between the upper and lower parts of the tank. The velocity of the flow into the tank should also be kept low in order to maintain the thermal stratification layers. Diffusers or other methods of flow distribution hardware can be applied if the flow velocity is a concern.

The detail design and optimisation of the system storage tank involves many aspects and falls outside the purpose of this study. Only a few of these aspects have been briefly discussed in this section to note its importance. Thermal storage systems and its design are comprehensively covered by Dincer & Rosen [24].

6.7. SYSTEM PERFORMANCE CONCLUSIONS

The investigations done in this chapter gave a good insight on the influences of certain system parameters on the performance.

Parameters that were of concern such as the connecting pipe diameter and storage tank dimensions turned out to have an insignificant effect on the performance. Other parameters that did not have a significant effect on the performance include the panel height and tilt angle.

Some parameters did however have a significant effect on the overall system performance. Two of the most influential parameters are the relative humidity and panel surface emissivity.

The information provided in this chapter can be used as design considerations for future radiative cooling system developments.

7. APPLIED MODEL: YEAR ROUND PERFORMANCE

7.1. INTRODUCTION

The purpose of the theoretical model is to simulate and predict the performance of a radiative cooling system. The model was therefore applied in several case studies to serve its purpose.

This chapter provides some baseline design parameters for a radiative cooling system involving the required panel surface and storage capacity. This design baseline was used to do a year round simulation of a radiative cooling system at various locations with differing meteorological conditions.

7.2. RADIATIVE COOLING SYSTEM DESIGN BASELINE

At the beginning of this study it was agreed that the goal of the radiative cooling system should be to provide a more constant heat sink for a thermodynamic cycle. To achieve this purpose a temperature range is needed for a design guideline. Such a temperature guideline was revealed in the previous study undertaken by Theunissen & Brink [27].

It was noted in that particular study that the storage tank temperature was very similar to the daily average of the ambient air temperature. The average ambient temperature is exactly the storage tank temperature that is required when the daily minimum and maximum ambient temperatures are to be evened out. This average temperature also turned out to be a viable guideline in terms of the required storage tank capacity and heat load input.

The daily average of the ambient temperature was therefore used as the design criterion for the mean storage tank temperature. The aim must be to keep the daily average of the storage tank temperature equal to or less than the average ambient temperature most of the time. The mean storage tank temperature should not show increasing trends above this average ambient temperature.

For the system to be effective as a heat sink it was decided that the system must be designed to absorb a temperature fluctuation of 5°C over a 12 hour period. This 5°C temperature range should be approximately equal to the average ambient temperature guideline set out.

The next design guideline that was decided upon involved the summer maximum conditions. The worst case scenario considered in the system design will occur in summer when the temperatures and relative humidity is usually at its peak. The annual maximum average ambient temperature usually occurs in the summer months of January and February in South African conditions. The design criterion therefore is for the system to be able to deliver adequate performance during this time of the year.

The required panel size and storage capacity must be based on the expected average heat loss per square meter of panel during this time. The winter conditions do not pose any threat in terms of the system performance. The cold ambient temperatures experienced in most parts of South Africa are preferable for good system performance although freeze resistance becomes a concern in some cases.

With the design guideline now established it was possible to scale up the model to a practical system size. The design parameters and calculations of the scaled up model are as follows:

The starting point of the design was the heat load that the system must be able to handle. A constant heat load input of 1 kW was chosen for the scaled up design.

The next step of the design was to calculate the required storage capacity to absorb the 5°C temperature increase with the 1 kW heat load. This is done with the following equation:

$$Q = mCp(\Delta T) \quad (56)$$

An assumption that is used in the design is that the energy input is over a 12 hour period during the day by the heat load. The energy supplied to the system is therefore:

$$Q = W * T \quad (57)$$

The values of W, T, Cp and ΔT were substituted in this equation to give the rounded up storage tank mass. For this design it was decided that water is used as the storage medium.

$$m = \frac{1 * 12 * 3600}{4.2 * 5} = 2057.14 \approx 2100 \text{ kg} \quad (58)$$

With the density of water assumed as 1000 kg/m³ it gives a storage capacity of 2100 litres.

From the historical meteorological data it was concluded that a typical South African summer night has an average temperature of 16°C and a relative humidity of 75%. This is therefore the most probable conditions under which the system must perform at night as a worst case scenario. The amount of Watt that a square meter of panel is able to dissipate at these conditions was determined by the method described in paragraph 3.6. By using the method described therein it was determined that the minimum Watt dissipated per square meter of panel are 40 W/m² during night time. This figure was used to calculate the total panel surface that is required to dissipate the storage tank heat load.

The required surface area of the panels is calculated by taking into account the amount of energy that needs to be dissipated during a night. If it is assumed that the heat load remains constant, the panel needs to dissipate this heat load and the accumulated energy of the heat load during the day. The panels should in essence dissipate double the daytime heat load input at night. The equation used for calculating the required panel surface is given below:

$$\text{Area} = 2 * \frac{W}{W/m^2} = 2 * \frac{1000}{40} = 50 \text{ m}^2 \quad (59)$$

A typical panel would be in the range of 1.5 to 2 metres long. If a length of 2 metres is used it means that the panels need to be 25 metres wide to provide the required surface area exposed to the night sky.

The calculated storage tank volume and subsequent required panel surface is used as the design baseline and applied in the practical model simulations. The performance at various locations and meteorological conditions is covered in the next section.

A summary of the design parameters is as follows:

Table 5 : Design baseline summary

Storage capacity	2100 litres
Panel surface	50 m ²
Panel length	2 m
Panel width	25 m
System height (h_1)	3 m
Storage medium	Water
Mean starting temperature	20°C

All other constants required in the scaled up model simulations are equal to the constants set out in chapter 4.3.1 in Table 3 and Table 4.

7.3. APPLIED THEORETICAL MODEL

The viability of a radiative cooling system for heat sink regulation was tested by simulating the performance at different locations throughout South Africa. The chosen locations are scattered throughout the country and are situated in very different meteorological climates. Basic simulations were done with the theoretical model in order to show the annual trend of the storage tank temperature.

Historical meteorological data for January to December of 2010 were used as input parameters to do the simulations at each of the locations [32]. The historical data that were used was given in six hour intervals. The simulations therefore gave crude predictions of the storage tank temperature throughout the year. This was not of any concern since the purpose of the simulations is to give an indication of the annual storage tank temperature trend. A comprehensive analysis of the system performance can be done by using more detailed weather data.

The effect of cloud cover or any other unusual weather conditions were not considered in these simulations due to the complex adjustments that are required to the theoretical model. It was therefore assumed that clear sky and windless conditions prevailed.

The chosen locations and their relevant system performance are described in the following paragraphs.

7.3.1. Simulation 1: Johannesburg

The city of Johannesburg was chosen because it represents the typical climate experienced in most parts of South Africa. Summer temperatures are usually above 25°C during the day and fall to between 15 to 20°C at night. Very cold winter temperatures are often experienced in this region. The winter daytime temperatures typically range between 15 and 20°C and night time temperatures range from below zero to 10°C.

The sky conditions are normally clear for most of the year especially during the winter months. Cloud cover is usually experienced in the form of summer thunderstorms or rainy overcast days that can last for a week or two. The humidity of this climate is ordinary and range on average from 70% in summer to 30% in winter.

The climate of Johannesburg therefore provides a broad spectrum of weather conditions that a radiative cooling system will be exposed to in practice.

The historical annual meteorological data of Johannesburg were used as input to the theoretical model. The resulting annual storage tank temperature is plotted in Figure 48.

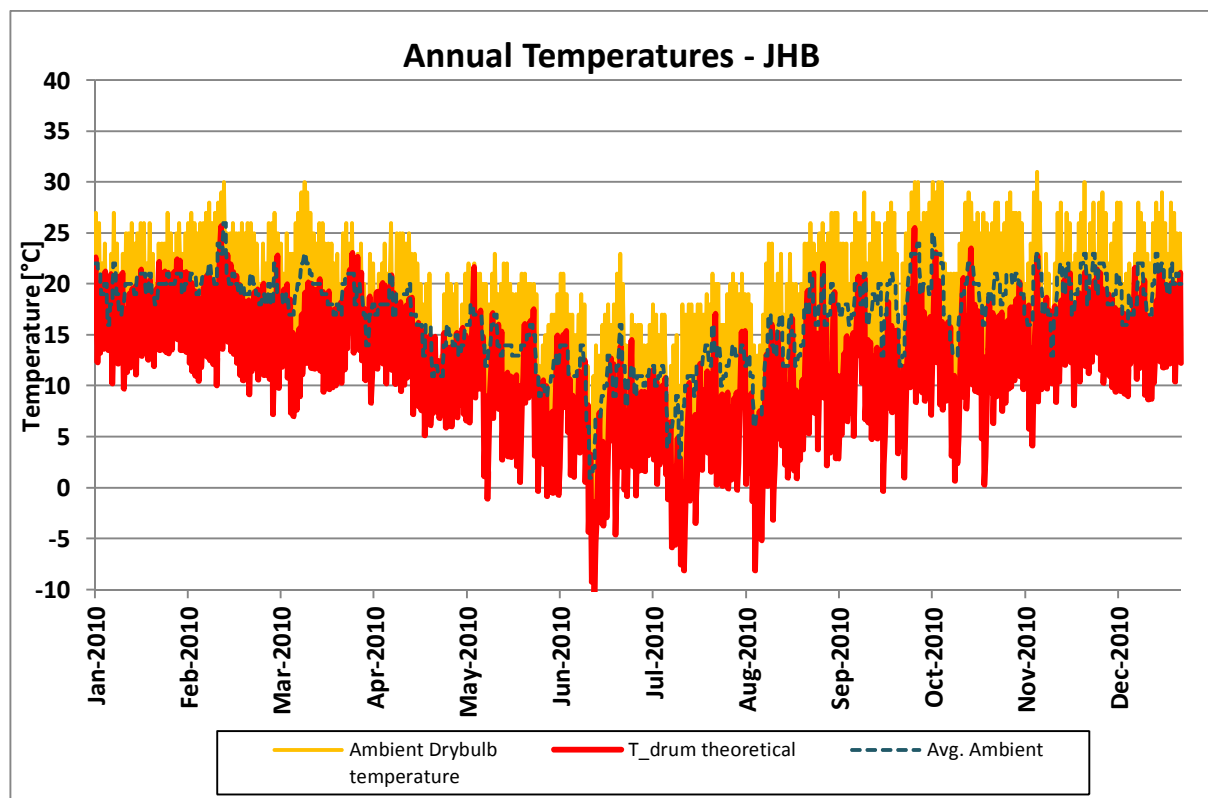


Figure 48 : Annual system performance for Johannesburg

The results given in the graph are very promising. It is evident that the storage tank temperature is able to remain equal to, or below the daily average ambient temperature throughout the year. The storage tank temperature did not indicate any increasing trend

apart from the winter to summer transition which was expected. This means that the chosen panel size and storage capacity is sufficient for the applied heat load. The graph also indicates that the radiative system was able to eliminate the daily maximum peaks that would otherwise have been the heat sink temperature.

The conclusion made from the results is that the system is able to provide sufficient performance in the climate of Johannesburg throughout the year.

7.3.2. Simulation 2: Pretoria

The climate and weather patterns of Pretoria are very similar to that of Johannesburg. One difference though is that Pretoria has a slightly higher average temperature throughout the year. Day time temperatures during summer typically reach 30°C and night time temperatures range between 15 and 20°C. Winter daytime temperatures range between 15 and 20°C and night time temperatures drops to between 5 and 10°C. The below zero night time temperatures common to Johannesburg are very seldom experienced in Pretoria.

The humidity and cloud cover is very similar to that of Johannesburg. Humidity is usually 70% in summer and around 30% in winter. Cloud cover is also experienced in the form of summer thunderstorms and occasional rainy overcast days that can last for a week or two.

Pretoria is a good climate to study the effect on performance of slightly warmer annual temperatures but similar conditions to that of Johannesburg.

The historical annual meteorological data of Pretoria were used as input to the theoretical model. The resulting annual storage tank temperature is plotted in Figure 49.

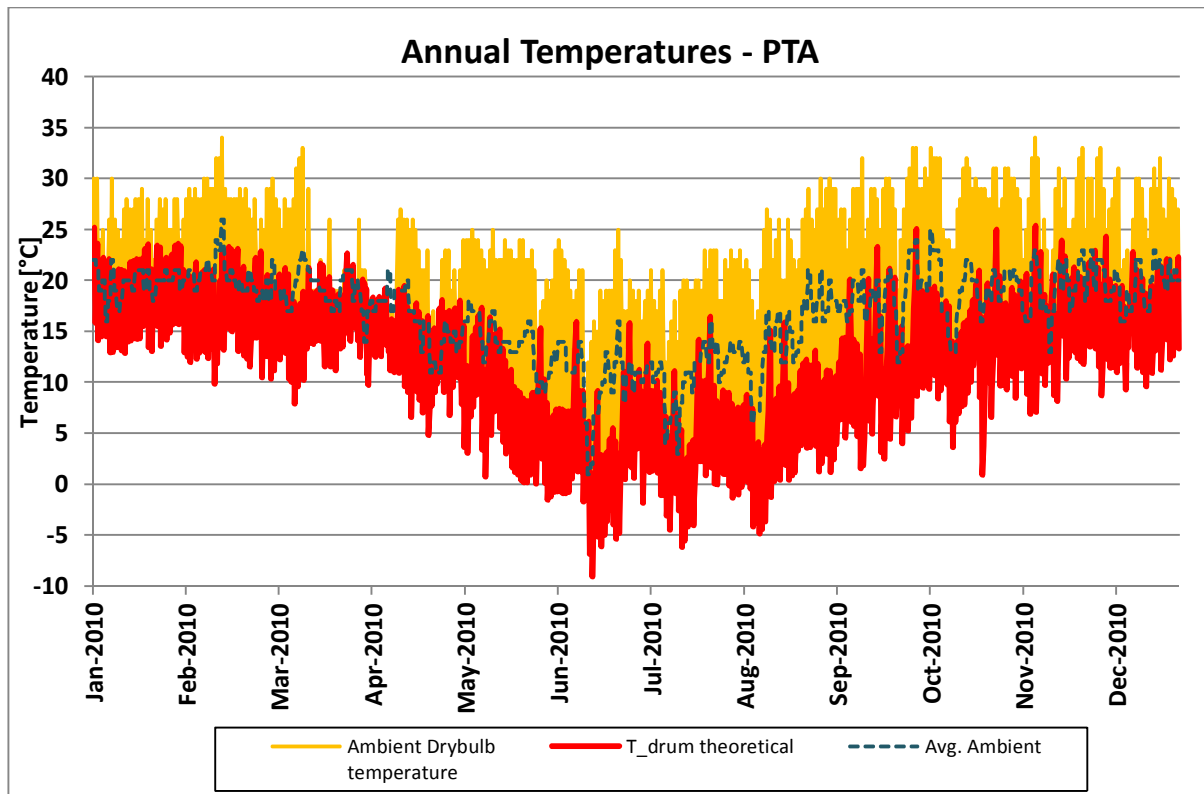


Figure 49 : Annual system performance for Pretoria

The results of the simulation for the climate of Pretoria are very similar to that of Johannesburg despite the slightly warmer temperatures. The explanation for this is the night time temperatures that are in the same range as that of Johannesburg. The annual temperature trend also does not differ considerably from that observed in the Johannesburg simulation. The satisfying results again indicated that the calculated panel size and storage capacity was adequate.

It was concluded from the results of this simulation that the system is able to perform sufficiently in the warm climate of Pretoria.

7.3.3. Simulation 3: Durban

The city of Durban is situated on the eastern coastline of South Africa and is renowned for its hot and very humid climate. The daytime temperatures in summer are normally above 25°C and drops to approximately 20°C at night. The winter temperatures experienced in this region are much warmer than the central parts of the country. Daytime temperatures during winter are usually above 20°C and night time temperatures are around 10 to 15°C. The summer to winter temperature differences is therefore much smaller than other parts of the country. The humidity in this region is easily above 70% throughout the year.

The climate of Durban is therefore good test of the system performance under high humidity and temperatures as well as a small summer-winter temperature difference.

The historical annual meteorological data of Durban were used as input to the theoretical model. The resulting annual storage tank temperature is plotted in Figure 50

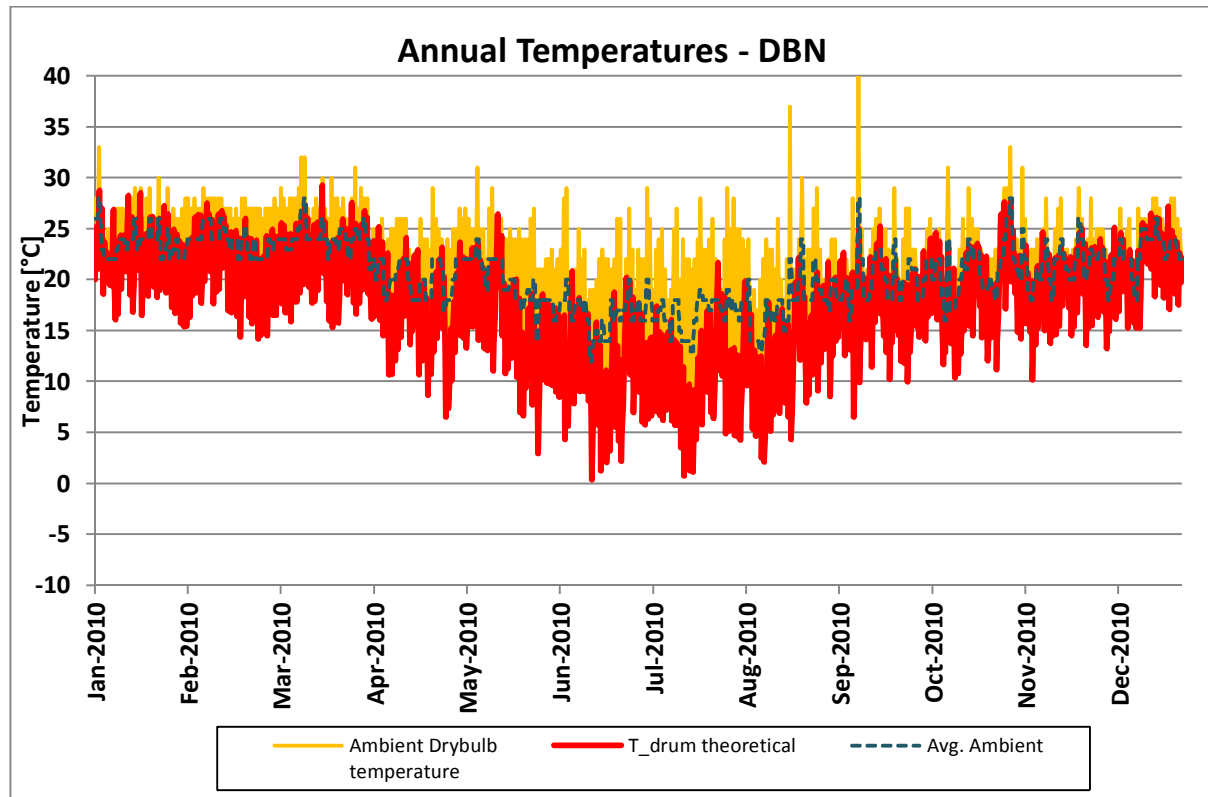


Figure 50 : Annual system performance for Durban

The results from this simulation indicated that the system is able to provide a level of radiative cooling even under the high humidity and night time temperature. The average storage tank temperature is much higher than that observed with Johannesburg and Pretoria. The storage tank temperature increased above the average dry bulb temperature at some stages. This is an indication that either the panel size or storage capacity or both are not sufficient. This problem can be mitigated to some extent by increasing the panel surface and storage capacity although the high humidity is still a significant limiting factor of the system performance in this climate.

It was concluded from this simulation that radiative cooling is possible under this climate conditions although it is significantly less than that experienced in other parts of the country. A detailed analysis should be conducted to determine the feasibility and performance of radiative cooling systems in climates with high temperatures and humidity.

7.3.4. Simulation 4: Cape Town

Cape Town is situated on the southwest coastline of South Africa. This area can experience quite severe weather systems in the form of cold fronts during winter and occasional heat waves in summer.

The summer day time temperatures usually peak around 30°C and easily exceeds 35°C during heat waves. Night time temperatures during summer are usually between 15 and 20°C. The winter daytime temperatures are normally around 20°C and falls to below 10°C at night.

The historical annual meteorological data of Cape Town were used as input to the theoretical model. The resulting annual storage tank temperature is plotted in Figure 51.

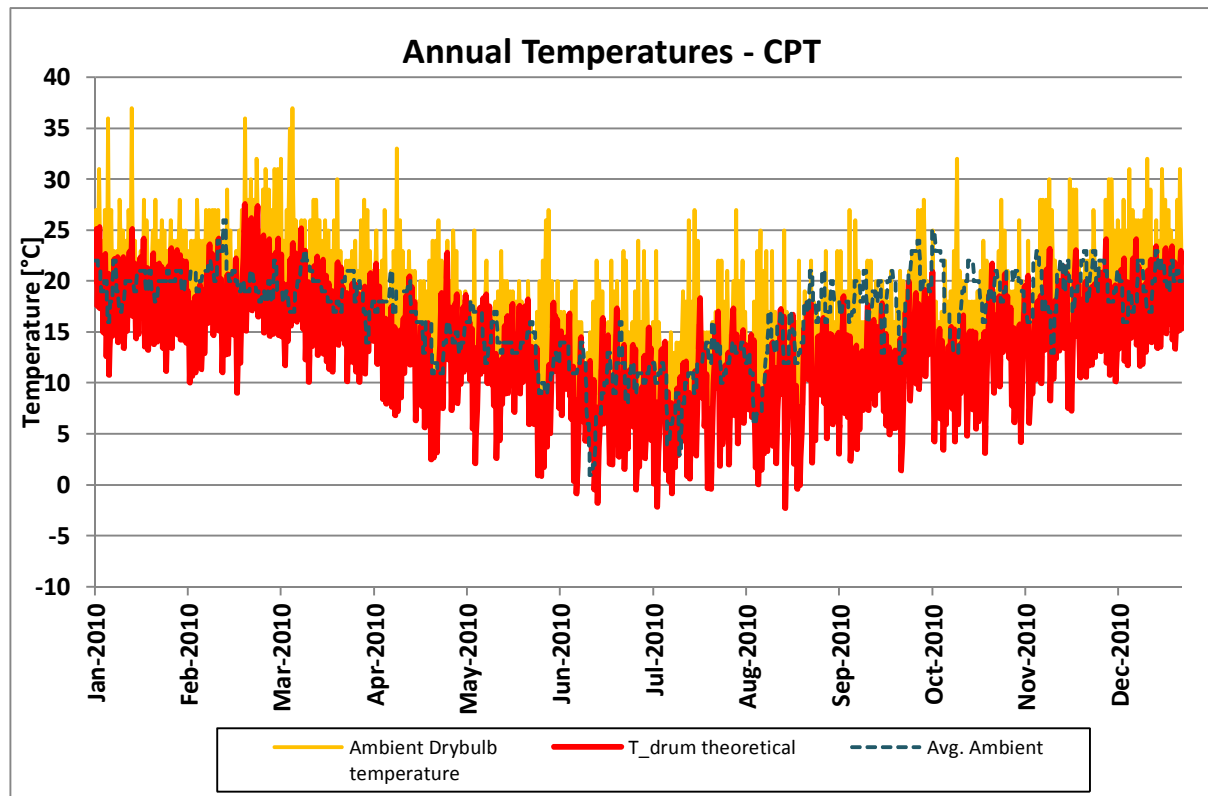


Figure 51 : Annual system performance for Cape Town

The results of this simulation indicated that the system can perform adequately under the weather conditions of Cape Town. The storage tank temperature trend throughout the year is very similar to that of Johannesburg and Pretoria. It was however noticed that the storage tank temperature change during the day is often more than the target of 5°C. This is not of any major concern since the same temperature change was restored most of the time during the night.

A larger storage tank can be used to ensure that the day time temperature change remains within the 5°C target value. It was estimated that a 2800 litre storage tank instead of the 2100 litres would be sufficient to achieve this.

Regardless of the slightly larger temperature changes noticed it was concluded that the system's performance was sufficient for this climate.

7.4. APPLIED MODEL CONCLUSION

The results obtained from the simulations of Johannesburg, Pretoria, and Cape Town were satisfactory. The main objective as set out at the beginning of the study was to even out the daily minimum and maximum temperature fluctuations. The simulations clearly indicated that this goal is achievable. The crude simulations proved that a radiative system is indeed capable of achieving the objective of providing a stabilised heat sink temperature throughout the year. The simulation of Durban is the only scenario that is of concern. Further studying of radiative cooling under high humidity is required to determine the actual performance and feasibility of radiative cooling in such climates.

The monthly average of the storage tank temperatures are indicated in Figure 52 below. From this graph it was again noticed that the system performance at Johannesburg, Pretoria and Cape Town are nearly similar in spite of the differences in climate. The effect of the higher temperature and humidity of Durban is clearly noticeable.

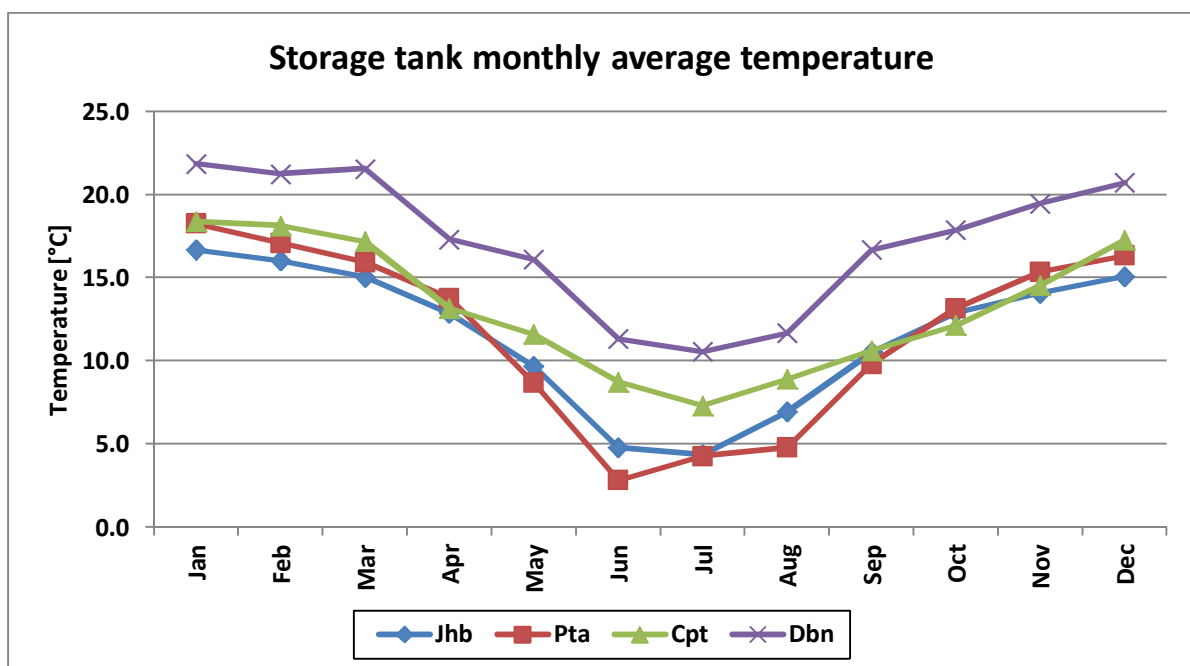


Figure 52 : Storage tank monthly average temperature comparison

The simulations confirm that the method used to determine the design baselines is sufficient for this application of a radiative cooling system. The baseline parameters such as the storage tank temperature change and the panel watts per square meter should be optimised to suite the application and weather conditions.

It should be stressed again that the simulation done in this chapter are only basic and crude. A detailed design and analysis is required to accurately determine the performance and feasibility of a radiative cooling system in a specific location.

8. CONCLUSIONS AND RECOMMENDATIONS

8.1. CONCLUSION

The need for energy saving and independence of fossil fuels has gained much popularity. This driving force has led to the research and development of a cooling system that utilises radiative cooling to the night sky.

The objective of this study was to develop a theoretical model to simulate and analyse the performance of a radiative cooling system. A literature study pointed out that all previous studies on radiative cooling systems were conducted on an experimental basis. Experimental studies are time consuming and costly exercises that impede the research and development of radiative cooling systems. The feasibility of radiative cooling systems in general was evaluated with the help of this model for various South African climate zones.

The theoretical model was developed with the help of models and information obtained from flat-plate solar water heating systems. The many similarities between a radiative cooling system and a flat-plate solar water heating system made it possible to use this knowledge. A mathematical model that was originally developed for a natural circulation solar water heater formed the basis of the radiative cooling system model. The heat gains in the original model were replaced by a night sky radiation and a convection heat transfer component for cooling. Fundamental heat transfer and fluid flow elements were also incorporated into the model.

The completed theoretical model was able to simulate the mean storage tank temperature with the ambient air temperature and relative humidity as the primary input parameters.

The theoretical model was verified with the help of an experimental setup. A number of deviations were observed when the experimental and theoretical results were compared. These differences were analysed to determine the cause. Corrective actions were applied where possible to improve the accuracy of the model. The final theoretical model delivered satisfactory results at the end and correlated well with the empirical data.

The model was used to analyse the impact of various parameters on the performance of a radiative cooling system. This gave a better understanding of the impact which each critical parameter had on the system performance. The relative humidity and panel emissivity turned out to have had the most significant influence on the performance.

The model was applied in a case study to analyse the performance of a radiative cooling system in various South African climate zones. The climates ranged from cold and dry conditions experienced in the inland regions of the country to the very hot and humid conditions of the coastal regions. The crude simulation of the model showed that a radiative cooling system is able to perform sufficiently under most climates. The system did however perform less admirably in hot and humid climates. This was expected because the humidity was known to have a great influence on the effective night sky temperature.

The overall size of the radiative cooling system was an important concern at the start of this study. An unfeasibly large system would render the practical application of a radiative

cooling system useless. The simulation of the model with reasonable input conditions showed that the system size is indeed practical. The design criteria that were used proved to be sufficient to determine the size of the storage tank and panel surface area.

The model that was developed served its purpose in providing a non-experimental method of research on radiative cooling systems.

8.2. RECOMMENDATIONS AND FUTURE DEVELOPMENTS

The theoretical model that was developed in this study is a basic model that served as a starting point for further research and development. The current model is restricted to a certain system layout and a temperature range. Parameters such as convection coefficients need to be revised for extremely high or low temperatures.

The model is also restricted to clear sky and windless conditions. The effect of wind can greatly increase the overall heat loss of the panel whilst overcast conditions can reduce the performance. The exact impact of overcast conditions on the radiative component of the heat transfer is still unclear and should be studied further to get a better understanding.

The possibility of an indirect freeze resistant thermosyphon loop should be investigated for a more cost effective design. This is particularly important for very cold climates when freezing of the panel can occur.

This study only analysed the performance of a natural circulation system. A comparative study can be done to gauge its performance against a forced flow system.

The aim of this study was to develop a system that is able to mitigate the ambient temperature fluctuations experienced by a heat sink. The system was able to provide a more stable heat sink temperature on a day-night cycle but a significant fluctuation is still present between summer and winter. Heating instead of cooling in winter, or the throttling of the cooling mass flow, should be investigated to try and maintain a set temperature range throughout the year.

A detailed analysis of the system performance under different climates and conditions should be undertaken to optimise the system design. The analysis in this study used a very crude dataset to look briefly at climates that are most likely to be encountered in South Africa.

The design of the radiative cooling system with natural circulation should be revised to try and optimise the performance. Aspects that need to be addressed are tube spacing on the panels, pipe network lengths and configuration, storage tank design and the mean system temperatures.

There are other applications of this initiative, which can be applied with innovation. An example is by simultaneously combining an upper storage tank (hot) with a lower storage tank (cold) to north facing solar panels (Southern hemisphere), with relatively simple plumbing. The operation would be the heating of e.g. water during day-time (in the upper reservoir) and the cooling of the water (in the lower reservoir) during night-time, in one direct

system. A spin-off would be the protection of the panels against freezing during the night without utilising an indirect system with an expensive freeze resistant working fluid. Direct systems are more efficient and less costly than indirect freeze resistant systems. Natural circulation also works adequately on both the heating and cooling modes of operation. The hot reservoir maintains its temperature during the night and so does the cold reservoir during daytime. This was proven in a test rig and was a pilot test which actually gave rise to this initiative for a more advanced application of the principle, as in this study [11].

8.3. CLOSURE

The intention of this study was to provide a better understanding of a radiative cooling system's performance. The lack of knowledge has certainly been filled with the help of the theoretical model that was developed in this study.

The importance and feasibility of radiative cooling systems in general was unclear at the start of this study, especially natural circulating systems. This study proved that a natural circulating system is indeed able to provide sufficient cooling performance with a feasible system size and layout.

Radiative cooling systems are an overlooked form of alternative energy and it can play an important role in the quest towards global energy efficiency. It must therefore receive more attention in future regarding development, refinement and new applications.

9. REFERENCES

- [1] "World Energy Outlook 2009," International Energy Agency, 2009.
- [2] "World Economic Outlook," International Monetary Fund, 2011.
- [3] "Digest of South African energy statistics 2009," Department of Energy South Africa, 2010.
- [4] "South African Energy Synopsis 2010," Department of Energy South Africa, 2010.
- [5] (2010) Eskom IDM. [Online]. www.eskomidm.co.za
- [6] Edward G. Pita, *Refrigeration Principles and Systems*.: John Wiley & Sons, 1984.
- [7] T.D. Eastop and A. McConkey, *Applied Thermodynamics for Engineering Technologists*, 3rd ed.: Longman Group Limited, 1978.
- [8] J.A. Duffie and W.A. Beckman, *Solar Engineering of Thermal Processes*.: John Wiley & Sons, 1974.
- [9] T.J. Jansen, *Solar Engineering Technology*.: Prentice-Hall, 1985.
- [10] Y. Shiran, A. Shitzer, and D. Degani, "Computerized design and economic evaluation of an aqua-ammonia solar operated absorption system," *Solar Energy*, vol. 29, no. 1, pp. 43-54, 1982.
- [11] J.G. Van Antwerpen, J.A. Bezuidenhout, and S.P. Oelofse, "Doeltreffendheid van die tweeluskonsep om 'n direkte sonwater verwarmers vriesbestand te maak," North-West University, Potchefstroom, Final year project report 2008.
- [12] Prof. C.P. Storm, Thermo fluid systems design - course notes, North-West University, 2009.
- [13] (2004) Passive Solar Heating and Cooling Design Booklet. [Online]. www.azsolarcentre.com
- [14] M.A. Al-Nimr, Z Kodah, and B Nassar, "A theoretical and experimental investigation of a radiative cooling system," *Solar Energy*, vol. 63, no. 6, pp. 367-373, 1998.
- [15] R.T. Dobson, "Thermal modelling of a night sky radiation cooling system," *Journal of Energy in Southern Africa*, vol. 16, no. 2, pp. 20-31, 2005.
- [16] S Ito and N Miura, "Studies of radiative cooling systems for storing thermal energy," *Journal of Solar Energy Engineering*, vol. 111, no. 3, pp. 251-256, 1989.
- [17] E. Erell and Y. Etzion, "Radiative cooling of buildings with flat-plate solar collectors," *Building and Environment*, vol. 35, no. 4, pp. 297-305, 2000.
- [18] M.G. Meir, J.B. Rekstad, and O.M. Løvvik, "A study of a polymer-based radiative cooling system," *Solar Energy*, vol. 73, no. 6, pp. 403-417, 2002.

- [19] A.W. Harrison and M.R. Walton, "Radiative cooling of TiO₂ white paint," *Solar Energy*, vol. 20, no. 2, pp. 185-188, 1977.
- [20] A Dimoudi and A Androutsopoulos, "The cooling performance of a radiator based roof component," *Solar Energy*, vol. 80, pp. 1039-1047, 2006.
- [21] D.J. Close, "The performance of solar water heaters with natural circulation," *Solar Energy*, vol. 6, no. 33, pp. 33-40, 1962.
- [22] F.P. Incropera, D.P. Dewitt, T.L. Bergman, and A.S. Lavine, *Fundamentals of Heat and Mass Transfer*, 6th ed.: John Wiley & Sons, 2007.
- [23] M. Pérez-García, "Simplified modelling of the nocturnal clear sky atmospheric radiation for environmental applications," *Ecological Modelling*, vol. 180, pp. 395-406, 2004.
- [24] I. Dinçer and M.A. Rosen, *Thermal energy storage*, 1st ed.: John Wiley & Sons, 2002.
- [25] S.M. Hasnain, "Review on sustainable thermal energy storage technologies, Part II: Cool thermal storage.," *Energy Conversion and Management*, vol. 39, no. 11, pp. 1139-1153, 1998.
- [26] J.A. Duffie and W.A. Beckman, *Solar Engineering of Thermal Processes*, 2nd ed.: John Wiley & Sons, 1991.
- [27] R. Theunissen and F. Brink, "Heat sink for solar powered device," North-West University, Potchefstroom, Final year project report 2009.
- [28] H.P. Garg, "Design and performance of a large-size solar water heater," *Solar Energy*, vol. Vol 14, pp. 303-312, 1971.
- [29] B.R. Munson, D.F. Young, and T.H. Okiishi, *Fundamentals of Fluid Mechanics*, 5th ed.: John Wiley & Sons, 2006.
- [30] A. Zerrouki, A. Boumédién, and K. Bouhadeb, "The natural circulation solar water heater model with linear temperature distribution," *Renewable Energy*, vol. 26, pp. 549-559, 2002.
- [31] E. Kreyszig, *Advanced Engineering Mathematics*, 8th ed.: John Wiley & Sons, 1999.
- [32] Weather Underground. [Online]. www.wunderground.com
- [33] R.E. Sontag, C. Borgnakke, and G.J. van Wylen, *Fundamentals of thermodynamics*, 6th ed.: John Wiley & Sons, 2003.
- [34] A. Sözen, D. Altıparmak, and H. Usta, "Development and testing of a prototype of absorption heat pump system operated by solar energy," *Applied Thermal Engineering*, vol. 22, no. 16, pp. 1847-1859, 2002.
- [35] G.L. Morrison and D.B.J. Ranatunga, "Thermosyphon circulation in solar collectors," *Solar Energy*, vol. 22, no. 2, pp. 191-198, 1980.

APPENDIX A: SAMPLE CALCULATION

A sample calculation is done in this section to illustrate the calculation steps and results of the theoretical model.

A 1: INPUT VARIABLES

The first part of the model is the calculating of the various input parameters that are required.

The following starting values at a specific time of step were used:

1. $T_{db} = 3.97 \text{ }^{\circ}\text{C}$
2. $T_m = 14.9 \text{ }^{\circ}\text{C}$
3. $T_{wb} = 2.3 \text{ }^{\circ}\text{C}$
4. $RH = 69 \%$ (Determined with T_{db} and T_{wb})
5. $Q_{load} = 30 \text{ W}$
6. $C_p = 3800 \text{ J/kgK}$
7. $m = 234.83 \text{ kg}$
8. $\varepsilon = 0.7$
9. $k = 0.045 \text{ W/m}^2\text{K}$
10. $x = 0.065 \text{ m}$
11. $A_{tank} = 2.332 \text{ m}^2$
12. $A_{panel} = 1 \text{ m}^2$

Effective sky temperature:

To calculate ε_{sky} the dew point temperature is required

$$\begin{aligned} T_{dp} &= RH^{\frac{1}{8}}(112 + 0.9T_{db}) + 0.1T_{db} - 112 \\ &= (0.69)^{\frac{1}{8}}(112 + 0.9(3.97)) + 0.1(3.97) - 112 = -1.2 \text{ }^{\circ}\text{C} \end{aligned}$$

The equivalent sky emissivity is:

$$\begin{aligned} \varepsilon_{sky} &= 0.741 + 0.62 \left(\frac{T_{dp}}{100} \right) \\ &= 0.741 + 0.62 \left(\frac{-1.2}{100} \right) = 0.734 \end{aligned}$$

The effective sky temperature is given below (with T_{sky} and T_{db} in Kelvin):

$$\begin{aligned} T_{sky} &= (\varepsilon_{sky})^{0.25} T_{db} \\ &= (0.734^{0.25} * (3.97 + 273.15)) - 273.15 = -16.7 \text{ } ^\circ\text{C} \end{aligned}$$

Storage tank thermal resistance:

The thermal resistance of the storage tank is given by:

$$\begin{aligned} R &= \sum R_t = \frac{x}{k} \\ &= \frac{0.065}{0.045} = 1.444 \end{aligned}$$

A 3: HEAT TRANSFER

Storage tank heat loss/gain:

The first heat transfer that is considered is that of the storage tank heat gain/loss calculated by:

$$\begin{aligned} Q_{tank} &= \frac{A_{tank}(T_{db} - T_m)}{R} \\ &= \frac{2.332(3.97 - 14.9)}{1.444} = -17.4 \text{ W} \end{aligned}$$

Radiation heat transfer:

The next heat transfer that is considered is the thermal radiation from the panel surface to the night sky. The thermal radiation heat transfer is given by:

$$\begin{aligned} Q_{rad} &= \varepsilon \sigma A (T_{sky}^4 - T_m^4) \\ &= 0.7 * 5.67051 * 10^{-8} * 1 * [(-16.7 + 273.15)^4 - (14.9 + 273.15)^4] \\ &= -101.4 \text{ W} \end{aligned}$$

Convective heat transfer:

The last heat transfer to be calculated is the convective heat transfer from the panel surface to the surrounding air.

The free convection coefficient h convective has to be calculated first before the convective heat transfer can be calculated.

The thermal properties of the air are:

$$\begin{aligned} \nu &= 1.35159 * 10^{-5} + 9.5 * 10^{-8} \left(\frac{T_{db} + T_m}{2} \right) \\ &= 1.35159 * 10^{-5} + 9.5 * 10^{-8} \left(\frac{3.97 + 14.9}{2} \right) = 1.44 * 10^{-5} \text{ m}^2/\text{s} \end{aligned}$$

$$\begin{aligned} k &= 0.0241 + 7.7 * 10^{-5} \left(\frac{T_{db} + T_m}{2} \right) \\ &= 0.0241 + 7.7 * 10^{-5} \left(\frac{3.97 + 14.9}{2} \right) = 0.0249 \text{ W/m}^2\text{K} \end{aligned}$$

$$\begin{aligned} \alpha &= 1.90077 * 10^{-5} + 1.4 * 10^{-7} \left(\frac{T_{db} + T_m}{2} \right) \\ &= 1.90077 * 10^{-5} + 1.4 * 10^{-7} \left(\frac{3.97 + 14.9}{2} \right) = 2.03 * 10^{-7} \text{ m}^2/\text{s} \end{aligned}$$

$$T_f = \frac{T_m + T_{db}}{2} = \frac{3.97 + 14.9}{2} = 9.4 \text{ }^\circ\text{C}$$

$$\beta = \frac{1}{(T_f + 273.15)} = \frac{1}{9.4 + 273.15} = 0.003539$$

The characteristic length of the panel is:

$$L_c = \frac{L * B}{2(L + B)} = \frac{1 * 1}{2 * (1 + 1)} = 0.25 \text{ m}$$

The Rayleigh number can now be calculated by:

$$Ra = \frac{g \sin \phi \cdot \beta (T_{db} - T_m) (L_c)^3}{\nu \alpha}$$

$$= \frac{9.81 \sin(40) * 0.003539 * (14.9 - 3.97) * (0.25)^3}{1.44 * 10^{-5} * 2.03 * 10^{-7}} = 1.303 * 10^7$$

With the Rayleigh number known the Nusselt number can be calculated:

$$Nu = 0.15 \cdot Ra^{\frac{1}{3}} \text{ for } (10^7 \leq Ra \leq 10^{11})$$

$$= 0.15(1.303 * 10^7)^{\frac{1}{3}} = 35.2$$

The free convection coefficient h is then calculated by:

$$h = Nu \cdot \frac{k}{L_c} = 35.2 \left(\frac{0.0249}{0.25} \right) = 3.505 \text{ W/m}^2\text{K}$$

With h now known the convective heat transfer is calculated:

$$Q_{conv} = hA(T_{db} - T_m) = 3.505 * 1 * (3.97 - 14.9) = -38.2 \text{ W}$$

A 4: MEAN STORAGE TANK TEMPERATURE

With Q_{rad} , Q_{conv} and Q_{tank} all know the mean storage tank temperature for a time step of 15 minutes (900 seconds) is calculated with:

$$T_{m(n+1)} = T_{m(n)} + x_{step} \cdot \left[\frac{(Q_{rad} + Q_{conv} + Q_{load} + Q_{tank} + Q_{ads}) \cdot Timestep}{c} \right]$$

$$= 14.9 + 1 * \frac{(-101.4 - 38.2 + 30 - 17.4 + 15) * 900}{8.923 * 10^5} = 14.7 \text{ } ^\circ\text{C}$$

with c calculated by:

$$c = m * Cp = 234.83 * 3800 = 8.923 * 10^5 \text{ J/K}$$

A 5: THERMOSYPHON MASS FLOW RATE

With the mean storage tank temperature known it is possible to calculate the thermosyphon mass flow rate with:

$$\left(\frac{Q_{tank} + Q_{load} + Q_{ads} - c \cdot \frac{dT_m}{d\theta}}{\dot{m}C_p} \right) (-2 \cdot 1.749 \cdot 10^{-6} \cdot T_m - 3.151 \cdot 10^{-4}) \cdot \left((h_1 - h_3) - 0.5(h_1 - h_2) - 0.5 \left(\frac{(h_5 - h_3)^2}{(h_5 - h_6)} \right) \right) = \left(\frac{128\dot{m}L_p\nu}{\pi ND_p^4} \right) \left(1 + N \left(\frac{L_{cp}}{L_p} \right) \left(\frac{D_p}{D_{cp}} \right)^4 \right)$$

The change in temperature $\frac{dT_m}{d\theta}$ is obtained by the difference between $T_{m(n+1)}$ and $T_{m(n)}$ over the time step.

$$\frac{dT_m}{d\theta} = \frac{14.75 - 14.88}{900} = -1.44 \cdot 10^{-4}$$

To simplify the mass flow equation solving the term in us taken out and the equation is then broken up in parts. The equation above was broken up as follow:

$$A = \left(\frac{Q_{tank} + Q_{load} - c \cdot \frac{dT_m}{d\theta}}{C_p} \right)$$

$$B = (-2 \cdot 1.749 \cdot 10^{-6} \cdot T_m - 3.151 \cdot 10^{-4})$$

$$C = \left((h_1 - h_3) - 0.5(h_1 - h_2) - 0.5 \left(\frac{(h_5 - h_3)^2}{(h_5 - h_6)} \right) \right)$$

$$D = \left(\frac{128L_p\nu}{\pi ND_p^4} \right)$$

$$E = \left(1 + N \left(\frac{L_{cp}}{L_p} \right) \left(\frac{D_p}{D_{cp}} \right)^4 \right)$$

The mass flow rate is then calculated with the simplified parts as follow:

$$\dot{m} = \sqrt{\left| \frac{A * B * C}{D * E} \right|}$$

The absolute value of the term under the square root is used since the sign convention used in the calculation will lead to a negative value under the square root.

The separate parts of the mass flow equation are calculated and the answers are as follow:

$$A = \left(\frac{-17.38 + 30 - 8.923 * 10^5 * (-1.44 * 10^{-4})}{3800} \right) = -0.03672$$

$$B = (-2 * 1.749 * 10^{-6} * 17.87 - 3.151 * 10^{-4}) = -0.0003667$$

$$C = \left((2.7 - 0.03) - 0.5(2.7 - 2.07) - 0.5 \left(\frac{(0.88 - 0.03)^2}{(0.88 - 0)} \right) \right) = 1.944$$

$$D = \left(\frac{128 * 1 * 1.31 * 10^{-6}}{\pi * 9 * 0.015^4} \right) = 0.01182$$

$$E = \left(1 + 9 \left(\frac{3.85}{1} \right) \left(\frac{0.015}{0.05} \right)^4 \right) = 1.281$$

The mass flow rate is then:

$$\dot{m} = \sqrt{\left| \frac{(-0.03672)(-0.0003667)(1.944)}{(0.01182)(1.281)} \right|} = 0.042 \text{ kg/s}$$

With the mean storage tank temperature and mass flow rate known the panel inlet and outlet temperatures is calculated with:

$$Q_{rad} + Q_{conv} + \dot{m} \cdot Cp \cdot T_2 = \dot{m} \cdot Cp \cdot T_1$$

and

$$T_m = \frac{T_1 + T_2}{2}$$

The outlet temperature at the panel outlet is:

$$Q_{rad} + Q_{conv} + \dot{m} \cdot Cp \cdot T_2 = \dot{m} \cdot Cp \cdot (2T_m - T_2)$$

$$-101.4 + -38.2 + (0.042)(3800)(T_2) = 0.042(3800)(2(14.7) - T_2)$$

$$T_2 = 15.14 \text{ } ^\circ\text{C}$$

and the inlet temperature is:

$$T_1 = 2T_m - T_2 = 2(14.7) - 15.14 = 14.26 \text{ } ^\circ\text{C}$$

The calculation steps represented above was for one 15 minute time step. The calculations are repeated for a number of steps with the corresponding input parameters to create a continuous series of data to indicate the system performance over a number of days.

APPENDIX B: THEORETICAL MODEL DATA EXTRACT

S1 Theoretical data extract – 5 October to 6 October 2010

Table 6 : S1 Theoretical data extract

S1														
Date	Time	Theta	T_db	RH	T_dp	ϵ_{sky}	T_sky	T_m (n-1)	Q_conv	Q_rad	Tank Q_ext	Heatload	Tank Heat loss/gain	T_drum theoretical
2010/10/05	00:14	1286	20.06	47%	8.5	0.793	3.6	20.7	-1.0	-63.2	15.0	30.0	-1.0	20.7
2010/10/05	00:29	1287	19.92	49%	8.7	0.795	3.6	20.7	-1.3	-63.1	0.0	30.0	-1.2	20.7
2010/10/05	00:44	1288	19.43	53%	9.5	0.800	3.5	20.7	-2.3	-63.2	0.0	30.0	-2.0	20.6
2010/10/05	00:59	1289	19.19	54%	9.7	0.801	3.4	20.6	-2.7	-63.4	0.0	30.0	-2.3	20.6
2010/10/05	01:14	1290	18.42	54%	9.0	0.797	2.3	20.6	-4.6	-66.8	0.0	30.0	-3.4	20.5
2010/10/05	01:29	1291	18.1	56%	9.1	0.797	2.0	20.5	-5.3	-67.6	0.0	30.0	-3.9	20.5
2010/10/05	01:44	1292	17.81	56%	8.9	0.796	1.7	20.5	-6.0	-68.7	0.0	30.0	-4.3	20.4
2010/10/05	01:59	1293	17.89	54%	8.3	0.793	1.5	20.4	-5.6	-69.2	0.0	30.0	-4.1	20.4
2010/10/05	02:14	1294	18.4	53%	8.5	0.794	2.0	20.4	-4.1	-67.0	0.0	30.0	-3.2	20.3
2010/10/05	02:29	1295	18.72	50%	8.0	0.791	2.1	20.3	-3.2	-66.8	0.0	30.0	-2.6	20.3
2010/10/05	02:44	1296	19.03	54%	9.4	0.799	3.1	20.3	-2.4	-63.1	0.0	30.0	-2.0	20.3
2010/10/05	02:59	1297	18.74	60%	10.8	0.808	3.6	20.3	-3.0	-61.4	0.0	30.0	-2.4	20.2
2010/10/05	03:14	1298	17.5	63%	10.3	0.805	2.2	20.2	-6.1	-66.0	0.0	30.0	-4.3	20.2
2010/10/05	03:29	1299	17.02	63%	10.0	0.803	1.5	20.2	-7.4	-68.0	0.0	30.0	-5.0	20.1
2010/10/05	03:44	1300	16.86	61%	9.2	0.798	1.0	20.1	-7.7	-69.6	0.0	30.0	-5.2	20.1
2010/10/05	03:59	1301	17.12	60%	9.2	0.798	1.2	20.1	-6.8	-68.5	0.0	30.0	-4.7	20.0
2010/10/05	04:14	1302	17.01	62%	9.6	0.801	1.3	20.0	-7.0	-67.9	0.0	30.0	-4.8	20.0
2010/10/05	04:29	1303	16.66	62%	9.4	0.799	0.9	20.0	-7.9	-69.3	0.0	30.0	-5.3	19.9
2010/10/05	04:44	1304	16.07	61%	8.4	0.793	-0.2	19.9	-9.5	-72.5	0.0	30.0	-6.1	19.9
2010/10/05	04:59	1305	15.97	62%	8.7	0.795	-0.2	19.9	-9.6	-72.1	0.0	30.0	-6.2	19.8

S1														
Date	Time	Theta	T_db	RH	T_dp	ϵ_{sky}	T_sky	T_m (n-1)	Q_conv	Q_rad	Tank Q_ext	Heatload	Tank Heat loss/gain	T_drum theoretical
2010/10/05	05:14	1306	15.89	60%	8.2	0.792	-0.5	19.8	-9.7	-73.0	0.0	30.0	-6.2	19.7
2010/10/05	05:29	1307	15.86	64%	9.0	0.797	-0.1	19.7	-9.6	-71.5	0.0	30.0	-6.2	19.7
2010/10/05	05:44	1308	15.15	63%	8.1	0.791	-1.2	19.7	-11.6	-74.8	0.0	30.0	-7.2	19.6
2010/10/05	05:59	1309	15	65%	8.3	0.793	-1.3	19.6	-11.9	-74.8	0.0	30.0	-7.4	19.6
2010/10/05	06:14	1310	15.57	61%	8.1	0.791	-0.8	19.6	-9.9	-73.1	0.0	30.0	-6.4	19.5
2010/10/05	06:29	1311	15.83	60%	8.0	0.791	-0.6	19.5	-8.9	-72.3	0.0	30.0	-5.8	19.4
2010/10/05	06:44	1312	16.75	56%	8.0	0.790	0.2	19.4	-6.1	-69.3	0.0	30.0	-4.3	19.4
2010/10/05	06:59	1313	17.73	54%	8.1	0.791	1.2	19.4	-3.3	-65.9	0.0	30.0	-2.6	19.3
2010/10/05	07:14	1314	18.8	47%	7.2	0.786	1.7	19.3	-0.8	-64.0	0.0	30.0	-0.9	19.3
2010/10/05	07:29	1315	20.42	46%	8.3	0.792	3.8	19.3	2.0	-56.8	15.0	30.0	1.8	19.4
2010/10/05	07:44	1316	20.69	44%	7.8	0.790	3.8	19.4	2.5	-57.0	15.0	30.0	2.1	19.4
2010/10/05	07:59	1317	22.55	39%	8.0	0.790	5.7	19.4	7.3	-50.9	15.0	30.0	5.0	19.5
2010/10/05	08:14	1318	24.96	40%	10.6	0.806	9.4	19.5	14.7	-38.2	15.0	30.0	8.8	19.5
2010/10/05	08:29	1319	23.66	40%	9.2	0.798	7.4	19.5	10.4	-45.4	15.0	30.0	6.6	19.6
2010/10/05	08:44	1320	23.83	40%	9.5	0.800	7.7	19.6	10.7	-44.4	15.0	30.0	6.8	19.6
2010/10/05	08:59	1321	23.4	38%	8.3	0.792	6.6	19.6	9.2	-48.4	15.0	30.0	6.0	19.7
2010/10/05	09:14	1322	24.34	36%	8.2	0.792	7.5	19.7	12.0	-45.7	15.0	30.0	7.4	19.7
2010/10/05	09:29	1323	25.21	35%	8.6	0.794	8.5	19.7	14.7	-42.2	15.0	30.0	8.7	19.8
2010/10/05	09:44	1324	25.92	31%	7.4	0.787	8.5	19.8	16.9	-42.3	15.0	30.0	9.8	19.8
2010/10/05	09:59	1325	26.75	32%	8.5	0.794	9.9	19.8	19.6	-37.6	15.0	30.0	11.0	19.9
2010/10/05	10:14	1326	26.04	27%	5.6	0.776	7.7	19.9	16.9	-45.9	15.0	30.0	9.8	19.9
2010/10/05	10:29	1327	29.24	25%	7.0	0.785	11.4	19.9	28.3	-32.5	15.0	30.0	14.8	20.0
2010/10/05	10:44	1328	29.77	25%	7.5	0.787	12.2	20.0	30.1	-30.1	15.0	30.0	15.6	20.1
2010/10/05	10:59	1329	29.94	27%	8.8	0.796	13.1	20.1	30.6	-26.9	15.0	30.0	15.7	20.1
2010/10/05	11:14	1330	29	25%	6.8	0.783	11.1	20.1	26.7	-34.6	15.0	30.0	14.1	20.2

S1														
Date	Time	Theta	T_db	RH	T_dp	ϵ_{sky}	T_sky	T_m (n-1)	Q_conv	Q_rad	Tank Q_ext	Heatload	Tank Heat loss/gain	T_drum theoretical
2010/10/05	11:29	1331	30.36	23%	6.8	0.783	12.4	20.2	31.7	-30.1	15.0	30.0	16.2	20.2
2010/10/05	11:44	1332	31.56	23%	7.8	0.789	14.0	20.2	38.6	-24.1	15.0	30.0	18.0	20.3
2010/10/05	11:59	1333	31.24	22%	7.0	0.784	13.3	20.3	34.7	-27.2	15.0	30.0	17.4	20.4
2010/10/05	12:14	1334	32.32	23%	8.3	0.793	15.1	20.4	41.5	-20.7	15.0	30.0	19.0	20.4
2010/10/05	12:29	1335	31.86	23%	8.0	0.791	14.5	20.4	39.1	-23.2	15.0	30.0	18.2	20.5
2010/10/05	12:44	1336	31.53	23%	8.2	0.792	14.3	20.5	37.3	-24.3	15.0	30.0	17.6	20.6
2010/10/05	12:59	1337	31.21	23%	7.9	0.790	13.8	20.6	33.5	-26.3	15.0	30.0	17.0	20.6
2010/10/05	13:14	1338	31.26	24%	8.5	0.794	14.2	20.6	33.5	-25.2	15.0	30.0	16.9	20.7
2010/10/05	13:29	1339	31.68	24%	8.5	0.794	14.6	20.7	34.9	-23.9	15.0	30.0	17.5	20.8
2010/10/05	13:44	1340	32.45	25%	9.9	0.802	16.1	20.8	40.3	-18.4	15.0	30.0	18.6	20.8
2010/10/05	13:59	1341	31.26	25%	8.7	0.795	14.3	20.8	32.7	-25.5	15.0	30.0	16.6	20.9
2010/10/05	14:14	1342	30.35	24%	7.9	0.790	13.0	20.9	29.0	-30.7	15.0	30.0	15.1	20.9
2010/10/05	14:29	1343	30.65	25%	8.3	0.793	13.5	20.9	29.9	-28.9	15.0	30.0	15.5	21.0
2010/10/05	14:44	1344	30.52	24%	7.6	0.788	13.0	21.0	29.2	-31.2	15.0	30.0	15.2	21.1
2010/10/05	14:59	1345	32.19	26%	10.5	0.806	16.2	21.1	37.7	-19.2	15.0	30.0	17.7	21.1
2010/10/05	15:14	1346	30.05	24%	7.2	0.786	12.3	21.1	26.9	-34.0	15.0	30.0	14.2	21.2
2010/10/05	15:29	1347	31.82	25%	9.2	0.798	15.1	21.2	33.5	-23.9	15.0	30.0	17.0	21.2
2010/10/05	15:44	1348	31.91	26%	10.2	0.804	15.7	21.2	33.6	-21.7	15.0	30.0	17.0	21.3
2010/10/05	15:59	1349	31.79	25%	9.7	0.801	15.3	21.3	32.9	-23.5	15.0	30.0	16.7	21.4
2010/10/05	16:14	1350	30.34	28%	10.0	0.803	14.1	21.4	27.1	-28.3	15.0	30.0	14.3	21.4
2010/10/05	16:29	1351	29.12	29%	9.5	0.800	12.7	21.4	22.3	-33.8	15.0	30.0	12.3	21.5
2010/10/05	16:44	1352	29.36	32%	10.9	0.808	13.7	21.5	23.0	-30.4	15.0	30.0	12.5	21.5
2010/10/05	16:59	1353	29.32	34%	12.0	0.816	14.3	21.5	22.6	-28.4	15.0	30.0	12.4	21.6
2010/10/05	17:14	1354	27.7	35%	10.9	0.809	12.1	21.6	16.7	-36.7	15.0	30.0	9.7	21.7
2010/10/05	17:29	1355	26.72	37%	10.6	0.807	11.1	21.7	13.3	-40.9	15.0	30.0	8.1	21.7

S1														
Date	Time	Theta	T_db	RH	T_dp	ϵ_{sky}	T_sky	T_m (n-1)	Q_conv	Q_rad	Tank Q_ext	Heatload	Tank Heat loss/gain	T_drum theoretical
2010/10/05	17:44	1356	25.59	43%	12.1	0.816	10.8	21.7	9.5	-42.1	15.0	30.0	6.2	21.8
2010/10/05	17:59	1357	24.1	44%	11.2	0.811	8.9	21.8	5.0	-49.1	15.0	30.0	3.7	21.8
2010/10/05	18:14	1358	23.05	47%	11.2	0.811	7.9	21.8	2.3	-52.8	15.0	30.0	2.0	21.9
2010/10/05	18:29	1359	22.28	49%	11.0	0.809	7.0	21.9	0.6	-56.0	15.0	30.0	0.7	21.9
2010/10/05	18:44	1360	21.55	48%	10.0	0.803	5.8	21.9	-0.5	-60.4	15.0	30.0	-0.6	21.9
2010/10/05	18:59	1361	21.29	46%	9.3	0.799	5.2	21.9	-0.9	-62.5	15.0	30.0	-1.0	21.9
2010/10/05	19:14	1362	20.97	50%	10.1	0.804	5.3	21.9	-1.5	-62.0	15.0	30.0	-1.4	21.9
2010/10/05	19:29	1363	20.5	48%	9.1	0.798	4.4	21.9	-2.6	-65.2	15.0	30.0	-2.2	21.8
2010/10/05	19:44	1364	20.43	47%	8.8	0.796	4.1	21.8	-2.7	-65.9	15.0	30.0	-2.2	21.8
2010/10/05	19:59	1365	20.23	45%	7.8	0.790	3.4	21.8	-3.1	-68.2	15.0	30.0	-2.5	21.8
2010/10/05	20:14	1366	20.09	47%	8.5	0.794	3.6	21.8	-3.4	-67.4	15.0	30.0	-2.7	21.7
2010/10/05	20:29	1367	19.81	50%	8.9	0.796	3.6	21.7	-4.0	-67.4	0.0	30.0	-3.1	21.7
2010/10/05	20:44	1368	18.73	52%	8.6	0.794	2.4	21.7	-6.8	-71.2	0.0	30.0	-4.7	21.6
2010/10/05	20:59	1369	18.42	52%	8.3	0.792	1.9	21.6	-7.6	-72.5	0.0	30.0	-5.1	21.6
2010/10/05	21:14	1370	18.19	51%	7.9	0.790	1.5	21.6	-8.1	-73.7	0.0	30.0	-5.4	21.5
2010/10/05	21:29	1371	18.41	47%	6.7	0.783	1.1	21.5	-7.3	-74.8	0.0	30.0	-5.0	21.5
2010/10/05	21:44	1372	18.69	51%	8.2	0.792	2.2	21.5	-6.3	-71.0	0.0	30.0	-4.4	21.4
2010/10/05	21:59	1373	18.42	52%	8.4	0.793	2.0	21.4	-6.9	-71.3	0.0	30.0	-4.8	21.4
2010/10/05	22:14	1374	18.02	53%	8.1	0.791	1.5	21.4	-7.9	-72.8	0.0	30.0	-5.3	21.3
2010/10/05	22:29	1375	17.57	55%	8.3	0.792	1.1	21.3	-9.1	-73.7	0.0	30.0	-6.0	21.3
2010/10/05	22:44	1376	17.49	57%	8.9	0.796	1.4	21.3	-9.2	-72.7	0.0	30.0	-6.0	21.2
2010/10/05	22:59	1377	17.29	56%	8.4	0.793	0.9	21.2	-9.6	-73.9	0.0	30.0	-6.2	21.1
2010/10/05	23:14	1378	17.3	54%	7.8	0.789	0.6	21.1	-9.4	-74.7	0.0	30.0	-6.1	21.1
2010/10/05	23:29	1379	17.29	57%	8.6	0.794	1.0	21.1	-9.3	-73.1	0.0	30.0	-6.0	21.0
2010/10/05	23:44	1380	16.99	56%	8.2	0.792	0.5	21.0	-10.0	-74.5	0.0	30.0	-6.4	21.0

S1														
Date	Time	Theta	T_db	RH	T_dp	ϵ_{sky}	T_sky	T_m (n-1)	Q_conv	Q_rad	Tank Q_ext	Heatload	Tank Heat loss/gain	T_drum theoretical
2010/10/05	23:59	1381	17.01	56%	8.1	0.791	0.5	21.0	-9.8	-74.4	0.0	30.0	-6.3	20.9
2010/10/06	00:14	1382	16.97	53%	7.3	0.786	0.0	20.9	-9.7	-75.7	0.0	30.0	-6.3	20.8
2010/10/06	00:29	1383	17.79	50%	7.3	0.786	0.8	20.8	-7.0	-72.9	0.0	30.0	-4.8	20.8
2010/10/06	00:44	1384	17.85	55%	8.7	0.795	1.6	20.8	-6.7	-70.0	0.0	30.0	-4.7	20.7
2010/10/06	00:59	1385	17.22	58%	8.7	0.795	1.0	20.7	-8.4	-71.7	0.0	30.0	-5.6	20.7
2010/10/06	01:14	1386	16.93	55%	7.6	0.788	0.2	20.7	-9.1	-74.2	0.0	30.0	-6.0	20.6
2010/10/06	01:29	1387	16.82	53%	7.1	0.785	-0.2	20.6	-9.3	-75.3	0.0	30.0	-6.0	20.5
2010/10/06	01:44	1388	16.64	56%	7.7	0.789	0.0	20.5	-9.6	-74.5	0.0	30.0	-6.2	20.5
2010/10/06	01:59	1389	16.36	56%	7.5	0.787	-0.4	20.5	-10.3	-75.5	0.0	30.0	-6.6	20.4
2010/10/06	02:14	1390	16.32	56%	7.4	0.787	-0.5	20.4	-10.3	-75.6	0.0	30.0	-6.5	20.4
2010/10/06	02:29	1391	16.33	54%	7.0	0.784	-0.7	20.4	-10.0	-75.9	0.0	30.0	-6.4	20.3
2010/10/06	02:44	1392	16.08	56%	7.3	0.787	-0.8	20.3	-10.6	-75.8	0.0	30.0	-6.7	20.2
2010/10/06	02:59	1393	16.13	56%	7.2	0.786	-0.8	20.2	-10.3	-75.7	0.0	30.0	-6.5	20.2
2010/10/06	03:14	1394	16.33	56%	7.5	0.787	-0.5	20.2	-9.4	-74.3	0.0	30.0	-6.1	20.1
2010/10/06	03:29	1395	16.28	54%	7.0	0.784	-0.8	20.1	-9.4	-75.1	0.0	30.0	-6.1	20.0
2010/10/06	03:44	1396	16.6	55%	7.4	0.787	-0.2	20.0	-8.3	-73.1	0.0	30.0	-5.5	20.0
2010/10/06	03:59	1397	16.51	55%	7.3	0.786	-0.4	20.0	-8.3	-73.4	0.0	30.0	-5.5	19.9
2010/10/06	04:14	1398	16.4	55%	7.3	0.786	-0.5	19.9	-8.5	-73.4	0.0	30.0	-5.6	19.9
2010/10/06	04:29	1399	16.4	57%	7.9	0.790	-0.2	19.9	-8.3	-72.2	0.0	30.0	-5.5	19.8
2010/10/06	04:44	1400	16.18	60%	8.3	0.792	-0.2	19.8	-8.8	-72.0	0.0	30.0	-5.8	19.8
2010/10/06	04:59	1401	15.96	55%	7.0	0.784	-1.1	19.8	-9.3	-74.7	0.0	30.0	-6.1	19.7
2010/10/06	05:14	1402	15.66	59%	7.6	0.788	-1.0	19.7	-10.1	-74.2	0.0	30.0	-6.4	19.6
2010/10/06	05:29	1403	15.31	57%	6.9	0.784	-1.7	19.6	-11.0	-76.3	0.0	30.0	-6.9	19.6
2010/10/06	05:44	1404	15	62%	7.7	0.789	-1.6	19.6	-11.8	-75.6	0.0	30.0	-7.3	19.5
2010/10/06	05:59	1405	14.77	58%	6.5	0.781	-2.4	19.5	-12.3	-78.0	0.0	30.0	-7.6	19.4

S1														
Date	Time	Theta	T_db	RH	T_dp	ϵ_{sky}	T_sky	T_m (n-1)	Q_conv	Q_rad	Tank Q_ext	Heatload	Tank Heat loss/gain	T_drum theoretical
2010/10/06	06:14	1406	14.86	58%	6.5	0.781	-2.4	19.4	-11.8	-77.5	0.0	30.0	-7.3	19.4
2010/10/06	06:29	1407	15.16	59%	7.2	0.785	-1.7	19.4	-10.6	-75.2	0.0	30.0	-6.7	19.3
2010/10/06	06:44	1408	15.76	56%	6.9	0.784	-1.3	19.3	-8.6	-73.6	0.0	30.0	-5.7	19.3
2010/10/06	06:59	1409	16.4	55%	7.4	0.787	-0.5	19.3	-6.5	-70.7	0.0	30.0	-4.5	19.2
2010/10/06	07:14	1410	17.07	52%	7.2	0.786	0.1	19.2	-4.5	-68.7	0.0	30.0	-3.4	19.2
2010/10/06	07:29	1411	17.89	50%	7.3	0.786	0.9	19.2	-2.3	-65.9	0.0	30.0	-2.0	19.1
2010/10/06	07:44	1412	18.5	46%	6.8	0.783	1.2	19.1	-0.9	-64.8	0.0	30.0	-1.0	19.1
2010/10/06	07:59	1413	19.87	42%	6.6	0.782	2.4	19.1	1.3	-60.6	0.0	30.0	1.3	19.1
2010/10/06	08:14	1414	21.02	43%	7.9	0.790	4.2	19.1	3.9	-54.7	15.0	30.0	3.1	19.2
2010/10/06	08:29	1415	22.05	41%	8.2	0.792	5.3	19.2	6.6	-51.1	15.0	30.0	4.6	19.2
2010/10/06	08:44	1416	23.4	34%	6.7	0.782	5.8	19.2	10.5	-49.8	15.0	30.0	6.7	19.3
2010/10/06	08:59	1417	24.66	33%	7.3	0.786	7.3	19.3	14.4	-44.7	15.0	30.0	8.6	19.3
2010/10/06	09:14	1418	26.04	31%	7.4	0.787	8.6	19.3	19.0	-40.1	15.0	30.0	10.7	19.4
2010/10/06	09:29	1419	27.52	29%	8.1	0.791	10.4	19.4	24.1	-34.0	15.0	30.0	13.0	19.4
2010/10/06	09:44	1420	27.25	27%	6.8	0.783	9.5	19.4	22.9	-37.7	15.0	30.0	12.5	19.5
2010/10/06	09:59	1421	28.6	27%	7.7	0.789	11.2	19.5	27.7	-31.5	15.0	30.0	14.5	19.5
2010/10/06	10:14	1422	29.28	24%	6.5	0.781	11.2	19.5	30.0	-31.8	15.0	30.0	15.5	19.6
2010/10/06	10:29	1423	30.68	24%	8.1	0.791	13.4	19.6	37.6	-23.9	15.0	30.0	17.7	19.7
2010/10/06	10:44	1424	30.61	24%	7.9	0.790	13.2	19.7	37.0	-24.8	15.0	30.0	17.4	19.7
2010/10/06	10:59	1425	31.4	22%	7.1	0.785	13.5	19.7	40.3	-24.0	15.0	30.0	18.6	19.8
2010/10/06	11:14	1426	32.65	20%	7.2	0.786	14.8	19.8	45.7	-19.5	15.0	30.0	20.5	19.9
2010/10/06	11:29	1427	33.37	21%	8.0	0.790	15.9	19.9	48.8	-15.6	15.0	30.0	21.5	19.9
2010/10/06	11:44	1428	33.58	20%	7.9	0.790	16.0	19.9	49.5	-15.4	15.0	30.0	21.8	20.0
2010/10/06	11:59	1429	33.48	19%	7.2	0.786	15.5	20.0	48.7	-17.4	15.0	30.0	21.5	20.1
2010/10/06	12:14	1430	34.96	18%	7.6	0.788	17.1	20.1	55.5	-11.6	15.0	30.0	23.7	20.1

S1														
Date	Time	Theta	T_db	RH	T_dp	ϵ_{sky}	T_sky	T_m (n-1)	Q_conv	Q_rad	Tank Q_ext	Heatload	Tank Heat loss/gain	T_drum theoretical
2010/10/06	12:29	1431	33.88	20%	7.9	0.790	16.3	20.1	49.9	-15.1	15.0	30.0	21.9	20.2
2010/10/06	12:44	1432	34.47	18%	6.8	0.783	16.2	20.2	52.4	-15.6	15.0	30.0	22.7	20.3
2010/10/06	12:59	1433	34.74	18%	7.3	0.786	16.8	20.3	53.4	-13.7	15.0	30.0	23.1	20.3
2010/10/06	13:14	1434	35.68	23%	11.6	0.813	20.1	20.3	57.7	-0.9	15.0	30.0	24.5	20.4
2010/10/06	13:29	1435	32.46	21%	7.2	0.786	14.6	20.4	42.0	-22.7	15.0	30.0	19.2	20.5
2010/10/06	13:44	1436	32.7	21%	7.6	0.788	15.0	20.5	42.8	-21.2	15.0	30.0	19.5	20.5
2010/10/06	13:59	1437	32.07	21%	7.4	0.787	14.3	20.5	39.6	-24.3	15.0	30.0	18.4	20.6
2010/10/06	14:14	1438	32.74	19%	5.9	0.777	14.1	20.6	42.3	-25.4	15.0	30.0	19.4	20.7
2010/10/06	14:29	1439	34.37	21%	9.3	0.799	17.6	20.7	49.7	-12.3	15.0	30.0	21.8	20.7
2010/10/06	14:44	1440	32.87	20%	7.2	0.786	15.0	20.7	42.3	-22.5	15.0	30.0	19.3	20.8
2010/10/06	14:59	1441	31.89	22%	7.9	0.790	14.4	20.8	37.6	-24.8	15.0	30.0	17.7	20.9
2010/10/06	15:14	1442	33.04	21%	8.0	0.791	15.6	20.9	42.5	-20.8	15.0	30.0	19.4	20.9
2010/10/06	15:29	1443	33.46	26%	11.6	0.813	18.0	20.9	44.1	-11.6	15.0	30.0	20.0	21.0
2010/10/06	15:44	1444	29.99	25%	7.8	0.789	12.6	21.0	27.2	-32.6	15.0	30.0	14.3	21.1
2010/10/06	15:59	1445	32.01	24%	9.0	0.797	15.1	21.1	34.7	-23.2	15.0	30.0	17.5	21.1
2010/10/06	16:14	1446	31.88	24%	8.9	0.796	15.0	21.1	34.0	-24.0	15.0	30.0	17.2	21.2
2010/10/06	16:29	1447	30.4	26%	9.0	0.797	13.6	21.2	28.0	-29.4	15.0	30.0	14.7	21.2
2010/10/06	16:44	1448	30.36	30%	10.8	0.808	14.6	21.2	27.6	-26.0	15.0	30.0	14.5	21.3
2010/10/06	16:59	1449	28.31	29%	8.6	0.794	11.5	21.3	19.9	-37.9	15.0	30.0	11.2	21.4
2010/10/06	17:14	1450	28.27	29%	8.6	0.795	11.4	21.4	19.6	-38.3	15.0	30.0	11.0	21.4
2010/10/06	17:29	1451	27.26	33%	9.6	0.801	11.0	21.4	15.9	-40.0	15.0	30.0	9.3	21.5
2010/10/06	17:44	1452	26.04	36%	9.7	0.801	9.9	21.5	11.7	-44.2	15.0	30.0	7.3	21.5
2010/10/06	17:59	1453	24.81	38%	9.5	0.800	8.6	21.5	7.8	-49.0	15.0	30.0	5.2	21.6
2010/10/06	18:14	1454	23.63	39%	8.7	0.795	7.1	21.6	4.3	-54.7	15.0	30.0	3.3	21.6
2010/10/06	18:29	1455	23.27	40%	9.0	0.797	6.9	21.6	3.3	-55.5	15.0	30.0	2.6	21.7

S1														
Date	Time	Theta	T_db	RH	T_dp	ϵ_{sky}	T_sky	T_m (n-1)	Q_conv	Q_rad	Tank Q_ext	Heatload	Tank Heat loss/gain	T_drum theoretical
2010/10/06	18:44	1456	22.63	43%	9.2	0.798	6.4	21.7	1.7	-57.4	15.0	30.0	1.5	21.7
2010/10/06	18:59	1457	22.4	41%	8.3	0.792	5.7	21.7	1.1	-60.0	15.0	30.0	1.1	21.8
2010/10/06	19:14	1458	22.67	67%	16.2	0.841	10.2	21.8	1.6	-44.5	15.0	30.0	1.5	21.8
2010/10/06	19:29	1459	17.43	73%	12.5	0.819	3.2	21.8	-11.1	-68.8	0.0	30.0	-7.0	21.7
2010/10/06	19:44	1460	17.2	65%	10.5	0.806	1.9	21.7	-11.7	-72.9	0.0	30.0	-7.3	21.7
2010/10/06	19:59	1461	17.7	64%	10.7	0.807	2.5	21.7	-9.9	-70.6	0.0	30.0	-6.4	21.6
2010/10/06	20:14	1462	17.6	61%	10.0	0.803	2.1	21.6	-10.0	-71.9	0.0	30.0	-6.4	21.6
2010/10/06	20:29	1463	17.9	54%	8.4	0.793	1.5	21.6	-8.9	-73.5	0.0	30.0	-5.8	21.5
2010/10/06	20:44	1464	19.09	47%	7.4	0.787	2.1	21.5	-5.3	-71.4	0.0	30.0	-3.9	21.5
2010/10/06	20:59	1465	20.44	47%	8.8	0.795	4.1	21.5	-1.8	-64.4	15.0	30.0	-1.6	21.4
2010/10/06	21:14	1466	20.31	49%	9.2	0.798	4.2	21.4	-2.0	-64.0	15.0	30.0	-1.8	21.4
2010/10/06	21:29	1467	19.73	47%	8.0	0.791	3.0	21.4	-3.4	-67.9	0.0	30.0	-2.7	21.4
2010/10/06	21:44	1468	20.19	48%	8.8	0.796	3.9	21.4	-2.2	-64.8	15.0	30.0	-1.9	21.3
2010/10/06	21:59	1469	19.59	54%	10.1	0.804	4.0	21.3	-3.5	-64.3	0.0	30.0	-2.8	21.3
2010/10/06	22:14	1470	18.75	56%	9.8	0.802	3.0	21.3	-5.7	-67.4	0.0	30.0	-4.1	21.3
2010/10/06	22:29	1471	18.36	59%	10.2	0.804	2.9	21.3	-6.6	-67.7	0.0	30.0	-4.6	21.2
2010/10/06	22:44	1472	18.06	59%	9.9	0.803	2.5	21.2	-7.4	-68.9	0.0	30.0	-5.0	21.2
2010/10/06	22:59	1473	17.75	58%	9.4	0.799	1.9	21.2	-8.1	-70.7	0.0	30.0	-5.4	21.1
2010/10/06	23:14	1474	17.61	59%	9.5	0.800	1.8	21.1	-8.4	-70.7	0.0	30.0	-5.6	21.0
2010/10/06	23:29	1475	17.4	61%	9.7	0.801	1.7	21.0	-8.8	-70.8	0.0	30.0	-5.8	21.0
2010/10/06	23:44	1476	17.19	59%	8.9	0.796	1.1	21.0	-9.3	-72.5	0.0	30.0	-6.1	20.9
2010/10/06	23:59	1477	17.42	62%	9.9	0.803	1.9	20.9	-8.4	-69.8	0.0	30.0	-5.6	20.9

S2 Experimental data extract – 5 October to 6 October 2010

Table 7 : S2 Theoretical data extract

S2														
Date	Time	Theta	T_db	RH	T_dp	ϵ_{sky}	T_sky	T_m (n-1)	Q_conv	Q_rad	Tank Q_ext	Heatload	Tank Heat loss/gain	T_drum theoretical
2010/10/05	00:14	1286	20.06	47%	8.5	0.793	3.6	16.1	9.7	-45.2	15.0	0.0	6.3	16.2
2010/10/05	00:29	1287	19.92	49%	8.7	0.795	3.6	16.2	9.2	-45.3	0.0	0.0	6.0	16.2
2010/10/05	00:44	1288	19.43	53%	9.5	0.800	3.5	16.2	7.7	-45.5	0.0	0.0	5.2	16.2
2010/10/05	00:59	1289	19.19	54%	9.7	0.801	3.4	16.2	7.0	-45.8	0.0	0.0	4.8	16.2
2010/10/05	01:14	1290	18.42	54%	9.0	0.797	2.3	16.2	4.9	-49.5	0.0	0.0	3.6	16.2
2010/10/05	01:29	1291	18.1	56%	9.1	0.797	2.0	16.2	4.0	-50.4	0.0	0.0	3.1	16.2
2010/10/05	01:44	1292	17.81	56%	8.9	0.796	1.7	16.2	3.3	-51.7	0.0	0.0	2.6	16.2
2010/10/05	01:59	1293	17.89	54%	8.3	0.793	1.5	16.2	3.4	-52.4	0.0	0.0	2.7	16.2
2010/10/05	02:14	1294	18.4	53%	8.5	0.794	2.0	16.2	4.8	-50.5	0.0	0.0	3.5	16.2
2010/10/05	02:29	1295	18.72	50%	8.0	0.791	2.1	16.2	5.6	-50.4	0.0	0.0	4.0	16.2
2010/10/05	02:44	1296	19.03	54%	9.4	0.799	3.1	16.2	6.5	-46.9	0.0	0.0	4.5	16.2
2010/10/05	02:59	1297	18.74	60%	10.8	0.808	3.6	16.2	5.7	-45.5	0.0	0.0	4.1	16.2
2010/10/05	03:14	1298	17.5	63%	10.3	0.805	2.2	16.2	2.5	-50.2	0.0	0.0	2.1	16.2
2010/10/05	03:29	1299	17.02	63%	10.0	0.803	1.5	16.2	1.4	-52.3	0.0	0.0	1.3	16.2
2010/10/05	03:44	1300	16.86	61%	9.2	0.798	1.0	16.2	1.1	-54.1	0.0	0.0	1.1	16.2
2010/10/05	03:59	1301	17.12	60%	9.2	0.798	1.2	16.2	1.6	-53.3	0.0	0.0	1.5	16.2
2010/10/05	04:14	1302	17.01	62%	9.6	0.801	1.3	16.2	1.4	-52.9	0.0	0.0	1.3	16.2
2010/10/05	04:29	1303	16.66	62%	9.4	0.799	0.9	16.2	0.7	-54.5	0.0	0.0	0.7	16.2
2010/10/05	04:44	1304	16.07	61%	8.4	0.793	-0.2	16.2	-0.1	-57.9	0.0	0.0	-0.2	16.1
2010/10/05	04:59	1305	15.97	62%	8.7	0.795	-0.2	16.1	-0.2	-57.5	0.0	0.0	-0.3	16.1
2010/10/05	05:14	1306	15.89	60%	8.2	0.792	-0.5	16.1	-0.2	-58.5	0.0	0.0	-0.3	16.0
2010/10/05	05:29	1307	15.86	64%	9.0	0.797	-0.1	16.0	-0.2	-57.0	0.0	0.0	-0.3	16.0

S2														
Date	Time	Theta	T_db	RH	T_dp	ϵ_{sky}	T_sky	T_m (n-1)	Q_conv	Q_rad	Tank Q_ext	Heatload	Tank Heat loss/gain	T_drum theoretical
2010/10/05	05:44	1308	15.15	63%	8.1	0.791	-1.2	16.0	-1.4	-60.3	0.0	0.0	-1.3	15.9
2010/10/05	05:59	1309	15	65%	8.3	0.793	-1.3	15.9	-1.6	-60.2	0.0	0.0	-1.4	15.8
2010/10/05	06:14	1310	15.57	61%	8.1	0.791	-0.8	15.8	-0.3	-58.6	0.0	0.0	-0.4	15.8
2010/10/05	06:29	1311	15.83	60%	8.0	0.791	-0.6	15.8	0.0	-57.7	0.0	0.0	0.1	15.8
2010/10/05	06:44	1312	16.75	56%	8.0	0.790	0.2	15.8	1.7	-55.0	0.0	0.0	1.5	15.8
2010/10/05	06:59	1313	17.73	54%	8.1	0.791	1.2	15.8	4.0	-51.8	0.0	0.0	3.1	15.8
2010/10/05	07:14	1314	18.8	47%	7.2	0.786	1.7	15.8	7.0	-50.1	0.0	0.0	4.8	15.8
2010/10/05	07:29	1315	20.42	46%	8.3	0.792	3.8	15.8	11.9	-43.1	15.0	0.0	7.4	15.8
2010/10/05	07:44	1316	20.69	44%	7.8	0.790	3.8	15.8	12.7	-43.1	15.0	0.0	7.8	15.8
2010/10/05	07:59	1317	22.55	39%	8.0	0.790	5.7	15.8	19.0	-37.0	15.0	0.0	10.7	15.9
2010/10/05	08:14	1318	24.96	40%	10.6	0.806	9.4	15.9	27.7	-24.1	15.0	0.0	14.5	15.9
2010/10/05	08:29	1319	23.66	40%	9.2	0.798	7.4	15.9	22.7	-31.3	15.0	0.0	12.4	15.9
2010/10/05	08:44	1320	23.83	40%	9.5	0.800	7.7	15.9	23.3	-30.1	15.0	0.0	12.6	15.9
2010/10/05	08:59	1321	23.4	38%	8.3	0.792	6.6	15.9	21.6	-34.1	15.0	0.0	11.9	16.0
2010/10/05	09:14	1322	24.34	36%	8.2	0.792	7.5	16.0	24.9	-31.2	15.0	0.0	13.3	16.0
2010/10/05	09:29	1323	25.21	35%	8.6	0.794	8.5	16.0	28.1	-27.7	15.0	0.0	14.7	16.0
2010/10/05	09:44	1324	25.92	31%	7.4	0.787	8.5	16.0	30.7	-27.6	15.0	0.0	15.8	16.1
2010/10/05	09:59	1325	26.75	32%	8.5	0.794	9.9	16.1	36.1	-22.9	15.0	0.0	17.0	16.1
2010/10/05	10:14	1326	26.04	27%	5.6	0.776	7.7	16.1	30.9	-31.1	15.0	0.0	15.9	16.1
2010/10/05	10:29	1327	29.24	25%	7.0	0.785	11.4	16.1	47.3	-17.6	15.0	0.0	20.9	16.2
2010/10/05	10:44	1328	29.77	25%	7.5	0.787	12.2	16.2	49.7	-15.0	15.0	0.0	21.7	16.2
2010/10/05	10:59	1329	29.94	27%	8.8	0.796	13.1	16.2	50.3	-11.7	15.0	0.0	21.9	16.2
2010/10/05	11:14	1330	29	25%	6.8	0.783	11.1	16.2	45.7	-19.4	15.0	0.0	20.3	16.3
2010/10/05	11:29	1331	30.36	23%	6.8	0.783	12.4	16.3	52.0	-14.7	15.0	0.0	22.5	16.3
2010/10/05	11:44	1332	31.56	23%	7.8	0.789	14.0	16.3	57.7	-8.6	15.0	0.0	24.3	16.4

S2														
Date	Time	Theta	T_db	RH	T_dp	ϵ_{sky}	T_sky	T_m (n-1)	Q_conv	Q_rad	Tank Q_ext	Heatload	Tank Heat loss/gain	T_drum theoretical
2010/10/05	11:59	1333	31.24	22%	7.0	0.784	13.3	16.4	55.9	-11.6	15.0	0.0	23.7	16.4
2010/10/05	12:14	1334	32.32	23%	8.3	0.793	15.1	16.4	61.1	-5.0	15.0	0.0	25.4	16.4
2010/10/05	12:29	1335	31.86	23%	8.0	0.791	14.5	16.4	58.6	-7.4	15.0	0.0	24.6	16.5
2010/10/05	12:44	1336	31.53	23%	8.2	0.792	14.3	16.5	56.8	-8.4	15.0	0.0	24.0	16.5
2010/10/05	12:59	1337	31.21	23%	7.9	0.790	13.8	16.5	55.0	-10.3	15.0	0.0	23.4	16.5
2010/10/05	13:14	1338	31.26	24%	8.5	0.794	14.2	16.5	55.0	-9.1	15.0	0.0	23.5	16.6
2010/10/05	13:29	1339	31.68	24%	8.5	0.794	14.6	16.6	56.9	-7.7	15.0	0.0	24.1	16.6
2010/10/05	13:44	1340	32.45	25%	9.9	0.802	16.1	16.6	60.6	-2.2	15.0	0.0	25.2	16.7
2010/10/05	13:59	1341	31.26	25%	8.7	0.795	14.3	16.7	54.4	-9.1	15.0	0.0	23.3	16.7
2010/10/05	14:14	1342	30.35	24%	7.9	0.790	13.0	16.7	49.8	-14.2	15.0	0.0	21.7	16.7
2010/10/05	14:29	1343	30.65	25%	8.3	0.793	13.5	16.7	51.1	-12.3	15.0	0.0	22.2	16.8
2010/10/05	14:44	1344	30.52	24%	7.6	0.788	13.0	16.8	50.3	-14.5	15.0	0.0	21.9	16.8
2010/10/05	14:59	1345	32.19	26%	10.5	0.806	16.2	16.8	58.3	-2.4	15.0	0.0	24.5	16.9
2010/10/05	15:14	1346	30.05	24%	7.2	0.786	12.3	16.9	47.6	-17.1	15.0	0.0	21.0	16.9
2010/10/05	15:29	1347	31.82	25%	9.2	0.798	15.1	16.9	56.0	-6.9	15.0	0.0	23.8	16.9
2010/10/05	15:44	1348	31.91	26%	10.2	0.804	15.7	16.9	56.3	-4.6	15.0	0.0	23.9	17.0
2010/10/05	15:59	1349	31.79	25%	9.7	0.801	15.3	17.0	55.5	-6.3	15.0	0.0	23.6	17.0
2010/10/05	16:14	1350	30.34	28%	10.0	0.803	14.1	17.0	48.3	-11.0	15.0	0.0	21.2	17.0
2010/10/05	16:29	1351	29.12	29%	9.5	0.800	12.7	17.0	42.4	-16.4	15.0	0.0	19.2	17.1
2010/10/05	16:44	1352	29.36	32%	10.9	0.808	13.7	17.1	43.3	-12.9	15.0	0.0	19.6	17.1
2010/10/05	16:59	1353	29.32	34%	12.0	0.816	14.3	17.1	43.0	-10.8	15.0	0.0	19.5	17.2
2010/10/05	17:14	1354	27.7	35%	10.9	0.809	12.1	17.2	35.4	-19.0	15.0	0.0	16.8	17.2
2010/10/05	17:29	1355	26.72	37%	10.6	0.807	11.1	17.2	29.3	-23.1	15.0	0.0	15.2	17.2
2010/10/05	17:44	1356	25.59	43%	12.1	0.816	10.8	17.2	24.9	-24.2	15.0	0.0	13.4	17.2
2010/10/05	17:59	1357	24.1	44%	11.2	0.811	8.9	17.2	19.4	-31.1	15.0	0.0	10.9	17.3

S2														
Date	Time	Theta	T_db	RH	T_dp	ϵ_{sky}	T_sky	T_m (n-1)	Q_conv	Q_rad	Tank Q_ext	Heatload	Tank Heat loss/gain	T_drum theoretical
2010/10/05	18:14	1358	23.05	47%	11.2	0.811	7.9	17.3	15.7	-34.7	15.0	0.0	9.2	17.3
2010/10/05	18:29	1359	22.28	49%	11.0	0.809	7.0	17.3	13.1	-37.8	15.0	0.0	7.9	17.3
2010/10/05	18:44	1360	21.55	48%	10.0	0.803	5.8	17.3	10.7	-42.1	15.0	0.0	6.7	17.3
2010/10/05	18:59	1361	21.29	46%	9.3	0.799	5.2	17.3	9.8	-44.3	15.0	0.0	6.3	17.4
2010/10/05	19:14	1362	20.97	50%	10.1	0.804	5.3	17.4	8.7	-44.0	15.0	0.0	5.8	17.4
2010/10/05	19:29	1363	20.5	48%	9.1	0.798	4.4	17.4	7.3	-47.4	15.0	0.0	5.0	17.4
2010/10/05	19:44	1364	20.43	47%	8.8	0.796	4.1	17.4	7.0	-48.3	15.0	0.0	4.8	17.4
2010/10/05	19:59	1365	20.23	45%	7.8	0.790	3.4	17.4	6.4	-50.8	15.0	0.0	4.5	17.4
2010/10/05	20:14	1366	20.09	47%	8.5	0.794	3.6	17.4	5.9	-50.1	15.0	0.0	4.2	17.5
2010/10/05	20:29	1367	19.81	50%	8.9	0.796	3.6	17.5	5.1	-50.3	0.0	0.0	3.7	17.5
2010/10/05	20:44	1368	18.73	52%	8.6	0.794	2.4	17.5	2.4	-54.3	0.0	0.0	2.0	17.5
2010/10/05	20:59	1369	18.42	52%	8.3	0.792	1.9	17.5	1.7	-55.8	0.0	0.0	1.5	17.5
2010/10/05	21:14	1370	18.19	51%	7.9	0.790	1.5	17.5	1.2	-57.3	0.0	0.0	1.2	17.5
2010/10/05	21:29	1371	18.41	47%	6.7	0.783	1.1	17.5	1.6	-58.6	0.0	0.0	1.5	17.5
2010/10/05	21:44	1372	18.69	51%	8.2	0.792	2.2	17.5	2.3	-55.1	0.0	0.0	1.9	17.5
2010/10/05	21:59	1373	18.42	52%	8.4	0.793	2.0	17.5	1.6	-55.6	0.0	0.0	1.5	17.5
2010/10/05	22:14	1374	18.02	53%	8.1	0.791	1.5	17.5	0.8	-57.4	0.0	0.0	0.9	17.5
2010/10/05	22:29	1375	17.57	55%	8.3	0.792	1.1	17.5	0.1	-58.5	0.0	0.0	0.2	17.5
2010/10/05	22:44	1376	17.49	57%	8.9	0.796	1.4	17.5	0.0	-57.7	0.0	0.0	0.0	17.5
2010/10/05	22:59	1377	17.29	56%	8.4	0.793	0.9	17.5	-0.2	-59.2	0.0	0.0	-0.3	17.4
2010/10/05	23:14	1378	17.3	54%	7.8	0.789	0.6	17.4	-0.1	-60.0	0.0	0.0	-0.2	17.4
2010/10/05	23:29	1379	17.29	57%	8.6	0.794	1.0	17.4	-0.1	-58.4	0.0	0.0	-0.1	17.3
2010/10/05	23:44	1380	16.99	56%	8.2	0.792	0.5	17.3	-0.4	-59.7	0.0	0.0	-0.5	17.2
2010/10/05	23:59	1381	17.01	56%	8.1	0.791	0.5	17.2	-0.3	-59.7	0.0	0.0	-0.4	17.2
2010/10/06	00:14	1382	16.97	53%	7.3	0.786	0.0	17.2	-0.2	-60.9	0.0	0.0	-0.3	17.1

S2														
Date	Time	Theta	T_db	RH	T_dp	ϵ_{sky}	T_sky	T_m (n-1)	Q_conv	Q_rad	Tank Q_ext	Heatload	Tank Heat loss/gain	T_drum theoretical
2010/10/06	00:29	1383	17.79	50%	7.3	0.786	0.8	17.1	1.1	-58.2	0.0	0.0	1.1	17.1
2010/10/06	00:44	1384	17.85	55%	8.7	0.795	1.6	17.1	1.2	-55.5	0.0	0.0	1.2	17.1
2010/10/06	00:59	1385	17.22	58%	8.7	0.795	1.0	17.1	0.1	-57.4	0.0	0.0	0.2	17.1
2010/10/06	01:14	1386	16.93	55%	7.6	0.788	0.2	17.1	-0.2	-60.2	0.0	0.0	-0.3	17.1
2010/10/06	01:29	1387	16.82	53%	7.1	0.785	-0.2	17.1	-0.3	-61.2	0.0	0.0	-0.4	17.0
2010/10/06	01:44	1388	16.64	56%	7.7	0.789	0.0	17.0	-0.5	-60.5	0.0	0.0	-0.6	16.9
2010/10/06	01:59	1389	16.36	56%	7.5	0.787	-0.4	16.9	-0.9	-61.5	0.0	0.0	-0.9	16.9
2010/10/06	02:14	1390	16.32	56%	7.4	0.787	-0.5	16.9	-0.8	-61.5	0.0	0.0	-0.9	16.8
2010/10/06	02:29	1391	16.33	54%	7.0	0.784	-0.7	16.8	-0.7	-61.9	0.0	0.0	-0.7	16.7
2010/10/06	02:44	1392	16.08	56%	7.3	0.787	-0.8	16.7	-1.0	-61.8	0.0	0.0	-1.0	16.7
2010/10/06	02:59	1393	16.13	56%	7.2	0.786	-0.8	16.7	-0.8	-61.7	0.0	0.0	-0.9	16.6
2010/10/06	03:14	1394	16.33	56%	7.5	0.787	-0.5	16.6	-0.4	-60.3	0.0	0.0	-0.4	16.5
2010/10/06	03:29	1395	16.28	54%	7.0	0.784	-0.8	16.5	-0.3	-61.1	0.0	0.0	-0.4	16.5
2010/10/06	03:44	1396	16.6	55%	7.4	0.787	-0.2	16.5	0.1	-59.1	0.0	0.0	0.2	16.5
2010/10/06	03:59	1397	16.51	55%	7.3	0.786	-0.4	16.5	0.0	-59.6	0.0	0.0	0.0	16.5
2010/10/06	04:14	1398	16.4	55%	7.3	0.786	-0.5	16.5	-0.1	-59.9	0.0	0.0	-0.1	16.4
2010/10/06	04:29	1399	16.4	57%	7.9	0.790	-0.2	16.4	0.0	-58.7	0.0	0.0	0.0	16.4
2010/10/06	04:44	1400	16.18	60%	8.3	0.792	-0.2	16.4	-0.2	-58.4	0.0	0.0	-0.3	16.3
2010/10/06	04:59	1401	15.96	55%	7.0	0.784	-1.1	16.3	-0.5	-61.1	0.0	0.0	-0.5	16.2
2010/10/06	05:14	1402	15.66	59%	7.6	0.788	-1.0	16.2	-0.9	-60.7	0.0	0.0	-0.9	16.2
2010/10/06	05:29	1403	15.31	57%	6.9	0.784	-1.7	16.2	-1.5	-62.8	0.0	0.0	-1.4	16.1
2010/10/06	05:44	1404	15	62%	7.7	0.789	-1.6	16.1	-2.0	-62.1	0.0	0.0	-1.8	16.0
2010/10/06	05:59	1405	14.77	58%	6.5	0.781	-2.4	16.0	-2.4	-64.5	0.0	0.0	-2.0	16.0
2010/10/06	06:14	1406	14.86	58%	6.5	0.781	-2.4	16.0	-2.0	-63.9	0.0	0.0	-1.8	15.9
2010/10/06	06:29	1407	15.16	59%	7.2	0.785	-1.7	15.9	-1.2	-61.7	0.0	0.0	-1.2	15.8

S2														
Date	Time	Theta	T_db	RH	T_dp	ϵ_{sky}	T_sky	T_m (n-1)	Q_conv	Q_rad	Tank Q_ext	Heatload	Tank Heat loss/gain	T_drum theoretical
2010/10/06	06:44	1408	15.76	56%	6.9	0.784	-1.3	15.8	-0.1	-60.1	0.0	0.0	-0.1	15.8
2010/10/06	06:59	1409	16.4	55%	7.4	0.787	-0.5	15.8	1.0	-57.2	0.0	0.0	1.0	15.8
2010/10/06	07:14	1410	17.07	52%	7.2	0.786	0.1	15.8	2.4	-55.4	0.0	0.0	2.0	15.8
2010/10/06	07:29	1411	17.89	50%	7.3	0.786	0.9	15.8	4.5	-52.8	0.0	0.0	3.4	15.8
2010/10/06	07:44	1412	18.5	46%	6.8	0.783	1.2	15.8	6.1	-51.8	0.0	0.0	4.3	15.8
2010/10/06	07:59	1413	19.87	42%	6.6	0.782	2.4	15.8	10.2	-47.8	0.0	0.0	6.5	15.8
2010/10/06	08:14	1414	21.02	43%	7.9	0.790	4.2	15.8	13.9	-41.8	15.0	0.0	8.3	15.8
2010/10/06	08:29	1415	22.05	41%	8.2	0.792	5.3	15.8	17.3	-38.1	15.0	0.0	9.9	15.8
2010/10/06	08:44	1416	23.4	34%	6.7	0.782	5.8	15.8	22.0	-36.7	15.0	0.0	12.0	15.9
2010/10/06	08:59	1417	24.66	33%	7.3	0.786	7.3	15.9	26.5	-31.5	15.0	0.0	14.0	15.9
2010/10/06	09:14	1418	26.04	31%	7.4	0.787	8.6	15.9	31.7	-26.8	15.0	0.0	16.2	15.9
2010/10/06	09:29	1419	27.52	29%	8.1	0.791	10.4	15.9	40.2	-20.6	15.0	0.0	18.5	16.0
2010/10/06	09:44	1420	27.25	27%	6.8	0.783	9.5	16.0	38.8	-24.2	15.0	0.0	18.0	16.0
2010/10/06	09:59	1421	28.6	27%	7.7	0.789	11.2	16.0	44.9	-17.9	15.0	0.0	20.1	16.0
2010/10/06	10:14	1422	29.28	24%	6.5	0.781	11.2	16.0	48.0	-18.1	15.0	0.0	21.1	16.1
2010/10/06	10:29	1423	30.68	24%	8.1	0.791	13.4	16.1	54.6	-10.0	15.0	0.0	23.3	16.1
2010/10/06	10:44	1424	30.61	24%	7.9	0.790	13.2	16.1	54.0	-10.9	15.0	0.0	23.1	16.2
2010/10/06	10:59	1425	31.4	22%	7.1	0.785	13.5	16.2	57.7	-9.9	15.0	0.0	24.3	16.2
2010/10/06	11:14	1426	32.65	20%	7.2	0.786	14.8	16.2	63.8	-5.4	15.0	0.0	26.2	16.2
2010/10/06	11:29	1427	33.37	21%	8.0	0.790	15.9	16.2	67.3	-1.4	15.0	0.0	27.3	16.3
2010/10/06	11:44	1428	33.58	20%	7.9	0.790	16.0	16.3	68.2	-1.1	15.0	0.0	27.6	16.3
2010/10/06	11:59	1429	33.48	19%	7.2	0.786	15.5	16.3	67.4	-3.0	15.0	0.0	27.4	16.4
2010/10/06	12:14	1430	34.96	18%	7.6	0.788	17.1	16.4	74.9	3.0	15.0	0.0	29.6	16.4
2010/10/06	12:29	1431	33.88	20%	7.9	0.790	16.3	16.4	69.0	-0.5	15.0	0.0	27.9	16.5
2010/10/06	12:44	1432	34.47	18%	6.8	0.783	16.2	16.5	71.9	-0.8	15.0	0.0	28.7	16.5

S2														
Date	Time	Theta	T_db	RH	T_dp	ϵ_{sky}	T_sky	T_m (n-1)	Q_conv	Q_rad	Tank Q_ext	Heatload	Tank Heat loss/gain	T_drum theoretical
2010/10/06	12:59	1433	34.74	18%	7.3	0.786	16.8	16.5	73.0	1.1	15.0	0.0	29.1	16.5
2010/10/06	13:14	1434	35.68	23%	11.6	0.813	20.1	16.5	77.8	14.1	15.0	0.0	30.5	16.6
2010/10/06	13:29	1435	32.46	21%	7.2	0.786	14.6	16.6	60.8	-7.7	15.0	0.0	25.3	16.6
2010/10/06	13:44	1436	32.7	21%	7.6	0.788	15.0	16.6	61.8	-6.1	15.0	0.0	25.6	16.7
2010/10/06	13:59	1437	32.07	21%	7.4	0.787	14.3	16.7	58.4	-9.0	15.0	0.0	24.6	16.7
2010/10/06	14:14	1438	32.74	19%	5.9	0.777	14.1	16.7	61.6	-10.0	15.0	0.0	25.6	16.7
2010/10/06	14:29	1439	34.37	21%	9.3	0.799	17.6	16.7	69.7	3.1	15.0	0.0	28.1	16.8
2010/10/06	14:44	1440	32.87	20%	7.2	0.786	15.0	16.8	61.8	-6.9	15.0	0.0	25.6	16.8
2010/10/06	14:59	1441	31.89	22%	7.9	0.790	14.4	16.8	56.7	-9.2	15.0	0.0	24.0	16.9
2010/10/06	15:14	1442	33.04	21%	8.0	0.791	15.6	16.9	62.3	-5.0	15.0	0.0	25.8	16.9
2010/10/06	15:29	1443	33.46	26%	11.6	0.813	18.0	16.9	64.2	4.3	15.0	0.0	26.4	17.0
2010/10/06	15:44	1444	29.99	25%	7.8	0.789	12.6	17.0	46.9	-16.6	15.0	0.0	20.8	17.0
2010/10/06	15:59	1445	32.01	24%	9.0	0.797	15.1	17.0	56.5	-7.1	15.0	0.0	23.9	17.0
2010/10/06	16:14	1446	31.88	24%	8.9	0.796	15.0	17.0	55.7	-7.8	15.0	0.0	23.7	17.1
2010/10/06	16:29	1447	30.4	26%	9.0	0.797	13.6	17.1	48.3	-13.1	15.0	0.0	21.3	17.1
2010/10/06	16:44	1448	30.36	30%	10.8	0.808	14.6	17.1	47.9	-9.6	15.0	0.0	21.1	17.1
2010/10/06	16:59	1449	28.31	29%	8.6	0.794	11.5	17.1	38.2	-21.4	15.0	0.0	17.8	17.2
2010/10/06	17:14	1450	28.27	29%	8.6	0.795	11.4	17.2	37.9	-21.7	15.0	0.0	17.7	17.2
2010/10/06	17:29	1451	27.26	33%	9.6	0.801	11.0	17.2	31.3	-23.3	15.0	0.0	16.0	17.2
2010/10/06	17:44	1452	26.04	36%	9.7	0.801	9.9	17.2	26.5	-27.4	15.0	0.0	14.0	17.3
2010/10/06	17:59	1453	24.81	38%	9.5	0.800	8.6	17.3	21.9	-32.1	15.0	0.0	12.0	17.3
2010/10/06	18:14	1454	23.63	39%	8.7	0.795	7.1	17.3	17.6	-37.7	15.0	0.0	10.1	17.3
2010/10/06	18:29	1455	23.27	40%	9.0	0.797	6.9	17.3	16.3	-38.4	15.0	0.0	9.5	17.3
2010/10/06	18:44	1456	22.63	43%	9.2	0.798	6.4	17.3	14.0	-40.2	15.0	0.0	8.4	17.4
2010/10/06	18:59	1457	22.4	41%	8.3	0.792	5.7	17.4	13.2	-42.8	15.0	0.0	8.0	17.4

S2														
Date	Time	Theta	T_db	RH	T_dp	ϵ_{sky}	T_sky	T_m (n-1)	Q_conv	Q_rad	Tank Q_ext	Heatload	Tank Heat loss/gain	T_drum theoretical
2010/10/06	19:14	1458	22.67	67%	16.2	0.841	10.2	17.4	14.0	-27.1	15.0	0.0	8.4	17.4
2010/10/06	19:29	1459	17.43	73%	12.5	0.819	3.2	17.4	0.0	-51.3	0.0	0.0	0.0	17.4
2010/10/06	19:44	1460	17.2	65%	10.5	0.806	1.9	17.4	-0.3	-55.6	0.0	0.0	-0.3	17.4
2010/10/06	19:59	1461	17.7	64%	10.7	0.807	2.5	17.4	0.5	-53.4	0.0	0.0	0.5	17.4
2010/10/06	20:14	1462	17.6	61%	10.0	0.803	2.1	17.4	0.3	-54.9	0.0	0.0	0.4	17.4
2010/10/06	20:29	1463	17.9	54%	8.4	0.793	1.5	17.4	0.8	-56.8	0.0	0.0	0.9	17.4
2010/10/06	20:44	1464	19.09	47%	7.4	0.787	2.1	17.4	3.5	-54.9	0.0	0.0	2.8	17.4
2010/10/06	20:59	1465	20.44	47%	8.8	0.795	4.1	17.4	7.2	-48.1	15.0	0.0	4.9	17.4
2010/10/06	21:14	1466	20.31	49%	9.2	0.798	4.2	17.4	6.7	-47.9	15.0	0.0	4.7	17.4
2010/10/06	21:29	1467	19.73	47%	8.0	0.791	3.0	17.4	5.0	-51.9	0.0	0.0	3.7	17.4
2010/10/06	21:44	1468	20.19	48%	8.8	0.796	3.9	17.4	6.3	-49.0	15.0	0.0	4.4	17.4
2010/10/06	21:59	1469	19.59	54%	10.1	0.804	4.0	17.4	4.6	-48.7	0.0	0.0	3.4	17.4
2010/10/06	22:14	1470	18.75	56%	9.8	0.802	3.0	17.4	2.5	-52.0	0.0	0.0	2.1	17.4
2010/10/06	22:29	1471	18.36	59%	10.2	0.804	2.9	17.4	1.6	-52.5	0.0	0.0	1.5	17.4
2010/10/06	22:44	1472	18.06	59%	9.9	0.803	2.5	17.4	1.0	-53.9	0.0	0.0	1.0	17.4
2010/10/06	22:59	1473	17.75	58%	9.4	0.799	1.9	17.4	0.4	-55.9	0.0	0.0	0.5	17.4
2010/10/06	23:14	1474	17.61	59%	9.5	0.800	1.8	17.4	0.2	-56.1	0.0	0.0	0.3	17.4
2010/10/06	23:29	1475	17.4	61%	9.7	0.801	1.7	17.4	0.0	-56.5	0.0	0.0	-0.1	17.4
2010/10/06	23:44	1476	17.19	59%	8.9	0.796	1.1	17.4	-0.2	-58.1	0.0	0.0	-0.3	17.3
2010/10/06	23:59	1477	17.42	62%	9.9	0.803	1.9	17.3	0.1	-55.5	0.0	0.0	0.2	17.3

APPENDIX C: EXPERIMENTAL DATA EXTRACT

S1 Experimental data extract – 5 October to 6 October 2010

Table 8 : S1 Experimental data extract

S1						
Date	Time	S1 Drum [°C]	S1 T_out [°C]	S1 T_in [°C]	Ambient temperature [°C]	T_WB [°C]
05-Oct-10	00:14:15	21.78	20.9	21.18	20.06	15.28
05-Oct-10	00:29:15	21.67	20.81	21.08	19.92	15.3
05-Oct-10	00:44:15	21.6	20.73	21.06	19.43	14.94
05-Oct-10	00:59:15	21.5	20.8	20.97	19.19	15.38
05-Oct-10	01:14:15	21.53	20.69	21.01	18.42	14.8
05-Oct-10	01:29:15	21.79	20.45	20.81	18.1	14.5
05-Oct-10	01:44:15	22.19	20.11	20.62	17.81	14.4
05-Oct-10	01:59:15	21.65	20.49	20.87	17.89	14.53
05-Oct-10	02:14:15	21.79	20.39	20.79	18.4	14.69
05-Oct-10	02:29:15	21.4	20.5	20.52	18.72	14.86
05-Oct-10	02:44:15	21.78	20.46	20.74	19.03	14.73
05-Oct-10	02:59:15	21.53	20.31	20.88	18.74	15.07
05-Oct-10	03:14:15	21.78	20.13	20.76	17.5	14.76
05-Oct-10	03:29:15	21.61	20.51	20.75	17.02	14.74
05-Oct-10	03:44:15	21.33	20.24	20.62	16.86	14.64
05-Oct-10	03:59:15	21.41	20.26	20.6	17.12	14.52
05-Oct-10	04:14:15	21.47	20.21	20.57	17.01	14.29
05-Oct-10	04:29:15	21	20.1	20.55	16.66	14.27
05-Oct-10	04:44:15	20.82	20.14	20.4	16.07	13.74
05-Oct-10	04:59:15	21.42	20.21	20.19	15.97	13.42
05-Oct-10	05:14:15	21.37	19.87	20.19	15.89	13.57
05-Oct-10	05:29:15	21.21	20.24	20.32	15.86	13.26
05-Oct-10	05:44:15	21.13	19.96	20.18	15.15	13.16
05-Oct-10	05:59:15	20.91	19.69	20.2	15	12.94
05-Oct-10	06:14:15	20.4	20.03	19.94	15.57	13.62
05-Oct-10	06:29:15	20.84	19.82	20.06	15.83	13.4
05-Oct-10	06:44:15	20.64	19.66	20.15	16.75	14.03
05-Oct-10	06:59:15	20.55	20.09	20.26	17.73	14.43
05-Oct-10	07:14:15	20.01	20.26	20.26	18.8	15.08
05-Oct-10	07:29:15	20.48	20.21	20.42	20.42	15.68
05-Oct-10	07:44:15	20.25	20.53	20.88	20.69	15.65
05-Oct-10	07:59:15	19.96	21.14	21.83	22.55	16.86

S1						
Date	Time	S1 Drum [°C]	S1 T_out [°C]	S1 T_in [°C]	Ambient temperature [°C]	T_WB [°C]
05-Oct-10	08:14:15	20.17	20.98	23.49	24.96	18.42
05-Oct-10	08:29:15	20.41	22.01	24.11	23.66	17.26
05-Oct-10	08:44:15	20.57	23.08	24.49	23.83	17.31
05-Oct-10	08:59:15	20.25	23.71	24.34	23.4	17
05-Oct-10	09:14:15	20.44	24.26	24.43	24.34	17.45
05-Oct-10	09:29:15	20.29	24.97	25.57	25.21	17.8
05-Oct-10	09:44:15	20.52	25.87	26.24	25.92	18.12
05-Oct-10	09:59:15	20.29	26.33	26.94	26.75	17.8
05-Oct-10	10:14:15	20.53	26.73	27.07	26.04	17.43
05-Oct-10	10:29:15	20.43	27.21	28.05	29.24	18.96
05-Oct-10	10:44:15	20.66	28.2	28.79	29.77	18.77
05-Oct-10	10:59:15	20.2	29.24	30	29.94	18.93
05-Oct-10	11:14:15	20.42	30.6	31.24	29	18.63
05-Oct-10	11:29:15	20.43	29.89	30.78	30.36	19.21
05-Oct-10	11:44:15	20.95	30.71	31.22	31.56	19.46
05-Oct-10	11:59:15	20.15	31.56	32.2	31.24	19.22
05-Oct-10	12:14:15	20.39	32.14	32.83	32.32	19.73
05-Oct-10	12:29:15	20.7	33.27	33.69	31.86	19.62
05-Oct-10	12:44:15	21.13	33.25	33.9	31.53	19.43
05-Oct-10	12:59:15	20.7	34.22	34.22	31.21	19.42
05-Oct-10	13:14:15	20.93	33.81	33.7	31.26	19.45
05-Oct-10	13:29:15	21.13	34.36	34	31.68	20
05-Oct-10	13:44:15	20.96	33.69	33.78	32.45	20.41
05-Oct-10	13:59:15	20.94	34.21	34.36	31.26	19.89
05-Oct-10	14:14:15	21	33.85	33.88	30.35	19.19
05-Oct-10	14:29:15	21.25	33.43	33.59	30.65	19.38
05-Oct-10	14:44:15	21.06	33.42	33.2	30.52	19.39
05-Oct-10	14:59:15	20.93	33.07	33.57	32.19	20.25
05-Oct-10	15:14:15	21.1	33.47	33.5	30.05	19.52
05-Oct-10	15:29:15	21.07	33.21	33.13	31.82	20
05-Oct-10	15:44:15	21.31	33.13	33.47	31.91	20.3
05-Oct-10	15:59:15	21.06	33.03	33.28	31.79	20.69
05-Oct-10	16:14:15	21.27	32.83	33.41	30.34	19.45
05-Oct-10	16:29:15	21.43	32.41	32.98	29.12	19.18
05-Oct-10	16:44:15	20.79	31.68	32.36	29.36	19.72
05-Oct-10	16:59:15	21.39	31.66	32.15	29.32	20.32
05-Oct-10	17:14:15	21.6	30.72	32.21	27.7	19.49
05-Oct-10	17:29:15	21.69	29.86	31.25	26.72	18.83
05-Oct-10	17:44:15	21.46	28.82	30.4	25.59	18.27
05-Oct-10	17:59:15	21.62	28.51	29.66	24.1	18.29
05-Oct-10	18:14:15	21.85	27.82	28.94	23.05	17.49

S1						
Date	Time	S1 Drum [°C]	S1 T_out [°C]	S1 T_in [°C]	Ambient temperature [°C]	T_WB [°C]
05-Oct-10	18:29:15	22.08	26.51	28.34	22.28	17.36
05-Oct-10	18:44:15	22.08	25.22	26.23	21.55	16.98
05-Oct-10	18:59:15	22.73	24.76	26.16	21.29	16.57
05-Oct-10	19:14:15	22.47	24.66	26	20.97	16.02
05-Oct-10	19:29:15	22.81	24.26	25.91	20.5	16.28
05-Oct-10	19:44:15	23.01	24.11	25.49	20.43	15.9
05-Oct-10	19:59:15	22.89	23.13	24.6	20.23	15.59
05-Oct-10	20:14:15	22.93	22.58	24.16	20.09	15.03
05-Oct-10	20:29:15	22.95	22.38	23.23	19.81	15.17
05-Oct-10	20:44:15	23.52	22.32	22.65	18.73	14.34
05-Oct-10	20:59:15	23.2	22.19	22.35	18.42	14.4
05-Oct-10	21:14:15	23.25	21.86	22.08	18.19	14.15
05-Oct-10	21:29:15	22.9	21.9	22.15	18.41	14.27
05-Oct-10	21:44:15	22.62	21.4	21.94	18.69	13.8
05-Oct-10	21:59:15	22.31	21.58	21.92	18.42	14.22
05-Oct-10	22:14:15	22.54	21.38	21.63	18.02	14.07
05-Oct-10	22:29:15	22.24	21.61	21.69	17.57	13.65
05-Oct-10	22:44:15	22.61	21.61	21.59	17.49	13.91
05-Oct-10	22:59:15	22.45	21.4	21.64	17.29	14.13
05-Oct-10	23:14:15	22.25	21.17	21.46	17.3	13.95
05-Oct-10	23:29:15	22.16	20.88	21.39	17.29	13.56
05-Oct-10	23:44:15	21.91	21.43	21.37	16.99	13.76
05-Oct-10	23:59:15	22.17	20.87	21.26	17.01	13.71
06-Oct-10	00:14:15	21.94	21.2	21.31	16.97	13.58
06-Oct-10	00:29:15	21.97	21.2	21.01	17.79	13.94
06-Oct-10	00:44:15	21.96	20.81	21.2	17.85	13.56
06-Oct-10	00:59:15	22.15	20.56	21.01	17.22	13.74
06-Oct-10	01:14:15	21.99	20.55	21.29	16.93	13.83
06-Oct-10	01:29:15	21.34	21.07	21.02	16.82	13.23
06-Oct-10	01:44:15	21.81	20.41	20.63	16.64	12.82
06-Oct-10	01:59:15	21.75	20.35	20.76	16.36	13.01
06-Oct-10	02:14:15	21.52	20.25	20.7	16.32	12.99
06-Oct-10	02:29:15	21.27	20.16	20.74	16.33	12.96
06-Oct-10	02:44:15	22.27	20.22	20.48	16.08	12.52
06-Oct-10	02:59:15	21.97	20.22	20.13	16.13	12.9
06-Oct-10	03:14:15	21.29	19.75	20.6	16.33	12.97
06-Oct-10	03:29:15	21.06	19.91	20.43	16.28	12.98
06-Oct-10	03:44:15	20.98	20.06	20.26	16.6	13.01
06-Oct-10	03:59:15	21.2	19.68	20.4	16.51	13
06-Oct-10	04:14:15	20.93	19.9	20.1	16.4	12.89
06-Oct-10	04:29:15	20.74	19.64	20.26	16.4	12.96

S1						
Date	Time	S1 Drum [°C]	S1 T_out [°C]	S1 T_in [°C]	Ambient temperature [°C]	T_WB [°C]
06-Oct-10	04:44:15	20.86	19.74	20.2	16.18	13.09
06-Oct-10	04:59:15	20.86	19.48	19.9	15.96	13.26
06-Oct-10	05:14:15	20.46	19.47	20.02	15.66	12.36
06-Oct-10	05:29:15	20.78	19.09	19.82	15.31	12.6
06-Oct-10	05:44:15	20.76	19.12	19.78	15	12.11
06-Oct-10	05:59:15	20.56	19.1	19.67	14.77	12.49
06-Oct-10	06:14:15	20.23	19.43	19.78	14.86	12.03
06-Oct-10	06:29:15	20.5	19.16	19.69	15.16	12.28
06-Oct-10	06:44:15	20.21	19.18	19.65	15.76	12.99
06-Oct-10	06:59:15	20.03	19.17	19.6	16.4	13.06
06-Oct-10	07:14:15	20.06	19.28	19.65	17.07	13.59
06-Oct-10	07:29:15	19.8	19.31	19.66	17.89	13.95
06-Oct-10	07:44:15	20.1	19.51	19.76	18.5	14.18
06-Oct-10	07:59:15	19.9	19.84	19.9	19.87	15.09
06-Oct-10	08:14:15	19.68	19.87	20.58	21.02	15.26
06-Oct-10	08:29:15	19.89	20.53	21.45	22.05	16.28
06-Oct-10	08:44:15	19.66	21.08	22.35	23.4	17.16
06-Oct-10	08:59:15	19.67	22.06	23.7	24.66	16.93
06-Oct-10	09:14:15	19.9	23.11	24.9	26.04	17.78
06-Oct-10	09:29:15	19.75	23.71	26.17	27.52	18.36
06-Oct-10	09:44:15	19.63	24.75	27.23	27.25	17.79
06-Oct-10	09:59:15	19.65	26.02	28.15	28.6	18.43
06-Oct-10	10:14:15	19.79	26.88	29.01	29.28	18.93
06-Oct-10	10:29:15	19.57	27.58	29.7	30.68	19.18
06-Oct-10	10:44:15	19.6	28.22	30.86	30.61	19.34
06-Oct-10	10:59:15	20.11	30.03	31.46	31.4	19.79
06-Oct-10	11:14:15	19.97	30.93	32.19	32.65	19.99
06-Oct-10	11:29:15	20.08	32.01	33.06	33.37	20.1
06-Oct-10	11:44:15	20.06	32.82	33.69	33.58	20.34
06-Oct-10	11:59:15	20.17	33.31	34.19	33.48	20.11
06-Oct-10	12:14:15	20.09	34.81	34.93	34.96	21.14
06-Oct-10	12:29:15	20.47	34.48	35.75	33.88	19.77
06-Oct-10	12:44:15	20.72	34.62	35.8	34.47	20.84
06-Oct-10	12:59:15	20.41	35.46	36.05	34.74	20.34
06-Oct-10	13:14:15	20.41	35.69	35.95	35.68	21.14
06-Oct-10	13:29:15	20.6	35.27	36.11	32.46	20.29
06-Oct-10	13:44:15	20.92	35.56	35.81	32.7	19.64
06-Oct-10	13:59:15	20.41	34.86	35.29	32.07	19.28
06-Oct-10	14:14:15	20.45	33.6	35.05	32.74	19.9
06-Oct-10	14:29:15	20.68	33.55	34.85	34.37	20.25
06-Oct-10	14:44:15	20.34	35.11	35.4	32.87	19.99

S1						
Date	Time	S1 Drum [°C]	S1 T_out [°C]	S1 T_in [°C]	Ambient temperature [°C]	T_WB [°C]
06-Oct-10	14:59:15	21.33	34.2	34.91	31.89	18.91
06-Oct-10	15:14:15	21.22	34.06	34.58	33.04	20.48
06-Oct-10	15:29:15	21.06	34.02	34.86	33.46	20.39
06-Oct-10	15:44:15	21.04	33.49	34.53	29.99	19.48
06-Oct-10	15:59:15	21.02	32.94	33.96	32.01	20.45
06-Oct-10	16:14:15	21.02	33.04	34.14	31.88	20.07
06-Oct-10	16:29:15	21.03	32.92	34.12	30.4	19.09
06-Oct-10	16:44:15	21.21	32.55	33.36	30.36	19.71
06-Oct-10	16:59:15	20.93	31.43	32.84	28.31	18.85
06-Oct-10	17:14:15	21.17	30.46	32	28.27	18.6
06-Oct-10	17:29:15	21.24	30.29	30.91	27.26	17.76
06-Oct-10	17:44:15	21.34	29.5	30.23	26.04	17.79
06-Oct-10	17:59:15	21.02	28.72	29.1	24.81	17.47
06-Oct-10	18:14:15	21.56	27.45	28.27	23.63	16.72
06-Oct-10	18:29:15	21.5	26.78	28.29	23.27	16.52
06-Oct-10	18:44:15	22.02	25.34	27.21	22.63	16.26
06-Oct-10	18:59:15	22.01	24.75	26.14	22.4	16.51
06-Oct-10	19:14:15	22.17	24.65	26.04	22.67	16.34
06-Oct-10	19:29:15	22.66	23.85	25.74	17.43	15.76
06-Oct-10	19:44:15	22.68	23.27	24.56	17.2	16.43
06-Oct-10	19:59:15	22.71	21.86	23.37	17.7	15.7
06-Oct-10	20:14:15	22.54	21.69	22.26	17.6	15.43
06-Oct-10	20:29:15	22.54	21.51	21.91	17.9	15.38
06-Oct-10	20:44:15	22.49	21.64	21.73	19.09	15.5
06-Oct-10	20:59:15	21.54	21.99	21.69	20.44	15.65
06-Oct-10	21:14:15	22.43	21.65	21.85	20.31	15.63
06-Oct-10	21:29:15	22.34	21.56	21.84	19.73	15.38
06-Oct-10	21:44:15	22.51	21.43	21.74	20.19	15.47
06-Oct-10	21:59:15	22.18	21.37	21.81	19.59	15.06
06-Oct-10	22:14:15	22.34	20.83	21.76	18.75	15.18
06-Oct-10	22:29:15	22.33	21.8	21.57	18.36	15.03
06-Oct-10	22:44:15	22.32	21.43	21.74	18.06	15.18
06-Oct-10	22:59:15	22.63	21.18	21.41	17.75	14.89
06-Oct-10	23:14:15	22.34	20.81	21.36	17.61	14.58
06-Oct-10	23:29:15	22.33	20.98	21.39	17.4	14.53
06-Oct-10	23:44:15	22.34	20.71	21.34	17.19	14.55
06-Oct-10	23:59:15	22.1	20.78	21.24	17.42	14.46

S2 Experimental data extract – 5 October to 6 October 2010

Table 9 : S2 Experimental data extract

S2						
Date	Time	S2 Drum [°C]	S2 T_out [°C]	S2 T_in [°C]	Ambient temperature [°C]	T_WB [°C]
05-Oct-10	00:14:15	16.79	20.36	20.58	20.06	15.28
05-Oct-10	00:29:15	16.83	20.16	20.24	19.92	15.3
05-Oct-10	00:44:15	16.78	20.16	20.26	19.43	14.94
05-Oct-10	00:59:15	16.79	20.14	19.91	19.19	15.38
05-Oct-10	01:14:15	17.03	20.04	19.82	18.42	14.8
05-Oct-10	01:29:15	16.86	19.92	19.53	18.1	14.5
05-Oct-10	01:44:15	16.86	19.64	19.35	17.81	14.4
05-Oct-10	01:59:15	16.81	19.26	18.68	17.89	14.53
05-Oct-10	02:14:15	16.88	18.78	18.51	18.4	14.69
05-Oct-10	02:29:15	16.32	18.35	18.37	18.72	14.86
05-Oct-10	02:44:15	16.84	18.93	18.65	19.03	14.73
05-Oct-10	02:59:15	16.81	18.99	18.62	18.74	15.07
05-Oct-10	03:14:15	17.03	18.62	18.44	17.5	14.76
05-Oct-10	03:29:15	16.98	17.98	18.34	17.02	14.74
05-Oct-10	03:44:15	17.13	18.18	18.23	16.86	14.64
05-Oct-10	03:59:15	16.98	18.02	18.09	17.12	14.52
05-Oct-10	04:14:15	17.06	17.61	17.89	17.01	14.29
05-Oct-10	04:29:15	17.06	17.72	17.77	16.66	14.27
05-Oct-10	04:44:15	16.93	17.61	17.64	16.07	13.74
05-Oct-10	04:59:15	16.81	17.82	17.49	15.97	13.42
05-Oct-10	05:14:15	16.98	17.58	17.61	15.89	13.57
05-Oct-10	05:29:15	17.02	17.73	17.65	15.86	13.26
05-Oct-10	05:44:15	16.87	17.32	17.57	15.15	13.16
05-Oct-10	05:59:15	17	17.2	17.52	15	12.94
05-Oct-10	06:14:15	16.91	17.51	17.36	15.57	13.62
05-Oct-10	06:29:15	16.9	17.43	17.36	15.83	13.4
05-Oct-10	06:44:15	16.86	17.59	17.79	16.75	14.03
05-Oct-10	06:59:15	16.62	17.73	17.85	17.73	14.43
05-Oct-10	07:14:15	16.73	17.92	18.39	18.8	15.08
05-Oct-10	07:29:15	16.77	18.4	19.32	20.42	15.68
05-Oct-10	07:44:15	16.65	18.99	20.2	20.69	15.65
05-Oct-10	07:59:15	16.73	19.56	21.27	22.55	16.86
05-Oct-10	08:14:15	16.64	20.7	22.73	24.96	18.42
05-Oct-10	08:29:15	16.73	21.63	23.83	23.66	17.26
05-Oct-10	08:44:15	16.71	22.82	24.19	23.83	17.31
05-Oct-10	08:59:15	16.87	23.4	24.2	23.4	17

S2						
Date	Time	S2 Drum [°C]	S2 T_out [°C]	S2 T_in [°C]	Ambient temperature [°C]	T_WB [°C]
05-Oct-10	09:14:15	16.81	23.96	24.37	24.34	17.45
05-Oct-10	09:29:15	16.69	24.29	24.82	25.21	17.8
05-Oct-10	09:44:15	17.04	25.4	25.96	25.92	18.12
05-Oct-10	09:59:15	16.81	26.02	26.58	26.75	17.8
05-Oct-10	10:14:15	16.8	27.34	26.94	26.04	17.43
05-Oct-10	10:29:15	16.95	28.33	27.78	29.24	18.96
05-Oct-10	10:44:15	17.35	28.7	28.23	29.77	18.77
05-Oct-10	10:59:15	16.88	30.09	29.77	29.94	18.93
05-Oct-10	11:14:15	16.78	30.93	30.68	29	18.63
05-Oct-10	11:29:15	17.03	30.37	30.64	30.36	19.21
05-Oct-10	11:44:15	17.24	30.99	31.08	31.56	19.46
05-Oct-10	11:59:15	17.09	31.89	31.89	31.24	19.22
05-Oct-10	12:14:15	17.16	33.54	32.88	32.32	19.73
05-Oct-10	12:29:15	17.08	33.54	33.58	31.86	19.62
05-Oct-10	12:44:15	17.33	34.04	34.33	31.53	19.43
05-Oct-10	12:59:15	17.27	34.53	34.22	31.21	19.42
05-Oct-10	13:14:15	17.15	34.39	34.14	31.26	19.45
05-Oct-10	13:29:15	16.81	34.73	34.45	31.68	20
05-Oct-10	13:44:15	17.35	34.29	34.26	32.45	20.41
05-Oct-10	13:59:15	17.52	34.86	34.7	31.26	19.89
05-Oct-10	14:14:15	17.39	34.43	34.01	30.35	19.19
05-Oct-10	14:29:15	17.37	33.59	34.06	30.65	19.38
05-Oct-10	14:44:15	17.26	33.28	34.09	30.52	19.39
05-Oct-10	14:59:15	17.31	33.76	34.33	32.19	20.25
05-Oct-10	15:14:15	17.33	33.61	34.23	30.05	19.52
05-Oct-10	15:29:15	17.2	33.9	34.47	31.82	20
05-Oct-10	15:44:15	17.62	33.58	34.36	31.91	20.3
05-Oct-10	15:59:15	17.44	33.45	34.64	31.79	20.69
05-Oct-10	16:14:15	17.5	33.42	34.36	30.34	19.45
05-Oct-10	16:29:15	17.55	32.87	34.12	29.12	19.18
05-Oct-10	16:44:15	17.58	32.14	33.71	29.36	19.72
05-Oct-10	16:59:15	17.44	31.71	33.19	29.32	20.32
05-Oct-10	17:14:15	17.41	31.06	32.68	27.7	19.49
05-Oct-10	17:29:15	17.79	30.2	32.13	26.72	18.83
05-Oct-10	17:44:15	17.32	29.53	31.29	25.59	18.27
05-Oct-10	17:59:15	17.77	28.78	30.57	24.1	18.29
05-Oct-10	18:14:15	17.91	28.03	29.46	23.05	17.49
05-Oct-10	18:29:15	17.93	26.82	27.45	22.28	17.36
05-Oct-10	18:44:15	17.72	25.81	26.97	21.55	16.98
05-Oct-10	18:59:15	17.83	24.09	25.98	21.29	16.57
05-Oct-10	19:14:15	17.73	24.32	25.77	20.97	16.02

S2						
Date	Time	S2 Drum [°C]	S2 T_out [°C]	S2 T_in [°C]	Ambient temperature [°C]	T_WB [°C]
05-Oct-10	19:29:15	18.04	23.76	25.49	20.5	16.28
05-Oct-10	19:44:15	17.53	23.49	24.65	20.43	15.9
05-Oct-10	19:59:15	17.63	23.01	23.99	20.23	15.59
05-Oct-10	20:14:15	18.31	22.73	23.35	20.09	15.03
05-Oct-10	20:29:15	18.13	22.34	22.7	19.81	15.17
05-Oct-10	20:44:15	17.81	21.41	21.77	18.73	14.34
05-Oct-10	20:59:15	18.12	21.53	21.07	18.42	14.4
05-Oct-10	21:14:15	17.81	20.74	20.98	18.19	14.15
05-Oct-10	21:29:15	18.04	20.29	20.28	18.41	14.27
05-Oct-10	21:44:15	17.77	19.78	19.53	18.69	13.8
05-Oct-10	21:59:15	17.96	19.15	19.39	18.42	14.22
05-Oct-10	22:14:15	18.15	19.15	18.99	18.02	14.07
05-Oct-10	22:29:15	18.19	18.82	19.12	17.57	13.65
05-Oct-10	22:44:15	17.69	18.93	19.14	17.49	13.91
05-Oct-10	22:59:15	17.89	18.78	18.73	17.29	14.13
05-Oct-10	23:14:15	18.22	18.25	18.67	17.3	13.95
05-Oct-10	23:29:15	18.07	18.83	18.46	17.29	13.56
05-Oct-10	23:44:15	17.96	18.46	18.61	16.99	13.76
05-Oct-10	23:59:15	17.89	18.48	18.27	17.01	13.71
06-Oct-10	00:14:15	17.92	19.15	18.47	16.97	13.58
06-Oct-10	00:29:15	18.32	18.31	18.43	17.79	13.94
06-Oct-10	00:44:15	18.16	18.79	18.37	17.85	13.56
06-Oct-10	00:59:15	18.13	18.42	18.41	17.22	13.74
06-Oct-10	01:14:15	17.69	18.35	18.36	16.93	13.83
06-Oct-10	01:29:15	17.68	18.79	18.4	16.82	13.23
06-Oct-10	01:44:15	17.37	18.21	18.45	16.64	12.82
06-Oct-10	01:59:15	17.58	18.33	18.5	16.36	13.01
06-Oct-10	02:14:15	17.48	18.3	18.36	16.32	12.99
06-Oct-10	02:29:15	17.4	18.31	18.37	16.33	12.96
06-Oct-10	02:44:15	17.11	18.21	18.56	16.08	12.52
06-Oct-10	02:59:15	17.43	17.95	18.73	16.13	12.9
06-Oct-10	03:14:15	17.23	18.67	17.87	16.33	12.97
06-Oct-10	03:29:15	17.3	18.32	18.39	16.28	12.98
06-Oct-10	03:44:15	17.18	18.52	18.19	16.6	13.01
06-Oct-10	03:59:15	17.11	18.08	18.15	16.51	13
06-Oct-10	04:14:15	17.11	17.71	18.01	16.4	12.89
06-Oct-10	04:29:15	17.34	17.8	17.91	16.4	12.96
06-Oct-10	04:44:15	17.12	17.83	17.98	16.18	13.09
06-Oct-10	04:59:15	16.85	17.79	17.91	15.96	13.26
06-Oct-10	05:14:15	17.32	17.6	17.92	15.66	12.36
06-Oct-10	05:29:15	16.84	17.6	17.94	15.31	12.6

S2						
Date	Time	S2 Drum [°C]	S2 T_out [°C]	S2 T_in [°C]	Ambient temperature [°C]	T_WB [°C]
06-Oct-10	05:44:15	17.27	17.94	17.73	15	12.11
06-Oct-10	05:59:15	17.04	17.54	17.76	14.77	12.49
06-Oct-10	06:14:15	16.91	17.38	17.66	14.86	12.03
06-Oct-10	06:29:15	16.97	17.45	17.67	15.16	12.28
06-Oct-10	06:44:15	16.88	17.66	17.64	15.76	12.99
06-Oct-10	06:59:15	16.81	17.73	17.57	16.4	13.06
06-Oct-10	07:14:15	16.73	17.84	17.71	17.07	13.59
06-Oct-10	07:29:15	16.73	18.13	17.98	17.89	13.95
06-Oct-10	07:44:15	16.72	18.47	18.47	18.5	14.18
06-Oct-10	07:59:15	16.8	18.76	19.42	19.87	15.09
06-Oct-10	08:14:15	16.76	19.6	19.48	21.02	15.26
06-Oct-10	08:29:15	16.67	20.22	20.97	22.05	16.28
06-Oct-10	08:44:15	16.62	20.96	21.72	23.4	17.16
06-Oct-10	08:59:15	16.54	22.28	23.1	24.66	16.93
06-Oct-10	09:14:15	16.77	22.94	24.14	26.04	17.78
06-Oct-10	09:29:15	16.71	24.07	25.18	27.52	18.36
06-Oct-10	09:44:15	16.72	25.31	26.39	27.25	17.79
06-Oct-10	09:59:15	16.73	26.67	27.33	28.6	18.43
06-Oct-10	10:14:15	16.82	27.63	28.35	29.28	18.93
06-Oct-10	10:29:15	16.53	28.99	29.38	30.68	19.18
06-Oct-10	10:44:15	16.86	29.58	30.05	30.61	19.34
06-Oct-10	10:59:15	16.73	29.96	30.79	31.4	19.79
06-Oct-10	11:14:15	17	30.93	31.55	32.65	19.99
06-Oct-10	11:29:15	16.97	31.81	32.78	33.37	20.1
06-Oct-10	11:44:15	16.41	32.02	33.72	33.58	20.34
06-Oct-10	11:59:15	17.23	33.62	34.36	33.48	20.11
06-Oct-10	12:14:15	16.9	34.26	34.91	34.96	21.14
06-Oct-10	12:29:15	16.87	35.14	36.04	33.88	19.77
06-Oct-10	12:44:15	17.28	36.03	36.14	34.47	20.84
06-Oct-10	12:59:15	17.36	36.52	36.57	34.74	20.34
06-Oct-10	13:14:15	17.65	36.86	36.88	35.68	21.14
06-Oct-10	13:29:15	17.14	36.43	36.65	32.46	20.29
06-Oct-10	13:44:15	17.47	35.96	36.01	32.7	19.64
06-Oct-10	13:59:15	17.36	35.19	35.74	32.07	19.28
06-Oct-10	14:14:15	17.44	34.21	35.24	32.74	19.9
06-Oct-10	14:29:15	17.65	34.24	35.2	34.37	20.25
06-Oct-10	14:44:15	17.6	34.91	35.93	32.87	19.99
06-Oct-10	14:59:15	17.44	34.9	35.08	31.89	18.91
06-Oct-10	15:14:15	17.33	34.08	34.88	33.04	20.48
06-Oct-10	15:29:15	17.8	34.48	35.68	33.46	20.39
06-Oct-10	15:44:15	17.76	34.04	34.93	29.99	19.48

S2						
Date	Time	S2 Drum [°C]	S2 T_out [°C]	S2 T_in [°C]	Ambient temperature [°C]	T_WB [°C]
06-Oct-10	15:59:15	17.71	33.33	34.37	32.01	20.45
06-Oct-10	16:14:15	17.78	33.63	34.36	31.88	20.07
06-Oct-10	16:29:15	17.99	33.55	34.09	30.4	19.09
06-Oct-10	16:44:15	17.84	32.83	33.7	30.36	19.71
06-Oct-10	16:59:15	17.98	31.98	33.06	28.31	18.85
06-Oct-10	17:14:15	17.91	31.33	32.27	28.27	18.6
06-Oct-10	17:29:15	17.92	30.52	31.41	27.26	17.76
06-Oct-10	17:44:15	18.17	29.82	30.73	26.04	17.79
06-Oct-10	17:59:15	18.18	29.05	29.71	24.81	17.47
06-Oct-10	18:14:15	17.98	28.34	27.84	23.63	16.72
06-Oct-10	18:29:15	18.14	26.86	27.37	23.27	16.52
06-Oct-10	18:44:15	18.12	26.08	26.56	22.63	16.26
06-Oct-10	18:59:15	18	25.57	25.85	22.4	16.51
06-Oct-10	19:14:15	18.33	24.84	25.46	22.67	16.34
06-Oct-10	19:29:15	18.29	22.95	25.51	17.43	15.76
06-Oct-10	19:44:15	18.54	21.48	22.72	17.2	16.43
06-Oct-10	19:59:15	18.3	20.31	20.38	17.7	15.7
06-Oct-10	20:14:15	18.17	19.85	20.07	17.6	15.43
06-Oct-10	20:29:15	18.34	19.8	20.31	17.9	15.38
06-Oct-10	20:44:15	18.33	19.83	19.49	19.09	15.5
06-Oct-10	20:59:15	17.57	19.84	20.31	20.44	15.65
06-Oct-10	21:14:15	18.32	20.31	20.77	20.31	15.63
06-Oct-10	21:29:15	18.27	20.66	20.79	19.73	15.38
06-Oct-10	21:44:15	18.1	20.48	20.47	20.19	15.47
06-Oct-10	21:59:15	18.01	20.96	20.01	19.59	15.06
06-Oct-10	22:14:15	18.26	20.51	19.75	18.75	15.18
06-Oct-10	22:29:15	18.3	20.06	19.59	18.36	15.03
06-Oct-10	22:44:15	18.24	19.61	19.33	18.06	15.18
06-Oct-10	22:59:15	18.23	19.07	19.14	17.75	14.89
06-Oct-10	23:14:15	18.22	19.12	19.02	17.61	14.58
06-Oct-10	23:29:15	18.17	19.02	18.98	17.4	14.53
06-Oct-10	23:44:15	17.93	18.74	19.01	17.19	14.55
06-Oct-10	23:59:15	18.52	18.95	18.99	17.42	14.46